Bending Creep of Corrugated Fibreboard in Cycling Relative Humidity

February 1999

Andrew David McKenzie

Bending Creep of Corrugated Fibreboard in Cycling Relative Humidity

A thesis presented in partial fulfilment of the requirements for the degree of

Master of Applied Science
in Agricultural Engineering at

Massey University

Andrew David McKenzie

February 1999

Abstract

Packaging of fresh fruit for export is a major use for corrugated fibreboard manufactured in New Zealand. However the cold and humid conditions used to preserve fruit quality are particularly detrimental to the strength of corrugated packaging.

The main objective of this study was to develop a method to measure the performance of corrugated fibreboard in high and cycling relative humidity environments. This method was then used to compare the performance of three corrugated fibreboards[1].

The creep performance of corrugated fibreboard was measured by subjecting samples to four point bending stress under controlled cyclic relative humidity conditions using a computer controlled testing apparatus. A mathematical model by Urbanik (1995) and an empirical exponential model were reviewed before selecting a three term model developed by Pecht (1985) to describe the deflection of the corrugated board.

Cyclic relative humidity accelerated the rate of creep compared to a static high humidity environment. The rate of creep in the machine direction was found to be considerably lower than that in the cross machine direction. It was also found that increasing the peak relative humidity from 80% to 90% RH dramatically changed the deflection response. This provides a solution to conflicting data in the literature on relative humidity cycling effects.

Isochronous deflection curves were used to compare the creep performance of the corrugated fibreboard samples in an environment cycling between 50% and 90% RH. Corrugated fibreboard sample *CB1* had a slightly lower creep stiffness than corrugated boards *CB2* (p=0.0580, n=8) and *CB3* (p=0.0398, n=8). However a greater number of tests would be required on a wider range of samples to conclusively determine if there were differences in board performance.

[1]For commercial reasons these will be referred to as 'CB1', 'CB2' and 'CB3'

Acknowledgments

I wish to express my sincere gratitude to my supervisors, Associate Professor Cliff Studman and Dr. Rob Steadman, for their encouragement and guidance during my study. I also wish to thank Dr. Bill Sampson for his contributions towards the modelling and Ian Chalmers for his support. Thanks to Reiner Hensel for his engineering expertise in the construction of the equipment.

Thanks must also go to PAPRO for allowing me to study and Carter Holt Harvey Pulp and Paper Limited for funding the research and allowing me to use it towards a degree.

Finally, special thanks to my wife Robyn for her confidence in me and to Hamish and Erin for their patience while I was working on the thesis.

Contents

List of Figures

List of Tables

Glossary of Terms

Creep: deformation caused by stress applied over time

Doublebacker Linerboard glued to single face corrugated board

Furnish: the mix of fibre and chemical used to make paper

Grammage: mass per unit area in g/m^2 of an air dried sheet (also called ***Basis weight***)

Hygroexpansion: dimensional changes due to the sorption of moisture

Isochronous curve: stress versus strain at constant time

Isometric curve: stress versus time at constant strain

Kraft: wood pulp made using sodium hydroxide and sodium sulphide to dissolve wood lignin

Kraft linerboard: contains not less than 80% kraft pulp fibre

Mechanosorption: nonlinear interaction between applied stress and changing moisture content exhibited in creep behaviour

Mechanosorptive creep: cumulative ratcheting of deformation following each change in material moisture content

Medium: Paperboard used to form the corrugated centre of corrugated fibreboard

Singleface corrugated board: Linerboard glued to corrugated medium

Single facer: First linerboard glued to corrugated medium

Stress induced hygroexpansion: additional dimensional changes due to stress during sorption

Viscoelastic creep: deformation caused by stress and the time required for deformation to respond to stress

Chapter 1

Introduction

1.1 Overview

Low temperature and high relative humidity conditions maintained in horticultural produce coolstores minimise fruit degradation. However, they also weaken the corrugated fibreboard packaging used to protect the fruit. Increasing pressure from overseas retailers for more easily handled point of sale packaging, possible packaging weight reduction legislation, and reduced grower profitability have resulted in packaging designs which are more complex and have lower strength margins. This has put greater emphasis on the performance of corrugated fibreboard, particularly in high and cycling relative humidity environments.

Modern coolstores involve not only high humidity but also considerable fluctuations in humidity during storage and shipment. There is considerable evidence to demostrate that corrugated board reacts in a complex fashion to changes in relative humidity (Söremark and Fellers, 1993; Urbanik, 1995).

There are methods to evaluate the high and cycling relative humidity performance of paper in New Zealand (Chalmers, 1994a) but there are no methods available to measure the long term performance of corrugated fibreboard used in the packaging under those conditions. As corrugated fibreboard is an engineered product made from paper, adhesives and sometimes coatings, it is important to determine the performance of the combined board.

This thesis focuses on the development of a method to evaluate the performance of corrugated fibreboard in a cycling relative humidity environment and the comparison of three types of corrugated board. Chapter 2 provides a background to the mechanical properties of paper and corrugated fibreboard. Chapter 3 summarises papers published in the field of moisture and load effects on paper, corrugated fibreboard and wood materials. The experimental methods and the models proposed by other researchers in this area are also discussed. Experimental methods and the design of the creep test apparatus are presented in Chapter 4.

Calibration of the creep test apparatus, characterisation of corrugated fibreboard bending creep and evaluation of the models discussed in Chapter 3 are covered in Chapter 5. The development of an alternative model is also discussed, before justifying the use of a model previously published for the evaluation of creep data. Chapter 6 presents the experimental plan and results of the main experiments. Chapter 7 discusses the cyclic response, model fit and creep performance of three corrugated fibreboards. The conclusions reached in Chapter 7 are summarised and recommendations made in Chapter 8.

1.2 Research Objectives

The following issues had to be addressed during the study:

1. Development of a suitable test apparatus.

2. Identification or development of a reliable model to describe creep under cycling relative humidity.

3. Generation of isochronous or isometric creep curves to quantify creep performance.

4. Evaluation of the creep performance of samples of three corrugated fibreboard products in cycling relative humidity[1].

[1]For commercial reasons full details of the three products cannot be provided in this thesis.

Chapter 2

Background to Corrugated Fibreboard and Creep

This chapter provides an overview of the relevant properties of corrugated fibreboard and the paper used in its manufacture. The information found in this chapter can be found in texts by Biermann (1996), Jönson (1993), Kocurek (1983-1993), Mark (1983) and Smook (1992).

Corrugated fibreboard is used in many packaging applications because of its low cost, light weight, high strength, recyclability and versatility. Over the years since its inception in the 1880s it has been continuously improved and there are now several common constructions which suit many different packaging applications. The most common construction is 'double face' corrugated board which has two flat outer plies and a corrugated centre ply, as shown in Figure 2.1. To increase the strength

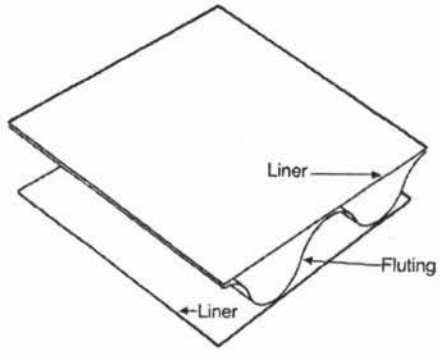

Figure 2.1: Double face corrugated board (Jönson, 1993)

of containers made from corrugated board either stronger paperboard or more layers of single face board are combined. In the case of fruit packaging dual-arch board (ie: two ply fluting) is sometimes used to increase the strength of corrugated fibreboard packaging.

Packaging fresh horticultural produce for export has unique requirements. Produce is stored at low temperature (0 - 0.5°C) and high relative humidity (85 to 95% RH) to minimise fruit spoilage. Unfortunately these conditions weaken corrugated board by increasing its moisture content. In the past wax has been added to the corrugated board to improve its water resistance but this has been phased out because of recycling difficulties.

Since the early 1990's some countries which import fresh fruit and produce have placed restrictions on packaging entering their countries. These require that packaging material weight must be reduced and be either returnable for reuse or recyclable. In order to satisfy these demands and those of exporters and growers for lighter, cheaper and yet better performing packaging, the performance of the corrugated board must be improved.

2.1 Overview of Paper Properties

Paper is the major component in the corrugated board used in corrugated packaging and as such plays a major role in its performance.

2.1.1 Manufacturing

Figure 2.2 shows the basic layout of a fourdrinier type paper machine typical of the type used to make corrugated packaging grade paper. It is formed by draining an approximately 0.5% w/w slurry of wood fibre pulp and chemical additives (stock) on a moving fabric followed by pressing and drying on heated cylinders.

The stock is pumped from the headbox through a narrow slice on to the fourdrinier forming section of the paper machine. Water is drained through a moving

fabric 'wire'. The weak paper web is put through a series of presses in the press section to force more water out, densify the sheet and improve the fibre to fibre bonding. The pulp fibres form hydrogen bonds at points of contact with other pulp fibres to form a laminar sheet as the paper dries. The paper web is dried on a series of steam heated rolls in the dryer section of the paper machine until the moisture content is between 5 to 10% w/w. The formed paper is often passed between heated calender rolls to smooth the paper before being reeled at the end of the paper machine. The reeled paper is slit to widths required by customers as it is rewound on to smaller customer reels.

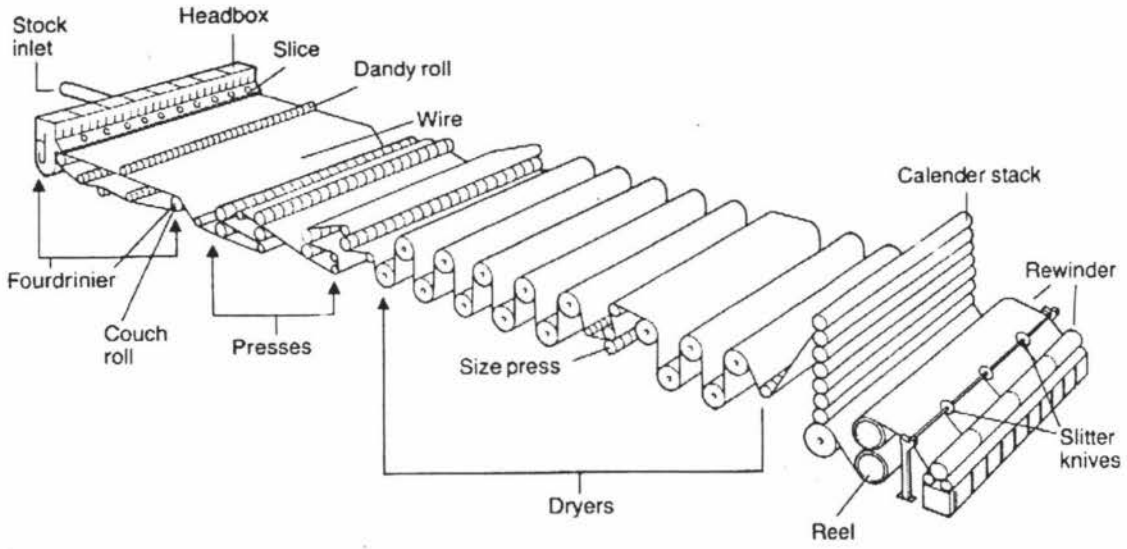

Figure 2.2: Layout of a fourdrinier type paper machine (Jönson, 1993)

Fibres tend to be oriented in the direction of manufacture, or the machine direction (MD) during the forming stage. The fibre orientation typically gives paper greater strength in the machine direction compared with the cross machine direction (CD). Figure 2.3 shows the terminology for the three basic directions of paper. The Z direction refers to the thickness of paper.

Throughout the process the paper is 'drawn' through the paper machine by running each section slightly faster than the previous section. Drawing the paper

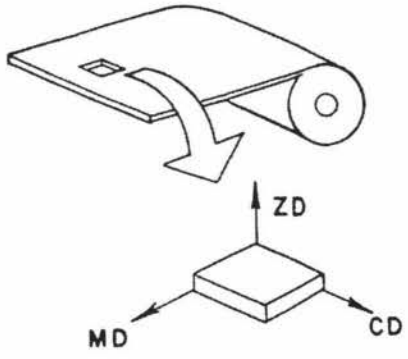

Figure 2.3: Basic directions of paper; MD, CD and ZD (Unknown source)

also stiffens the fibres. Straining the fibres while the fibre components are above their glass transition point straightens the microstructure of the fibre. As paper dries the fibre components move below their glass transition point and the strains are 'frozen' into the fibre.

As the fibres dry they shrink, mostly in the radial direction. The draw on a paper machine limits shrinkage in the machine direction. There is no similar restraint in the CD. This makes paper less dimensionally stable in the CD when its moisture content is changed during use.

The two classes of paper used in corrugated board are linerboard, for the flat surfaces of corrugated fibreboard and corrugating medium (or medium[1]), which is the paper used in the centre of the corrugated fibreboard. Kraft linerboard[2] is usually made from fibre obtained by chemically pulping softwood trees but often includes recycled fibre and semichemical hardwood fibre in the furnish[3]. Linerboard manufactured from recycled fibre is called testliner. Virgin medium is usually semichemically pulped hardwood species mixed with kraft softwood pulp. Recycled medium is manufactured from recycled fibre.

Apart from its fibre components most packaging grade paper contains water-

[1]Also called fluting, as in Figure 2.1
[2]Kraft linerboard contains not less than 80% kraft pulp fibre
[3]Furnish: the mix of fibre and chemicals used to make paper.

proofing chemicals and starch to enhance its performance. Paper is sold on its strength characteristics and on its weight per square metre or 'basis weight'.

At the time of writing, all linerboard manufactured in New Zealand was produced at Carter Holt Harvey Pulp and Paper Limited's Kinleith Mill, and was unusual in that it used predominantly *Pinus Radiata* kraft softwood fibre. Approximately 20% of the furnish is recycled fibre. Carter Holt Harvey Pulp and Paper Limited also manufactured virgin and recycled fibre medium.

2.1.2 Engineering Properties

Paper is an anisotropic laminar material with property differences in the planar directions and through the thickness. The laminar fibre structure of paper often means that standard engineering concepts cannot necessarily be applied due to difficulties in measuring properties such as the thickness and the cross sectional area. For example stress is defined as the load per unit cross sectional area but the cross section of paper contains cross sections of fibres and air gaps between the fibres.

The measured thickness of paper depends on the measurement technique. If, for instance, the elastic modulus of paper was determined using the cross sectional area determined by a standard technique which uses a micrometer with a specified foot area and pressure to measure thickness, it would seriously underestimate the true elastic modulus because the actual stress bearing thickness is much less (Markström, 1991). Compounding this are variations in surface roughness and grammage[4]. Markström (1991) reported that deviations between the standardised thickness and the strength-effective thickness may amount to 25%. This is one of the reasons that many paper properties are indexed to the basis weight.

Tensile stiffness is often used instead of modulus of elasticity because it does not require thickness to be known (Equation 2.1). Tensile stiffness index (E^*) is obtained by dividing tensile stiffness by grammage, and is equivalent to specific

[4]Grammage (or basis weight) is the weight per unit area in g/m^2 of an air dried sheet.

elastic modulus, or elastic modulus divided by density. This is a useful measure of the level of tensile stiffness for a given weight and can serve as a basis for comparing paper with other materials.

$$S_t = E \times t = \frac{F}{b} \times \frac{1}{\epsilon} \tag{2.1}$$

where

S_t	=	tensile stiffness (N/m)
E	=	elastic modulus (N/m^2)
t	=	thickness (m)
F	=	force (N)
b	=	width (m)
ϵ	=	strain m/m

The primary strength properties of paperboard which influence the compression strength of corrugated containers are CD compression strength and tensile stiffness. CD compression strength directly affects the edgewise compression strength of corrugated board, while the tensile stiffness affects the bending stiffness of corrugated board. The bending stiffness resists compression loads when the sides start to buckle under compression.

Paper is also described as a viscoelastic material (Brezinski, 1956). Properties such as tensile strength and failure strain are affected by the rate of strain. On a larger time scale the viscoelastic nature influences the long term loading characteristics of paper. The strain caused by loading over long periods of time is referred to as 'creep'. The viscoelastic nature of paper makes modelling the creep of paper very difficult.

2.1.3 Effect of Moisture on Paper

Paper adsorbs or desorbs moisture when exposed to non-equilibrium relative humidity or temperature conditions. Raising the relative humidity at constant temperature or reducing the temperature of the surrounding environment at constant relative humidity will increase the moisture content of paper. The reverse is also true.

The relationship between relative humidity and moisture content is non-linear and best described as a sigmoidal shape. Furthermore, paper also exhibits a hysteresis when the relative humidity is changed. Figure 2.4 from Wink (1961) shows typical moisture isotherms for pulp and paper. Curve A is the first complete desorption and the first complete absorption is shown by curve B. These curves define the outer boundaries of an equilibrium area and any subsequent changes in relative humidity will fall within these boundaries.

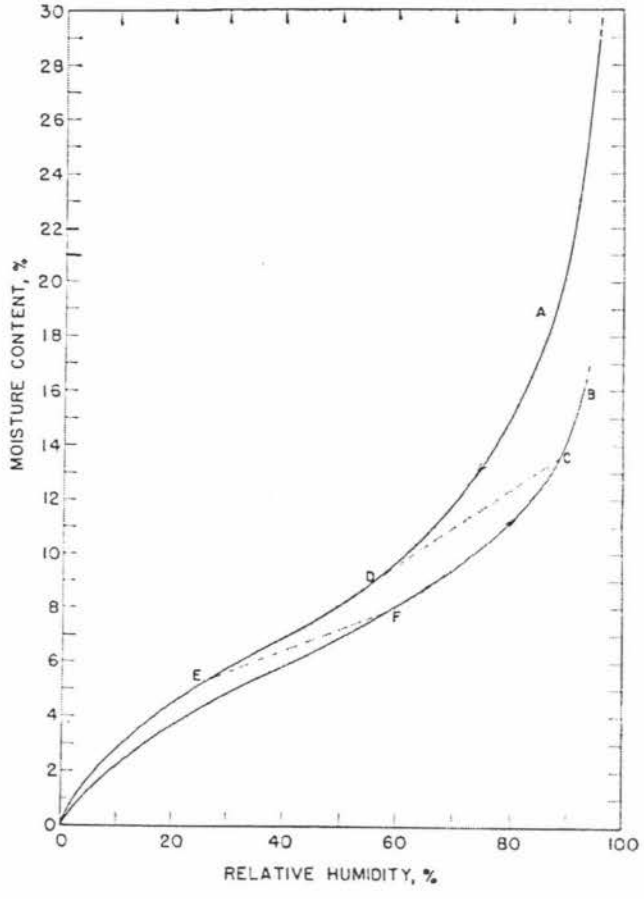

Figure 2.4: Typical moisture hysteresis isotherms for pulp and paper (Wink, 1961)

If paper is cycled between two intermediate relative humidities the moisture content moves from one isotherm to the other and shows a hysteresis effect. Partial adsorption to a relative humidity shown as point C in Figure 2.4 followed by desorption would result in an isotherm represented by line CD. Similarly partial adsorption

from point E would result in the line EF.

This means that the equilibrium moisture content of paper at a given relative humidity depends on whether the paper has adsorbed or desorbed water to reach equilibrium. In Figure 2.4 this could mean an equilibrium moisture content ranging between 6.8% and 8% at 50% RH. In practice this can make a large difference in the mechanical properties of paper, especially in the high relative humidity regions above 80% RH. The level of moisture and the moisture sorption rate is also dependent on factors such as the rate of change and magnitude of the change of relative humidity as well as the physical and chemical characteristics of the paper.

As paper absorbs and desorbs moisture it expands and shrinks. This is termed *hygroexpansion* and is a function of the moisture content, orientation, manufacturing draw and the previous moisture history.

The tensile and compressive strengths of paper are reduced by increasing the moisture content. At constant temperature strength is almost linearly related to the moisture content up to about 17% moisture content.

Increasing the moisture content of paper at constant temperature above the glass transition point of some of the fibre components (eg: above about 12% at room temperature) releases some of the dried-in stresses which affect properties such strain to failure, the amount of tensile strain energy absorbed to cause failure, and hygroexpansivity (Salmén, 1993). Like the adsorption of moisture, dried in stresses are released more rapidly and there is greater relaxation above about 80% RH per % RH increase.

2.2 Corrugated Fibreboard Properties

Corrugated fibreboard is an engineered structure made from paper components and adhesive. It is manufactured by gluing two flat linerboards to corrugated medium with starch based adhesive. The medium is corrugated by heating it with steam showers and passing it between heated corrugating rolls in the 'labyrinth'. The

corrugating rolls heat the paper to about 170°C which is above the glass transition temperature of the lignin and hemicellulose in the wood fibre. The fibres are easily deformed under these conditions and retain their shape when the medium cools rapidly after leaving the labyrinth. The first linerboard is glued to the corrugated medium immediately after the medium is corrugated. This forms *single face* corrugated fibreboard. Double face corrugated fibreboard, as used in corrugated containers, is made by gluing a second linerboard to the other side of the corrugated medium. A diagram of a corrugator is shown in Figure 2.5.

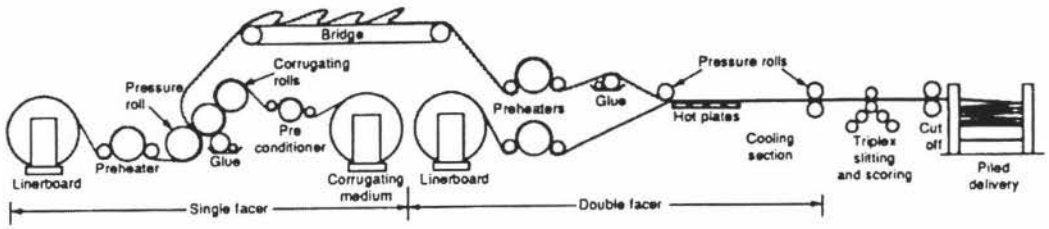

Figure 2.5: Corrugated board manufacture (Jönson, 1993)

Corrugated fibreboard retains the machine and cross machine directions of paper because of the way the paper components are unwound to form a continuous sheet of corrugated board. Figure 2.6 shows these directions.

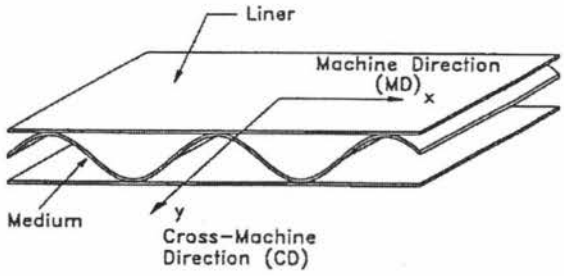

Figure 2.6: Basic geometry and component materials of corrugated board (Luo et al. (1995)

The first linerboard glued to the medium is termed the 'single facer'. The second linerboard is called the 'doublebacker'. The two linerboards are not necessarily the

same basis weight. When the construction is asymetrical the heavier basis weight linerboard is used on the inside of the corrugated container. This improves the container strength because it puts the heavier, and stronger, paper in compression when the container begins to bulge while the weaker paper is in tension which is paper's stronger stressing direction.

The two main characteristics which determine the end use performance of corrugated fibreboard are its bending stiffness and its compression strength in the plane of the board. In 1963 McKee et al. proposed Equation 2.2 for determining the compression strength of corrugated containers. The 'McKee' equation is still used extensively today for estimating the strength of containers.

$$P = a\, {P_m}^b \left(\sqrt{D_x\, D_y}\right)^{1-b} Z^{2b-1} \tag{2.2}$$

where

P	=	container compression strength (N)
P_m	=	edgewise compression strength of corrugated board (kN/m)
$D_x\ D_y$	=	corrugated board bending stiffness, MD and CD respectively (N.m)
Z	=	container perimeter (m)
a, b	=	constants (2.028, 0.746)

Edgewise compression strength is measured by compressing small columns of board in the CD. There are several standard methods which vary primarily in the size and shape of the test specimen and whether it has reinforced edges or not. Bending stiffness is based on the four point method to eliminate shear.

Although the compression strength of combined board can be estimated from the compression strength of the individual components, none of these tests accurately predict the long term stacking performance of corrugated containers in high or cycling relative humidity conditions. Crude rule of thumb allowances have been used to build in 'correction factors' for these and other conditions found in the storage and transport chain (Jönson, 1993).

2.3 Creep

'Creep' describes the deformation, or strain, over time. Plotting strain versus time with a constant load gives a characteristic creep curve (Figure 2.7) which, if the sample is taken to failure, normally exhibits three distinct regions of strain rate. The first region features a rapid increase in strain and has an element of elastic strain as the material is stressed. This is the primary creep zone. As the rate of strain decreases it enters the secondary creep zone. This is characterised by a relatively long period of constant strain rate. Tertiary creep occurs immediately before catastrophic failure and is characterised by a rapid increase in strain rate leading to collapse of the structure (Bronkhorst, 1997).

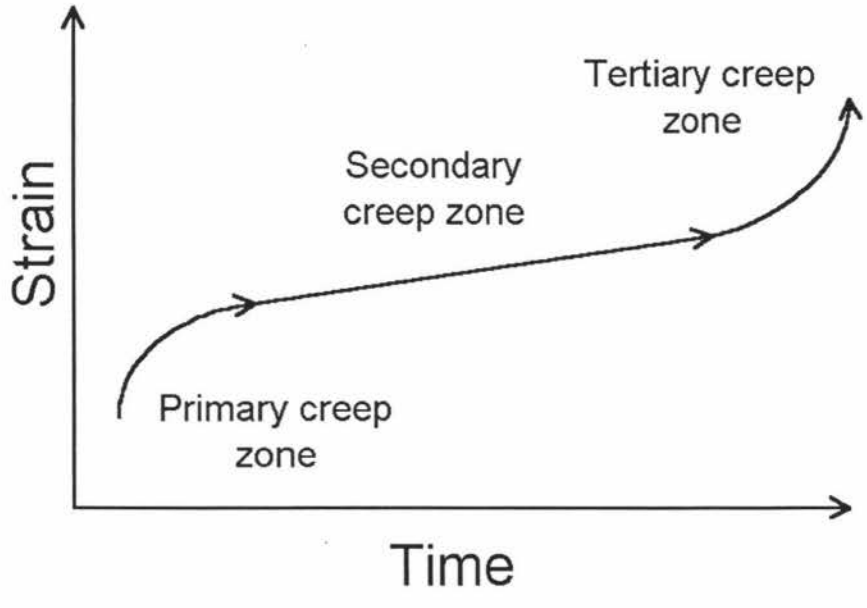

Figure 2.7: Example creep curve.

Chapter 3

Literature Review

3.1 Introduction

Creep in paper has been studied for many years (Brezinski, 1956). In 1972 Byrd published a paper showing that paper subjected to tensile stress would creep faster in a cyclic relative humidity environment than in a static high relative humidity.

In the 1980's paper and packaging companies searching for a competitive advantage turned towards lighter weight packaging and greater use of recycled fibre. At the same time plastic started to threaten paperboard as a source of packaging material. One advantage that plastic had over corrugated board was its relative insensitivity to relative humidity fluctuations. Understanding the causes of cyclic relative humidity creep and evaluating the long term stacking performance of containers became a priority for many corrugated board packaging companies in an effort improve the performance of their product.

There have been many papers published on creep of paper, but relatively few on creep of corrugated board. The major exceptions are publications since 1990 by researchers at the U.S. Department of Agriculture's Forest Products Laboratory (FPL), and those at the Swedish Forest Products Laboratory (STFI).

3.2 Corrugated Fibreboard Creep Measurement Methods

Gunderson and Laufenberg (1994) described a device for measuring the bending and column creep of corrugated fibreboard at FPL (Figure 3.1). The device could test up to 70 specimens for column creep or 50 specimens for bending creep. Normally it was configured to test 28 specimens for column creep and 30 specimens for bending creep. The column creep sample was 51mm wide by 38mm high and paraffin wax

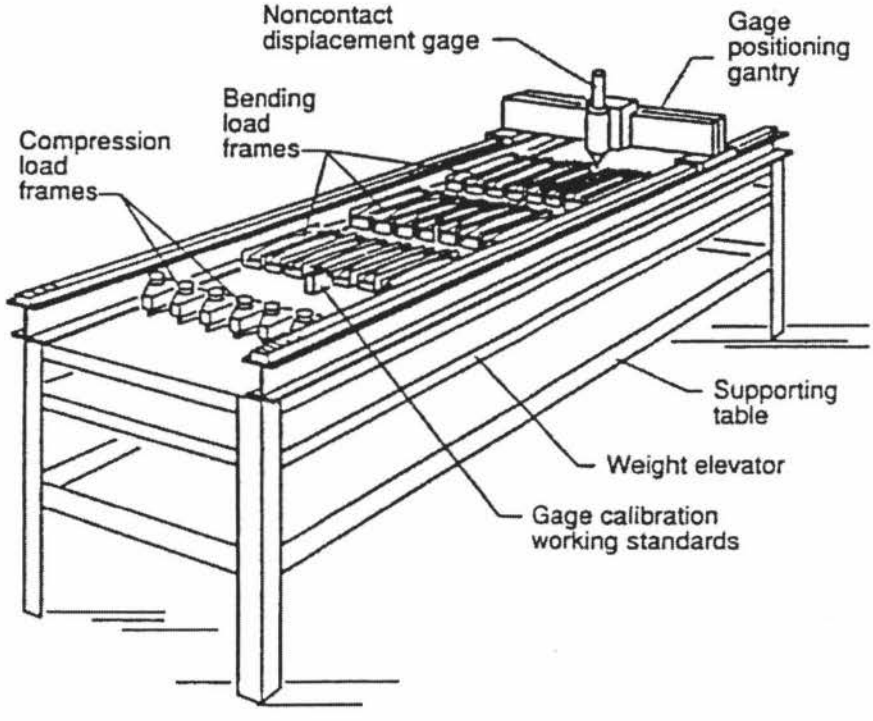

Figure 3.1: FPL corrugated fibreboard creep measurement device.(Gunderson and Laufenberg, 1994)

treated, as specified in the TAPPI procedure for measuring the edgewise compression of corrugated fibreboard[1]. Time to fail and deformation rate were the principal parameters used to evaluate sample performance.

The bending creep test pieces were 280mm long by 40mm wide and a four point bending system was used to create a constant moment, zero shear region in the

[1]TAPPI Test method T811 om-88

middle of the test piece. Deformation was measured by the vertical displacement of the test piece at the centre of the specimen portion subjected to constant moment load. Similar to column creep, performance was measured by time to failure and deformation rate. Figure 3.2 shows the bending creep set-up.

Loading was done with dead weights and used a remote system to load all the test pieces at the same time. Displacement measurements were made by moving a non-contact LVDT from specimen to specimen throughout the duration of the test. The LVDT resolution was 0.013mm. Each cycle of measurements took about 15 minutes. The whole device was placed in a humidity and temperature controlled room.

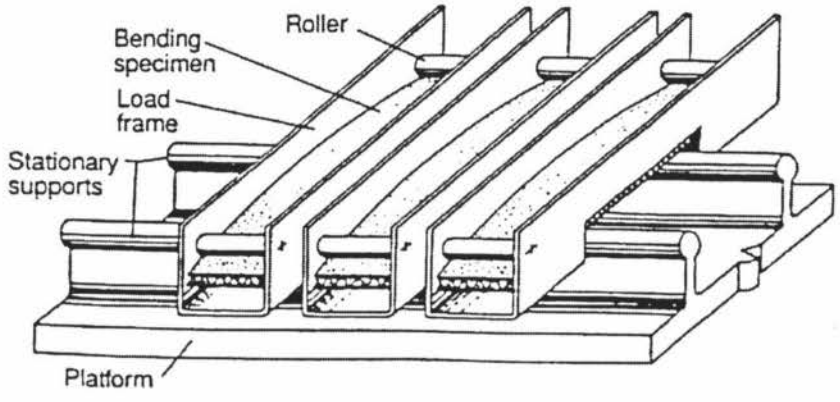

Figure 3.2: Bending creep in the FPL tester. (Gunderson and Laufenberg, 1994)

Söremark and Fellers (1993) at STFI used a Lorentzen and Wettre four point bending stiffness tester to measure corrugated board bending creep. This used a 460mm long by 100mm wide test specimen in four point bending mode and measured the deflection of the specimen in the middle of the centre span. The tester was placed in a humidity and temperature controlled cabinet which enabled experiments under high and cycling relative humidity conditions to be conducted. Creep and hygroexpansion in tension and compression was measured by substituting one of the liners of the corrugated board with a steel strip.

3.3 Creep Test Stressing Mode

Laufenberg (1991) found bending mode creep was more sensitive to changes in corrugated board construction compared to column creep. This agreed with Padanyi (1991) who said mechanosorptive effects are more pronounced in bending mode than in compression and tension because the outer layers have a proportionally greater influence on bending stiffness and this is where sorption of moisture first occurs. This geometry is therefore particularly suitable for characterising the sorption-dependent behaviour of paper.

Further evidence for using bending creep instead of column creep was given by Thorpe and Choi (1992) who reported the major portion of the vertical panels near corrugated fibreboard container corners are under compression load while the mid-portion of the vertical panels usually support compression load in a bending mode. This is typical of panels with pinned sides subjected to compression stress greater than a critical level. With stacked containers in a cyclic humidity environment the effect of successive hygroexpansions caused by the cycling relative humidity lessens the portion of the vertical panels supporting the load under compression loading and increases the portion supporting the load under bending. Just before a container collapses an area of high shear strain forms within the vertical panel where the bending portion of the vertical panel meets the compression portion of the panel.

3.4 Mechanosorption

Researchers in the field of structural wood products have been aware of the 'mechanosorptive' effect since 1960 (Hoffmeyer and Davidson, 1989). Mechanosorption is described as the nonlinear interaction between applied stress and changing moisture content exhibited in creep behaviour (Fridley et al. (1992). Mechanosorptive creep describes the cumulative ratcheting of deformation following each change in material moisture content. The features of mechanosorption (in wood) were documented by

Hoffmeyer and Davidson (1989). The following list is taken from their paper.

Table 3.1: Typical Features of Mechanosorption (Hoffmeyer and Davidson, 1989)

1. Deformations increase during desorption.
2. The first sorption step causes an increase in deformation. All following sorption steps normally cause a decrease in deformation at low or moderate stresses and an increase of deformations at high stresses.
3. The mechanosorptive deformation is virtually time independent and influenced only by the magnitude of the moisture change at or below fibre saturation.
4. The increase in deformation of initially saturated wood is much greater than in initially dry wood.
5. Instantaneous elastic recovery following unloading is equal to or greater than the initial elastic deformation. Thus, the anatomical features responsible for mechanosorptive effects increase the elastic 'spring back' of the wood.
6. Deformations are 'frozen' for constant moisture content. After unloading and instantaneous recovery, a large proportion of the total deformation is maintained. The deformations are "thawed" by further moisture cycling. Larger recovery during adsorption than during desorption.
7. Constant moisture flow through wood, causing no local changes of moisture content, does not result in any mechanosorptive effect.
8. Mechanosorption leads to failure in shorter time and/or at lower loads.
9. Modulus of elasticity is progressively reduced. Bethe (1969) demonstrated a linear relationship between total creep and MOE after termination of a series of six moisture cycles. A reduction of up to 40% was found.
10. The amplitude of the oscillation of the mechano-sorptive creep curve tends to increase linearly with total creep.
11. Unloading causes the amplitude of the oscillation of the creep curve to drop. It then tends to stay constant regardless of total creep.

A significant proportion of research on the long term stress-strain relationship of wood products has concentrated on the mechanosorptive effect as it has been identified as a major contributor to the long term performance of these products in the field. While the attributes of mechanosorption have been documented for some time, the phenomenon is not well understood and there have been several models

suggested to explain the mechanism of mechanosorption.

In particular, a model of slip-planes being formed in the wood cell wall under compression was included in a more complex model, with additional effects due to the matrix material of the wood structure by Mohager and Toratti (1993).

The wood matrix may have a parallel situation in the hydrogen bonding in paper, making this model potentially useful in describing the creep characteristics of corrugated fibreboard. However this was not explored futher in this study.

3.5 Environmental Conditions

High humidity conditions increase the moisture content of paper and paper products as illustrated in Figure 2.4. Increasing the moisture content reduces the compression strength and stiffness of paper (Salmén, 1993), thus weakening corrugated fibreboard. It is also accepted that cycling relative humidity increases the rate of creep since Byrd (1972) reported that paper with a tensile load in cycling relative humidity conditions had a greater rate of creep than paper under the same load in static high humidity conditions. This occurred even though the average moisture content of the paper in the cycling RH was lower.

Other researchers have also compared the effects of cyclic and static RH. The conclusion reached by all was the same as Byrd's. Gunderson and Tobey (1990) showed that the amount of creep of paper under tension was independent of the frequency and depended only of the number of relative humidity cycles.

Leake and Wojcik (1993) subjected corrugated containers under load to cycling relative humidity and found that they had a shorter life span than those exposed to a static RH environment. They also reported that longer cycle times had a more adverse affect than short cycle times and that the longer cycle times caused greater moisture changes and greater hygroexpansion.

The manner in which the relative humidity is cycled is thought to influence the response of paper in cyclic relative humidity creep tests (Haslach, 1997). There have

been several methods used, depending on the desired response or limitations of the equipment used to control the environment. Some researchers have used a square wave or step function (Söremark and Fellers, 1993), others have used sawtooth or constant rate of RH change cycles (Haslach et al., 1991) and others used sinusoidal relative humidity variation (Laufenberg, 1991; Urbanik, 1995).

Mechanosorptive creep is thought to be a response to changing moisture content (Fridley et al., 1992). Therefore, as pointed out by Haslach (1997) it is inappropriate just to bring the test specimens to moisture equilibrium, as would happen in a square wave or stepped RH function, when investigating a dynamic response. Using a sawtooth variation implies that a linear rate of change must be chosen. There have been contradictory results in the literature on how the rate of change affects creep (Considine et al., 1994). Varying the relative humidity in a sinusoidal manner also varies the rate of change in a sinusoidal cycle thereby eliminating the need to choose a specific rate of change. Haslach (1997) suggested that sinusoidal variation might be useful because random variation can be resolved as a sum of sinusoidal functions. It was also noted however that no one has investigated whether or not the separate responses of two different humidity patterns can be superposed to obtain the same response as that due to the sum of the two humidity variations.

Urbanik and Lee (1995) showed that the hygroexpansive and phase relationship of the cyclic relative humidity creep response of corrugated fibreboard is dependent on the frequency of the cyclic RH and proposed a swept sine RH schedule in which the cycle frequency varies logarithmically with time.

Temperature also affects the equilibrium moisture content of paper and the rate at which it adsorbs and desorbs moisture from the surrounding air. Reducing the temperature at constant relative humidity increases the equilibrium moisture content and vice versa. Compounding the temperature / moisture content interaction is that adsorption of moisture is an exothermic reaction. This affects the moisture sorption rate as the temperature of the paper changes.

It was agreed by delegates at the 3^{rd} International Symposium on Moisture and Creep Effects on Paper, Board and Containers that further work in the field of creep response in cycling humidities needs to be done on a cycle ranging from 50 to 90% relative humidity (Chalmers, 1997 p.271). This was a compromise between two groups wanting either 80% or 95% relative humidity to be the maximum relative humidity, and provides a basis for comparison of results. Cycle period and ramp times were left to individual researchers to best fit the work or equipment being used.

3.6 Material Characteristics Affecting Creep

Creep tests, by their very nature are long term tests and may take days or weeks to complete single tests. At the forefront of research have been attempts to predict creep performance from traditional tests of paper products. Considine (1992) reported that hygroexpansive strain was the best predictor of paperboard creep performance, and postulated that compressive strength did not predict the compressive creep performance, probably due to the greater influence of viscoelastic behaviour over the longer term (Considine et al., 1994). Kuskowski et al. (1995) reported that CD hygroexpansivity could be used to gauge the cyclic creep performance of components and combined board under compressive load.

Recently Urbanik (1998) suggested that stiffness may be a good predictor of paper creep, and that bending stiffness of corrugated board has also been correlated with corrugated fibreboard creep behaviour but this requires experimental confirmation.

3.7 Characteristics of Cyclic Relative Humidity Creep of Corrugated Fibreboard

Column compression creep of corrugated board follows the characteristic creep curve shown in Figure 2.7 (Urbanik, 1995). The specimen shows a cyclic response related

to the level of relative humidity. Increased relative humidity causes the specimen to expand, reducing the strain, and vice versa.

When Söremark and Fellers (1993) measured the deflection of corrugated fibreboard subjected to bending stress in a square wave profile cyclic relative humidity atmosphere they observed that after the initial cycle the corrugated fibreboard increased deflection when the relative humidity was reduced from 80% to 40%. This was contrary to the expected response and led the authors to propose that not only does stress affect the hygroexpansion of paper, but there is greater hygroexpansion in compression compared with tension.

Söremark and Fellers (1993) substituted one or other of the linerboards of the corrugated fibreboard with a steel ribbon. Because the steel ribbon was not affected by relative humidity measuring the bending creep response of these specimens under cyclic relative humidity allowed them to remove the hygroexpansive response of either the linerboard in compression or tension. This resulted in the separate measurement of the hygroexpansion of linerboard under compression and tension. They calculated the stress induced hygroexpansion (SIH) component of the cyclic creep to be +15% and -11% compared to unloaded corrugated board for compression and tension respectively i.e.: linerboard under compression is more hygroexpansive and linerboard under tension is less hygroexpansive than unloaded linerboard.

SIH was reported to be opposite in direction and higher than the sum of the elastic and creep strains when the humidity was changed. They also observed that corrugated fibreboard exhibited an increase in creep rate and a decrease in stiffness under cyclic relative humidity conditions compared to creep in a constant climate.

This result fitted the model of slip-planes being formed in the cell wall under compression (Hoffmeyer and Davidson, 1989) and also supports Mohager and Toratti's (1993) view that mechanosorption behaviour differed for tension compared to compression.

However, contrary to this observation, bending creep experiments carried out at

FPL showed less deflection at low RH (Laufenberg, 1991). It was not clear why, and no explanation was given. The experiments at FPL used a sinusoidal relative humidity profile ranging from 50 to 90% RH.

When Hoffmeyer and Davidson (1989) listed the features of mechanosorption they said that the level of stress influenced the direction of the deformation (Table 3.1, page 18). Norimoto et al. (1992) suggested that the increase in deflection with reduced moisture, and vice versa, may be a geometrical and elastic effect. Thus the response observed by Laufenberg (1991) may fit the features of mechanosorption.

Although Haslach et al. (1991) conducted experiments on paper when they subtracted unloaded sample hygroexpansive strain from measured tensile creep strain in cyclic relative humidity creep experiments too much strain was subtracted to account for the hygroexpansive response. This is what may be expected if tension reduced the hygroexpansivity of paper. Instead they subtracted the creep strain from the cyclic minima of the measured strain to determine the swelling response. Using this method of calculation they noted that hygroexpansive swelling strain decreased on subsequent cycles, and suggested that perhaps the load had a damping effect. They also noted that the unloaded specimens showed hysteresis in the swelling cycles as the relative humidity was cycled. This can be expected if the hygroexpansion is proportional to the moisture content, knowing that paper exhibits a moisture hysteresis when relative humidity is cycled.

Haslach (1997) later reported that there were differing results in the literature on the dampening of the cyclic response.

3.8 Mathematical Modelling of Creep

One of the aims of this research was to characterise bending creep deflection using a mathematical model. Ideally this would be a mechanistic model in which the terms represented physical characteristics of the sample, or at least represent characteristics of the creep response, which could be used to predict behaviour from material

characteristics. Achieving this would enable the comparison of different corrugated fibreboard constructions and enhance our understanding of the mechanisms of mechanosorptive creep.

A descriptive empirical model would also be useful to assist analysis of creep curves by smoothing experimental data and possibly allowing extrapolation of experimental data.

3.8.1 Wood Products

Since paper is a wood based product, it is possible that models developed for other wood products may be of value to the understanding of corrugated fibreboard creep characteristics.

Researchers in the area of wood products, such as timber and chipboard, have built up a large body of knowledge of the effects of moisture and creep at high and cycling humidity. Much of the modelling has been based on linear models of spring and dash-pot systems to account for the elastic, viscoelastic and viscous behaviour of timber and woodfibre based chipboard (Fridley et al., 1992; Pierce et al., 1979).

3.8.2 Paper and Corrugated Fibreboard

3.8.2.1 Creep Response

Bresinski (1956) found that the creep response of paper under tension could best be described by an exponential function at low stresses or short times (Equation 3.1), but when subjected to high stresses or stress over a long time the deformation was best described by a logarithmic function (Equation 3.2).

$$\epsilon = Bt^a + C \tag{3.1}$$

$$\epsilon = K \log t + C' \tag{3.2}$$

where

ϵ	=	strain (mm/mm)
t	=	time (s)
B, a, C, K, C'	=	constants

Haraldsson et al. (1993) reviewed several creep models, including Brezinski's, and concluded that a model using a power function to describe the time element combined with a non-linear hyperbolic tangent model to describe the stress-strain relationship could predict long term behaviour of paperboard products (Equation 3.3).

$$\sigma^w = (t/t_0)^n . \alpha_1 . \tanh(\varepsilon . \alpha_2/\alpha_1) \tag{3.3}$$

where

σ^w	=	specific stress (force/width.grammage), $\mathrm{Nm.kg^{-1}}$
t	=	time (s)
t_0	=	constant (1 s)
n, α_1, α_2	=	material constants
ε	=	strain (mm/mm)

The model worked well at constant relative humidity where the stress-strain relationship could be measured. They concluded that paperboard products could then be designed using engineering principles with more confidence than was previously possible.

It is logical to suggest that combining the performance of the individual components to predict the performance of corrugated board may be appropriate. However this approach should be treated with caution as Urbanik (1981) showed that corrugated fibreboard could not be treated as a sum of the components with respect to compression strength.

Pecht (1985) proposed a curve fitting model which used a combination of loga-

rithmic and exponential terms to describe constant moisture content tensile creep of paper at fixed stress and temperature conditions. In this model the strain is the sum of an initial strain and a creep term of the form in Equation 3.4.

$$\epsilon(t) = c\ln[1 + \beta(\sigma, m)t^n] \tag{3.4}$$

where

$\epsilon(t)$	=	Strain at time t
c	=	Constant
β	=	Function of σ and m
σ	=	Constant axial stress
m	=	Constant moisture content
t	=	Time
n	=	Material constant

This was used by Haslach et al. (1991) in the analysis of tensile creep of paper. For constant RH, and therefore constant moisture content in a static load creep test σ and m are both constants and can be included in a single term, B (Haslach et al., 1991):-

$$\epsilon(t) = c\ln[1 + Bt^n] \tag{3.5}$$

where

B	=	time shift factor on a master creep curve

Equation 3.5 implies that a given creep strain at a given time can be obtained by changing either the stress or moisture content. B therefore moves the creep response along the time scale as a result of σ and m.

Haslach et al. (1991) used this equation to model the tensile creep response of paper in a cyclic relative humidity environment. They assumed that when the RH returned to its initial level there would be no swelling component in the strain measurement. They fitted the Pecht Model (Equation 3.5) to the creep strain which corresponded to 30% RH when cycling the relative humidity from 30% to 90% after starting at 30% RH. An example of this is shown in Figure 3.3.

Urbanik (1995) also suggested that the overall cyclic relative humidity creep

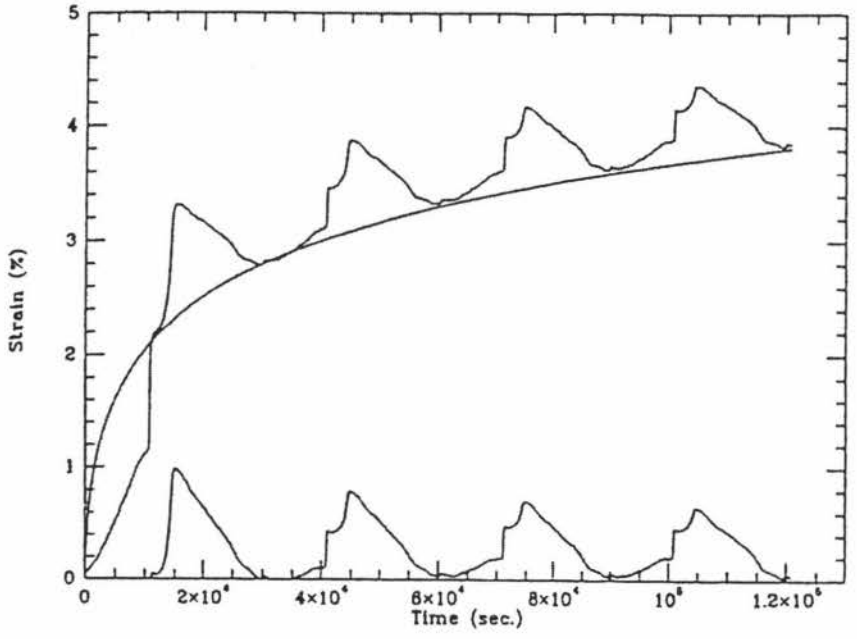

Figure 3.3: Equation 3.5 fitted to the cyclic minima of tensile creep in a cyclic RH environment (Haslach et al., 1991)

deformation function is the sum of a mechanosorption creep function and a hygroexpansion function (Equation 3.6) and developed a model which described the compression creep of corrugated fibreboard by separating the response of the two phenomenon.

$$X(t) = X_h(t) + X_c(t) \tag{3.6}$$

where
$X(t)$ = cyclic creep deformation function
$X_h(t)$ = hygroexpansive function
$X_c(t)$ = mechanosorptive creep function

The model had terms for primary and secondary creep rates, a time constant for the exponential change from primary to secondary creep and the magnitude and amplitude and phase lag of the cyclic deformation. The mechanosorption function was assumed to be a function of the rate of change of moisture and equal in magnitude for both increasing and decreasing moisture content. It then used specimen

hygroexpansion to predict creep rate.

3.8.2.2 Hygroexpansive Response

Uesaka et al. (1992) and Niskanen et al. (1997) have shown that the cross machine (CD) hygroexpansion of paper is linearly related to moisture content but not relative humidity. However, Urbanik (1995) observed that the hygroexpansion of unloaded test pieces varied with the same form as relative humidity. Therefore, for those conditions moisture content was directly proportional to relative humidity. This made it valid for Urbanik's hygroexpansion function $[X_h(t)]$ (Equation 3.7) to be related to the time base of the relative humidity variation.

$$X_h(t) = A_0 + A\sin(\omega t + \phi - \theta) \tag{3.7}$$

where

$X_h(t)$	=	hygroexpansive function
A_0	=	magnitude
A	=	amplitude
ω	=	frequency
t	=	time
ϕ	=	phase offset
θ	=	phase lag relative to relative humidity

The moisture content of unstressed paper and corrugated fibreboard is close to linearly related to relative humidity over the range of about 40% to 80% relative humidity (Figure 2.4 on page 9) for either adsorption or desorption of water. However there is a significant hysteresis when changing the direction of the moisture sorption. This would lead to inaccuracies in Urbanik's assumption. The relationship between relative humidity and moisture content becomes very nonlinear above 80% RH which invalidates the assumption at high relative humidities. The assumption would have to remain true at 80% and higher RH for the model to be applicable to coolstore conditions.

Urbanik's model does not account for stress induced hygroexpansion in using

the rate of hygroexpansion to predict the rate of change in moisture content to calculate the rate of mechanosorptive creep. In the case of bending creep however the sample is subjected to both compression and tension stress. It is therefore unclear if hygroexpansion would be a good predictor of moisture content and hence mechanosorption.

Before using Urbanik's model it must be examined under conditions of 90+% relative humidity.

3.8.2.3 Analysis of Results

There are several ways to analyse data from creep experiments. A creep model such as Urbanik's (1995) fitted to the data which had terms such as the secondary creep rate can make comparisons relatively simple, particularly if specimen life-time can be related to the terms (Bronkhorst, 1997). A mechanistic model derived from fundamental material properties would also be beneficial as those properties could be engineered to improve the creep performance. It is also possible to use an empirical model to describe creep response and plot the creep response on isochronous or isometric curves. This method is commonly used in the analysis of the creep of plastics (Haraldsson et al., 1993).

Data from constant load creep experiments consists of the strain measured at given times from the beginning of the test. Data are plotted to give creep curves of the form shown in Figure 3.4. In this example three levels of stress (σ_1, σ_2 and σ_3) were used to generate three creep curves. The data in the creep curves can be rearranged to plot isometric and isochronous curves.

An isometric curve is a graph of the stress required to reach a nominated level of strain or deflection at a corresponding time (Figure 3.5). This form is useful in predicting the maximum load (stress) which can be applied to a structure to give a known lifetime if the structure fails at a critical strain. This may be the case for corrugated containers (Haraldsson et al., 1997). In Figure 3.5 points t_1, t_2 and t_3 at

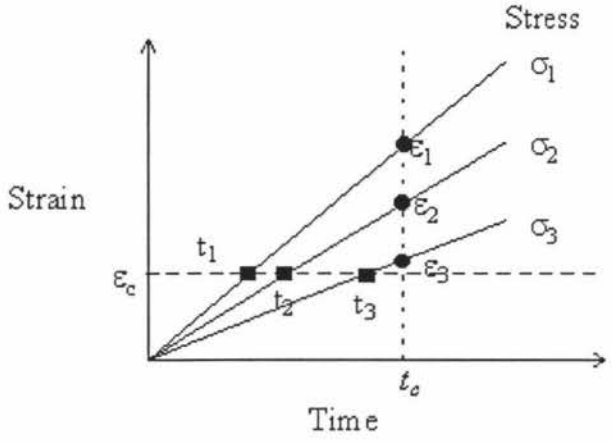

Figure 3.4: Example creep curves

strain ε_c were taken from Figure 3.4 and plotted on stress versus time axes.

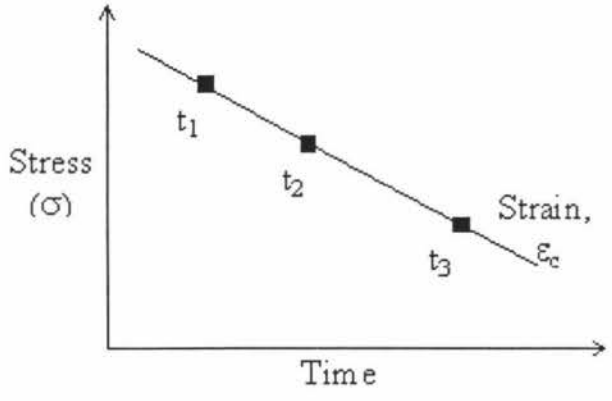

Figure 3.5: Example isometric curve

An isochronous graph shows the creep stress versus strain or deflection for a nominated time. This makes it easier to visualise the relationship between stress and strain at a given time. In Figure 3.6 points ε_1, ε_2 and ε_3 at time t_c were taken from Figure 3.4 and plotted on stress versus strain axes.

Söremark et al. (1993) suggested using isochronous stress strain curves and comparing these on the basis of the initial slope, or *creep modulus*. Lower creep modulus reflects poorer creep performance. Haraldsson et al. (1993) used isometric curves at a critical strain which reflected the strain at failure. An advantage of isochronous and isometric creep analysis is that the curves can be determined from experimental

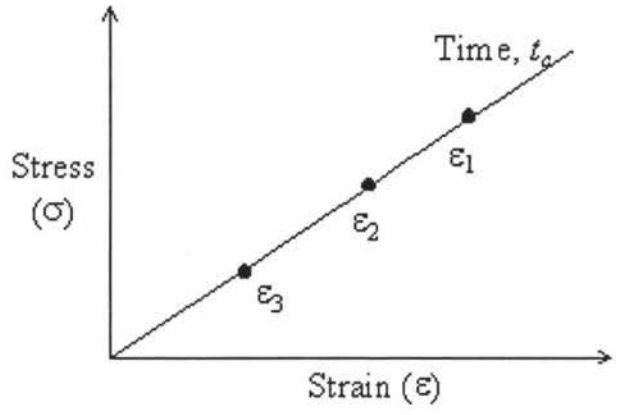

Figure 3.6: Example isochronous curve

data. Modelling the data is not always necessary.

3.8.3 Finite Element Modelling of Corrugated Fibreboard and Corrugated Containers

McDougall (1994) summarised much of the literature available on finite element modelling (FEM) of corrugated fibreboard and corrugated fibreboard cases. McDougall also repeated an experiment performed by Peterson (1983), modelling a cross-machine direction (CD) corrugated beam under three point bending stress.

It was found that modelling corrugated fibreboard beams in three point bending required a large number of elements to account for the shape of the corrugations. It was not practical to model the individual liners and medium of corrugated fibreboard separately to produce a model of a corrugated container using a PC based finite element package because of the number of elements. One possible approach was to treat the corrugated fibreboard as a plate structure with orthotropic properties of the combined board for modelling corrugated container structures. Models employed by other researchers in this area have generally used simplified linear elastic approximations to the behaviour of the paper elements of corrugated fibreboard.

McDougall concluded that, while it is difficult to model corrugated fibreboard and corrugated containers, finite element modelling has the potential to be able to

model corrugated fibreboard and incorporate complex design elements, such as hand and ventilation holes, in corrugated containers. Continued advances in computing power and finite element software would allow a model to be developed which could assist corrugated container designers.

Nordstrand and Hägglund (1997) used isochronous stress strain curves in an anisotropic elastic-plastic material model for use in a finite element model to predict the sagging of the base of corrugated board fruit trays. The model was based on constant 90% relative humidity atmosphere and did not cover moisture transients found in a cycling relative humidity environment. Nordstrand and Hägglund (1997) believed this work could also be used to predict sagging in a cycling relative humidity environment if suitable isochrones could be obtained.

3.9 Summary and Conclusions

Researchers have conducted cyclic relative humidity creep tests of corrugated board with specimens subjected to compression and four point bending stress. Bending creep tests were found to be more sensitive to differences in construction. In this study the differences between corrugated board types were likely to be small so bending creep was chosen to evaluate the samples.

Environmental conditions play a major role in the creep response of paper and corrugated board, with the waveform of cyclic relative humidity possibly influencing the deformation mechanism. Previous researchers felt that a sinusoidal cycling relative humidity at constant temperature probably provided the best test conditions. Conditions for testing are arbitrary, but should be in keeping with cool store conditions. Alternatively the relative humidity should be cycled between 50% and 90% RH.

Researchers have found that simple paper strength tests do not predict cyclic creep performance. However, hygroexpansivity and possibly stiffness measurements are thought to rank specimens in a similar order to cyclic creep performance.

Modelling both static and cyclic relative humidity creep has largely been empirical. The model proposed by Haraldsson et al. (1993) is only applicable to a steady state climate, not a cyclic RH. Although Urbanik's (1995) model was developed using cyclic RH creep data, it is not necessarily applicable to the harsh conditions found in the end use of corrugated containers such as found in cool stores. It was also developed using compression creep data. An advantage of Urbanik's model is the clearly understood parameters.

The Pecht model (1985) appears to work for both static and cyclic relative humidity creep, but has only been tested on tensile creep. The simplicity of this model made it worthwhile investigating.

Analysing bending creep curves was still possible if a suitable model was not developed. The use of stress-strain isochrones could be used to determine creep stiffness as a measure of creep performance. Finite element modelling is a powerful tool but requires considerable expertise and was beyond the scope of the proposed study.

The experiments in this study were based on measuring the bending creep of corrugated fibreboard in a sinusoidally cycled relative humidity ranging from 50% to at least 90% RH. The cycle time and temperature were determined based on limitations of available time and equipment. The following Chapter details the planned experiments and the design and construction of the test equipment.

Chapter 4

Experimental

4.1 Corrugated Fibreboard Samples

Commercial corrugated fibreboard samples were supplied by Carter Holt Harvey Pulp and Paper Limited. The samples were chosen to be similar to those used in export horticultural produce packaging. Samples used in the preliminary experiments were identified as 'R' and 'S'. Corrugated board samples used in the main part of the study were identified as CB1, CB2 and CB3. For commercial reasons full details of the corrugated boards cannot be provided in this thesis.

Test pieces measuring 50 ± 0.5mm wide and 300 ± 20mm long were cut from the samples. Test pieces were cut in both the machine direction and the cross-machine direction. Figures 4.1 and 4.2 show the two orientations.

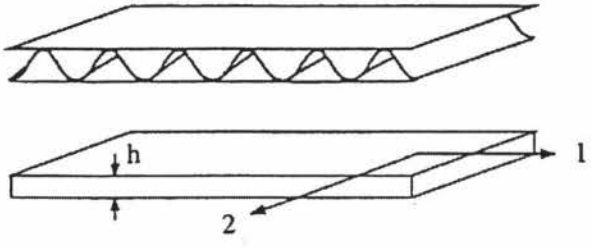

Figure 4.1: Diagram of a MD test piece (Luo et al., 1995) Direction 1 is the MD, 2 is the CD and 'h' is the thickness

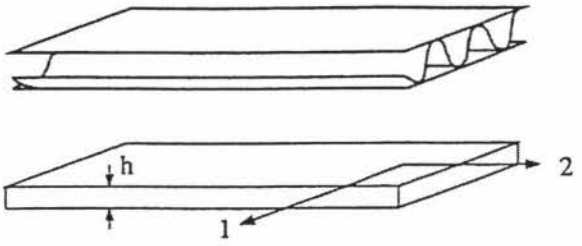

Figure 4.2: Diagram of a CD test piece (Luo et al., 1995)

4.2 Experimental Conditions

4.2.1 Environmental Conditions

An objective of the study was to develop a method to evaluate the performance of corrugated fibreboard in a cycling relative humidity environment. It was decided to cycle the relative humidity between 50 and 90% RH at 23°C consistent with recent international recommendations (Chalmers, 1997) and limitations of the equipment used for this study.

The cycle form was sinusoidal in order to keep the moisture content of the specimens in a non-equilibrium condition and also to have a dynamic rate of moisture change. Assuming the moisture content and cyclic defection followed the form of the relative humidity cycle it would allow analysis of the cyclic response by FFT. The relative humidity cycle period of 12 hours was a compromise between the need to get as many cycles as possible in a short time, while still allowing the corrugated board to react to the changes in relative humidity.

Unless otherwise noted the experimental conditions were 23°C and the relative humidity cycled sinusoidally between 50 and 90% RH over a 12 hour period.

Test specimens were preconditioned by exposing them to cycling relative humidity test conditions without load for at least 4 cycles prior to testing. Other researchers have used this technique to relieve stress in the paper (Söremark et al., 1993; Söremark and Fellers, 1993), although Haslach et al. (1991) did not expose their samples to a cyclic RH, but preconditioned at 30% RH. If the samples are not

stress relieved the hygroexpansion in the first moisture cycle is likely to be different from subsequent cycles (Niskanen et al., 1997; Uesaka et al., 1992).

To avoid uncontrolled moisture extremes the samples were stored at 23°C / 50% RH until tested.

4.2.2 Load

Loads used were chosen to give a broad range of creep responses. Unlike compression or tensile testing there is no clear breaking load or other end point to bending tests. It was not possible to set the load as a proportion of the ultimate load as is frequently done in compression or tension creep tests.

Samples were put in the load frames (Figure 4.3) and placed on the stationery supports on the creep test apparatus.

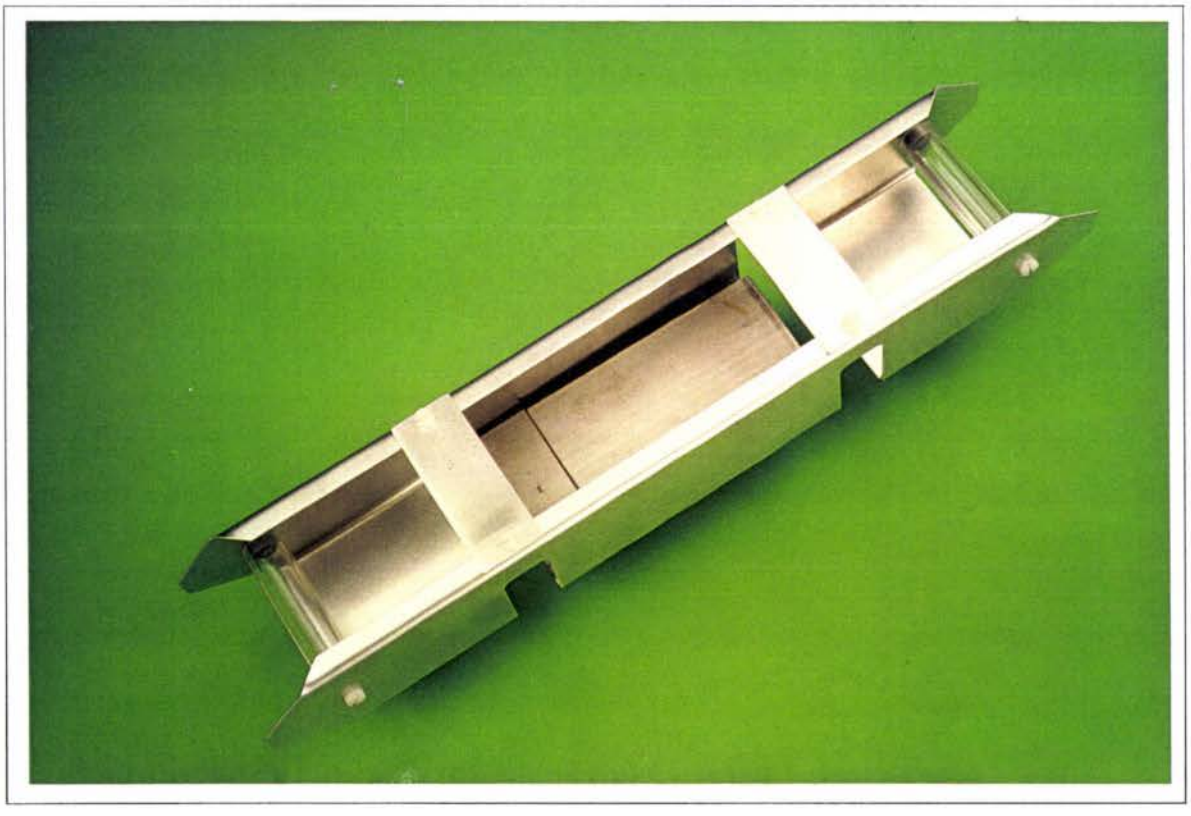

Figure 4.3: Corrugated board specimen load frame

Measurements were started about 3 minutes after loading. This delay removed

initial (elastic) strain from the measurements, leaving only strain from creep and hygroexpansion to be measured during the experiment. This practice is similar to that used by Haslach, Pecht and Wu (1991). Each aluminium load frame weighed approximately 74g. Stainless steel weights were added to obtain the desired load.

4.3 Experimental Design

Up to six specimens were tested during each experiment. Replication allowed testing of either two or three samples, with 3 or 2 replicates respectively, in each experiment. Previous experience with other environmental chambers gave reason to suspect there may be relative humidity and temperature gradients within the test space of the cabinet. Experiments were therefore blocked from front to back on the creep test apparatus to account for possible variations in the relative humidity within the environmental cabinet. Test pieces were therefore grouped to minimise any influence of the position of the test pieces within the cabinet. Sample positions were identified by their order from the back of the environmental cabinet; position 1 was closest to the back of the cabinet, and position 13 closest to the door. Positions 1, 2, 3, 11, 12 and 13 were occupied by specimens for testing. Positions 4 to 10 were occupied by a calibration block to provide reference measurements during the experiment. A typical experiment to test double treatment samples using a single bending stress with replication may look like Table 4.1.

Details of the specimens used in each experiment are given in Sections 5.3.1 and 6.2 of Chapters 5 and 6 respectively.

Preliminary experiments were performed to determine the the effect of experimental variables. These were specimen orientation, load and cyclic versus constant relative humidity environments. Using data from these experiments different models were investigated. The main experiments were then performed on samples *CB1*, *CB2* and *CB3*.

The main experiments were five experiments to measure the cyclic relative hu-

ht

Table 4.1: Sample experimental design

Corrugated fibreboard samples							
Position:	1	2	3	4 - 10	11	12	13
Run (1)	CB1	CB2	CB3	Calibration Block	CB1	CB2	CB3
Run (2)	CB3	CB2	CB1	Calibration Block	CB3	CB2	CB1

midity creep performance under four load conditions to generate isometric and isochronous creep curves. Two constant relative humidity experiments were conducted as indicators of the relative magnitude of the detrimental effect of cyclic relative humidity on creep performance.

One experiment was planned to test the hypothesis that a lower top relative hummidity (80% cf. 90%) would reduce the cyclic and long term creep deflection.

4.4 Data Analysis

4.4.1 Curve Fitting

Calibrated deflection data were copied from Microsoft Excel into Microcal Origin for non-linear model fitting using the Levenberg-Marquardt algorithm. If the data were not smooth enough to allow reliable data analysis it was smoothed by 5 point moving mean. A smoothing routine using waveform analysis was still being developed.

4.4.2 Statistical Analysis

Data from the isochrones were analyed using the General Linear Model in SAS. The isochrones were analysed by treating the deflection as a continuous variable to represent the creep modulus. Deflection was treated as a class variable when analysing the variance of the isochronous data.

4.5 Equipment

The extended testing time of creep tests necessitated using an automated data logging system to record the experimental data. All 6 test pieces of corrugated fibreboard were measured during each experiment using one transducer moved on guides from test piece to test piece while recording the position and the displacement. This had a significant influence on the design of the data collection system. The displacement and environmental data collected had to be coordinated with the position of the displacement transducer. An advantage of using one transducer was that any drift over time affected all test pieces equally and was readily compensated by calibrating the measurement on each measurement cycle. Figure 4.4 shows the creep test apparatus with six specimens in the load frames.

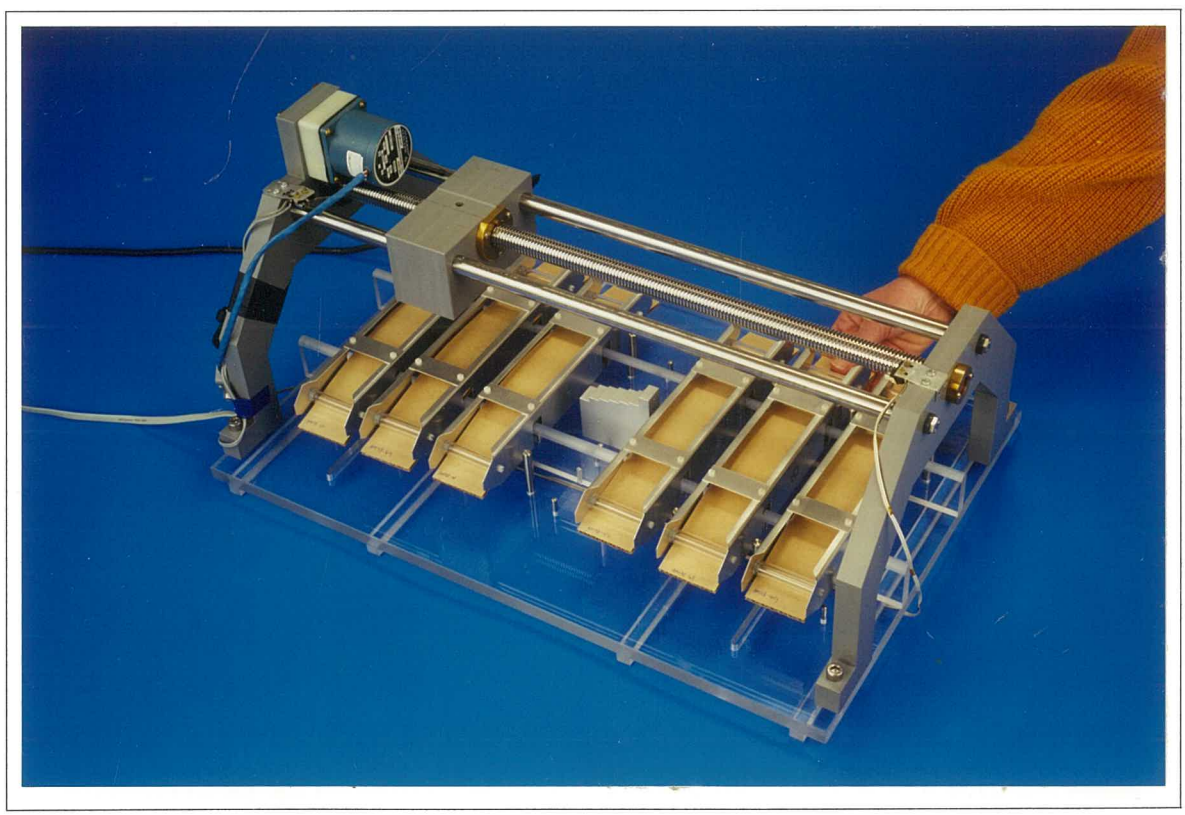

Figure 4.4: Four point bending creep apparatus

The design was based on the equipment described by Gunderson and Laufenberg

(1994). The load frames (Figure 4.3) were made from 0.7mm aluminium plate and had low friction rollers where they contacted the test specimens. The rollers were spaced 230mm apart. The stationery supports on the creep tester base plate were 12mm acrylic plate centred 114mm apart and had a 6mm radius where they contacted the test specimens.

The displacement transducer was mounted in a sealed PVC block to protect it from the high humidity. The PVC block was mounted on two guide rods and an acme thread transport screw in between. The screw was turned by a stepper motor at one end of the apparatus. The combination of stepper motor resolution and acme thread gave a positioning resolution of 0.015mm. Also shown in Figure 4.4 is the seven level aluminium calibration block situated in the middle of the base plate between two sets of three load frames.

The bending creep measurement apparatus was placed inside a Thermoline environmental cabinet which cycled the relative humidity at constant temperature. Figure 4.5 shows the creep apparatus positioned in the Thermoline environmental cabinet.

4.5.1 Measurements Required

The measured response of the corrugated board to the four point bending stress and environment was the deflection at the centre of the test piece. Measuring the deflection over time gave the creep response. Load, relative humidity, temperature, specimen moisture content and time were recorded as these affect the creep response.

4.5.2 Selection of Displacement Transducer

A requirement for all measurements was that they did not interfere with the experimental system. Displacement is often measured through the movement of a sensor such as the core of a linear variable differential transformer (LVDT) or the legs of an extensometer, but these methods can impart a measurement induced displace-

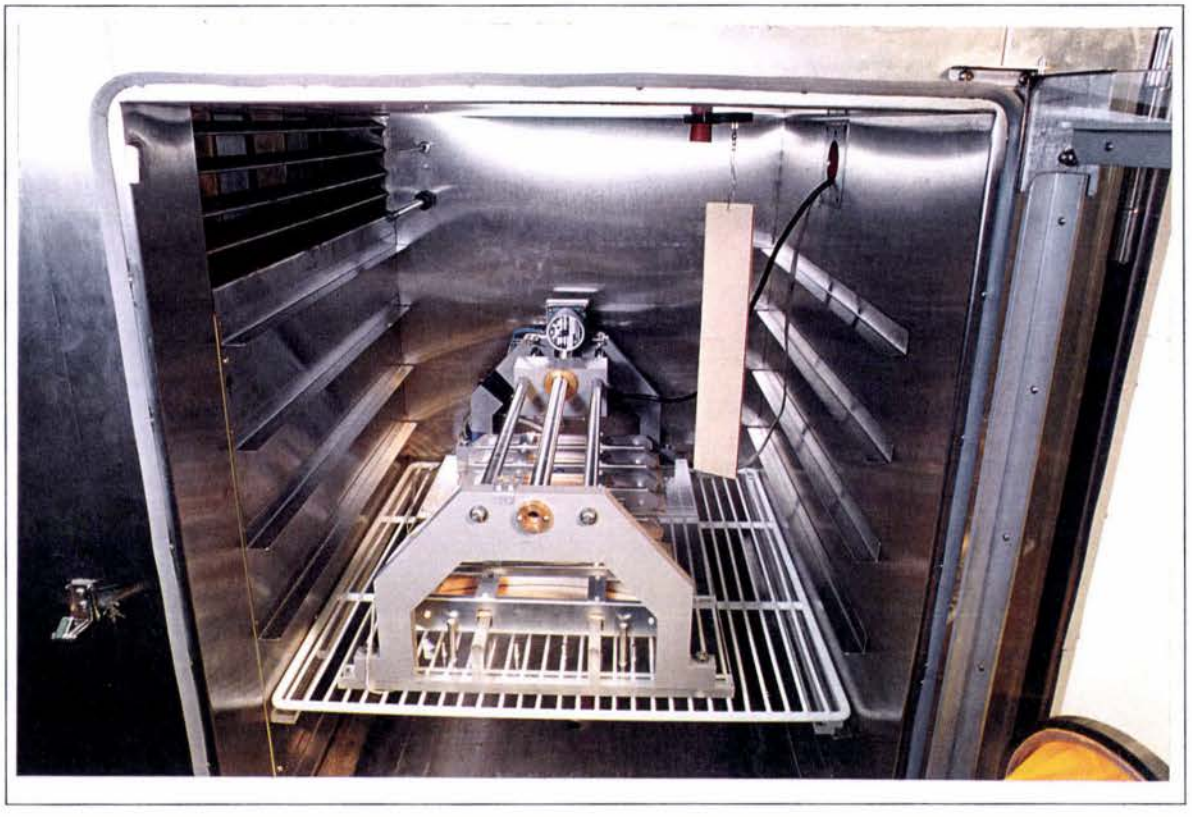

Figure 4.5: Bending creep apparatus in the Thermoline environmental cabinet

ment error. The solution is to use a non-contact transducer, using methods such as magnetic induction or laser. As it was necessary to measure corrugated fibreboard directly, its poor magnetic properties would not provide a suitable target for an inductance type sensor. Laser displacement transducers (LDT) do not suffer from this problem. However they can be sensitive to temperature and moisture changes. The measurement range and resolution of LDTs is very wide. In this experiment the measurement range was up to 10mm, but the transducer had to be at least 30mm from the test piece in order to clear the load frames as it was moved. Resolution of 0.05mm or better was required, as some of the creep responses were expected to be as small as 1mm deflection. The "Koden" LDT chosen met these requirements (Table 4.2) as well as being small enough to seal in a housing to protect it from high humidity. Experiments were conducted at constant temperature so there were no significant temperature induced errors.

Table 4.2: Laser displacement transducer specifications

Range	90±40mm
Resolution	0.05mm
Linearity	0.06% FS

4.5.3 Relative Humidity Measurement

The most significant variable in this project was the relative humidity of the atmosphere surrounding the specimens. Relative humidity is difficult to measure accurately, especially at high levels ($> 90\%$) and low temperature ($< 5°C$). An error of 1% below 90% RH is acceptable, but realistically 2% accuracy above 90% RH is all that can be guaranteed with present technology. The relative humidity sensor needed to have a response time of less than 15 seconds in order to pick up any transient spikes in relative humidity.

Experience has shown wet and dry bulb psychrometers to be the most reliable but due to their size and the limited space available in the environmental cabinet they were not practical. Chilled mirror devices, which are accurate and rely on measuring temperature to determine the relative humidity were also not suitable because of their slow measurement cycle times and high cost.

Instead, a capacitive sensor met most of the requirements. Response time was typically 10 seconds or less with acceptable accuracy. The Thermoline Environmental cabinet was therefore equipped with a Vaisala combination relative humidity (capacitive type) and temperature probe for control purposes. The temperature sensor was a Pt100 platinum resistance thermometer. The signals from the Vaisala sensor were used by a Eurotherm PID controller to control the relative humidity and temperature inside the Thermoline cabinet. The Eurotherm had the capability to communicate with a PC via an RS-232 serial port and transmit the measured temperature and relative humidity from the Vaisala sensor. The ability to get accurate temperature and relative humidity measurements from the controller meant

that it was not necessary to purchase an additional sensor. The manufacturers specifications for the sensor were ±2% up to 90% RH and ±3% above 90% RH.

4.5.4 Humidity Sensor Calibration

Calibration of relative humidity sensors is difficult. Temperature based sensors can be accurately calibrated, but verification in a known relative humidity atmosphere is difficult to conduct. Most relative humidity sensor types require a known relative humidity atmosphere for calibration and use saturated salt solutions to generate the relative humidity.

The location of the Thermoline Vaisala relative humidity sensor made salt solutions difficult to use. Instead a portable Vaisala sensorwas purchased for the sole purpose of providing a reference device for all of the relative humidity probes in PAPRO. This device was calibrated by Industrial Research Limited using a technique to generate precise relative humidities.

The Thermoline cabinet RH sensor was compared with the reference probe at about 2 monthly intervals. The Thermoline sensor was found to be within 1% at 90% RH and approximately 2% RH low when reading 50% RH.

The long term drift of the reference probe was checked at 50% RH in the PAPRO paper testing laboratory kept at 23±°C and 50 ± 2% RH which is monitored by a calibrated wet and dry bulb Pt100 psychrometer. Less than 1% RH drift was found during the course of the experiments.

4.5.5 Temperature Measurement

Temperature was measured using the Pt 100 sensor in the Vaisala combination relative humidity / temperature probe. The accuracy of this sensor over the range of -20 to 80°C was specified as ±0.2°C.

4.5.6 Time Measurement

An advantage of using a PC based data logging system was the availability of the computer system time clock. An alternative was to purchase a dedicated timer card for the data logging PC if the system clock was not accurate enough but time drift was less than 1 minute per week (0.01%) and was considered acceptable.

4.5.7 Moisture Content Measurement

A balance was used to measure the weight of a piece of corrugated board suspended in the Thermoline environmental cabinet to determine its moisture content. After the experiment was finished the test piece was oven dried at 105°C and weighed, allowing the moisture content to be calculated throughout the experiment. The moisture content of the creep test specimens were inferred by the moisture content of the test piece suspended from the balance. This technique has been used by others (Uesaka et al., 1992; Niskanen et al., 1997).

4.5.8 Data Logging System Hardware

A PC data logging system was chosen for its flexibility in terms of connecting inputs and outputs (I/O) and in also for the ability to modify the system if required.

4.5.8.1 Analogue Inputs and Digital I/O

With a number of signal sources and types it was important to make the signal conditioning and analogue to digital conversion (ADC) as flexible and robust as possible. Previous experience had shown the long term benefits of separating the signal conditioning from the ADC PC board. Although the initial cost was higher the flexibility and electrical isolation justified the additional expense.

The National Instruments 12 bit ADC board had 16 single ended analogue voltage input channels which could be re-configured to 8 differential inputs if there was too much noise in the signal. Sampling speed in this experiment was very slow which

meant this was not a significant factor in the choice of ADC board. Data acquisition card specifications are listed in Appendix A.

Initially it was thought there would be voltage and current inputs and digital I/O. Using hardware signal conditioning blocks on a PCB backplane reduced interconnection difficulties by providing linearising circuitry and conversion of 4-20mA current loop input to voltage. The conditioning blocks provided the correct input impedance to match the transducers. In addition to this the output impedance matched the input impedance of the ADC board. This avoided the need for custom built circuitry. Connecting new signal sources into the data acquisition system required no specialist electronics knowledge.

Each channel on the I/O backplane could be connected to a different source type, giving great flexibility. Programming the data logging PC was simplified as each signal conditioning block output $\pm$5V to the ADC at full scale input. This meant that each ADC channel was set to the same gain to get the greatest sensitivity and minimise settling times when different channels were sampled.

In the original data acquisition design it was planned to monitor relative humidity and temperature using a combination sensor with 4-20mA outputs for each and either a voltage or current input for the displacement transducer. However, interrogating the Thermoline controller for relative humidity and temperature data via a serial data link eliminated the need for a second sensor and conditioning modules. The only analogue input was the LDT, with a range of $\pm$4V. The characteristics of the conditioning module are given in Appendix A.

Digital input modules were installed to allow monitoring of mains voltage air and water heaters and the refrigeration solenoid on the Thermoline cabinet. A digital output module from the data acquisition system was installed to switch a relay in the Thermoline to stop the circulating fans just before readings were taken from the balance used to measure moisture content of the separate sample. This stopped the specimen from being blown around and gave a more accurate weight measurement.

4.5.8.2 Serial Data Communication

Four serial (Com) ports were used to control equipment during experiments:-

1. The stepper motor used to move the LDT carriage was controlled via a serial interface.

2. The PC set the relative humidity setpoint and logged the actual temperature and relative humidity from the Eurotherm 900EPC PID controller on the Thermoline environmental cabinet.

3. The data logging PC communicated with a Mettler PM3600 balance via an RS-232 serial interface to record the weight of an unloaded test piece suspended in the test environment from the balance to monitor the moisture content of the test piece.

4. An external modem was connected to the PC to dial a pager to alert the operator when an alarm condition existed.

Figure 4.6 shows an overview of the data acquisition and control system.

4.5.9 Data Logging Software

4.5.9.1 Language Attributes

There were several factors which the data acquisition software required in order to be effective. These were:

- PC based
- Capable of RS-232 Serial communication
- Operate under Microsoft Windows
- Flexible
- Easy to learn
- Good support
- Industry standard

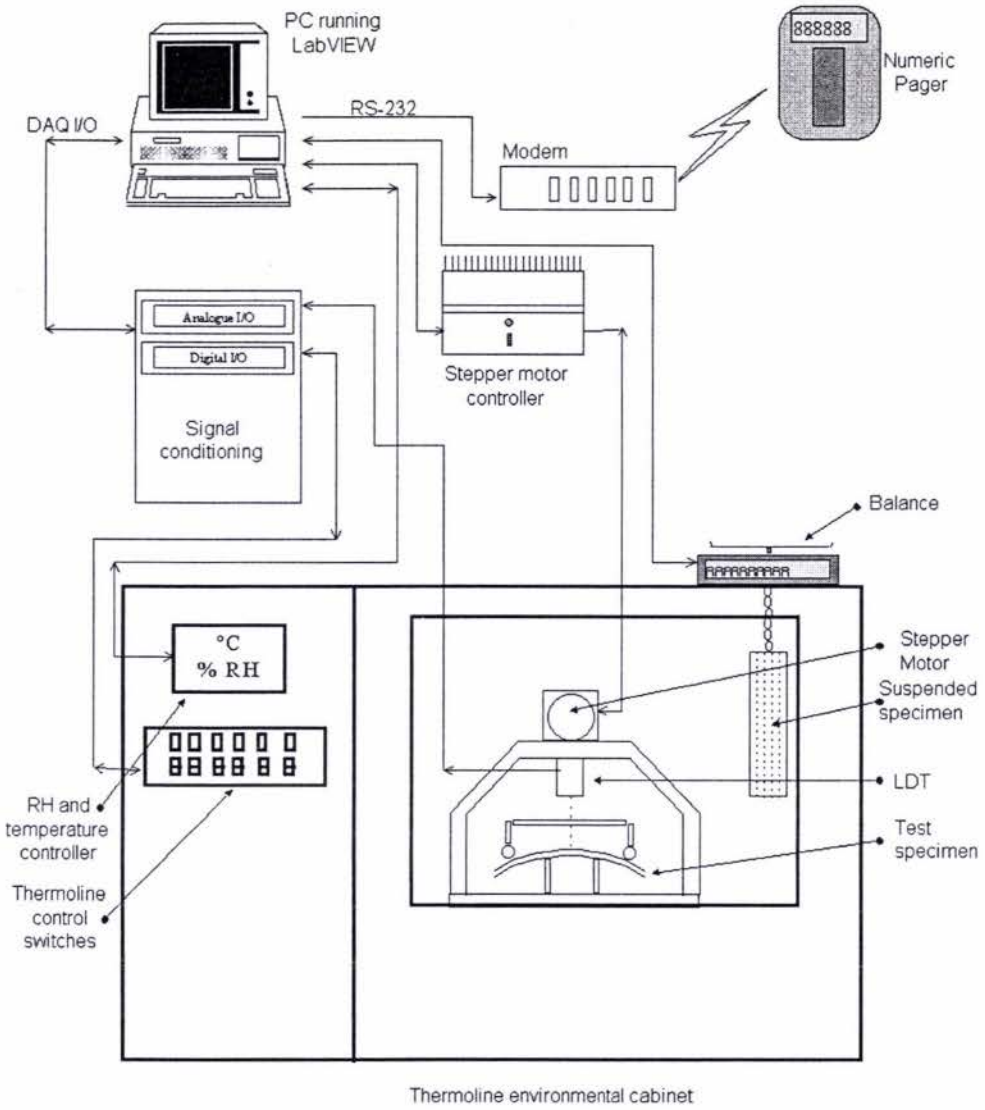

Figure 4.6: Data Acquisition Hardware Overview

Newer data acquisition and control languages are graphics based, using icons to describe functions. They can be powerful while relatively easy to learn, thereby minimising the time before a system can be operating.

The data acquisition program is the operator interface for the instrument so must be both informative and easy to use. A list of attributes for both the interface and the functionality was developed. The programme had to allow:

- Changing of hardware settings for each test,
- Comments to be logged at the beginning and during the test,

- Real-time graphing of data, re-scalable during an experiment,
- Secure logging of data in case of power failure,
- Data to be saved in a format which could be imported by analysis software.

LabVIEW was selected as the best option to meet these requirements. LabVIEW is programmed by 'wiring' functional icons together. The icons are termed 'Virtual Instruments' or VI's. A program was written in LabVIEW to achieve the attributes listed previously.

4.6 Creep Tester Program

4.6.1 Program Initialisation

The operator had to set the following fields prior to starting a test;

- Sample and test description,
- LDT measurement positions (mm from motor end *home* position),
- Pager activation checkbox,
- Environmental conditions error limits,
- Time delay (if any) between measurement cycles,
- Balance Com port/activation selectors,
- Thermoline fan control,
- Time between balance readings,
- Check box to record data file.

4.6.2 Program Operation

This section describes the operation of the creep apparatus program. Operating the test apparatus is described in Section 4.8. The program block diagram is shown in Appendix B.

If the check-box on the screen was selected to record data, a file name for the data was requested. When a file name was entered the file was opened and the data headers, test conditions, any comments and the program file name were recorded. The data file was then closed.

The LDT carriage was moved forward about 5mm before returning to a home position set by a limit switch. The stepper motor position counter was zeroed at this physical reference. The carriage returned to this mechanical position rather than an electrical zero position determined from the motor controller. This method ensured that false readings could not be taken if there was a communications glitch or if the LDT carriage jammed and the motor slipped because a new test measurement cycle could not begin until the limit switch had been set.

A voltage reading was then taken from the LDT and stored in the first position of a one dimensional data array. This voltage was proportional to the distance from the LDT to the first specimen. The PC then instructed the stepper motor to move the number of steps corresponding to the distance to the next test piece. The carriage halted while the ADC measured the voltage representing the second specimen deflection and stored the reading in the next position of the data array. This process was repeated until readings were taken from all of the test pieces and seven levels of the calibration block.

If a balance reading was to be recorded a digital output from the ADC was activated to stop the Thermoline circulating fans for 10 seconds prior to recording the balance reading. The fans were switched on immediately after the weight was recorded. The decision to record a weight was determined from the initial settings of the balance recording frequency and the elapsed testing time i.e.: if the time since the last balance reading was equal to or had exceeded the set time a recording was made.

Relative humidity, temperature and control data were read from the Thermoline's Eurotherm controller and added to the data array after the last LDT reading was stored. Any operator comments were appended to the data array before a time stamp was added.

At the end of each measurement cycle the data was stored on the PC hard disk in a tab delimited ASCII file. The data file was opened, the data array appended

to the data file and the data file closed. Minimising the length of time the data file was open reduced the likelihood of data loss due to PC hardware problems. The stepper motor returned to the mechanical micro-switch home position ready to start the next measurement cycle.

Measurements were made when the LDT carriage was moving in one direction only to minimise positional errors from drive train backlash and free play (a significant amount of free play was allowed in the drive train to compensate for different thermal expansion rates among the plastics and metals used in the construction of the apparatus, but this procedure avoided the potential problem).

Data from the LDT and the Eurotherm was also stored in a circular (first in first out) buffer in memory for plotting on the screen. This allowed monitoring of creep and Thermoline cabinet variables during the experiment. Depending on the sample rate, data from the previous 72 hours or more could be plotted on the screen.

An error checking loop was programmed to monitor the environmental conditions and the state of the stepper motor. If the environmental conditions exceeded the maximum error level from the set point on two consecutive measurement cycles or the stepper motor had not returned to the mechanical home position within 5 minutes an alarm panel appeared on the screen. If the Pager check box was selected a modem dialled a pager and sent a numeric message to alert the operator. A stepper motor delay may be caused by mechanical failure of the carriage mechanism or data loss from the serial interface. The system attempted to re-initialise the stepper motor controller before it entered an alarm condition. Two consecutive temperature or relative humidity readings outside the allowable limits were required to activate the alarm to eliminate false alarms from one off spikes or communication errors.

4.7 Cyclic Relative Humidity Profile Control

A separate program was written to control the relative humidity set point. This program ran concurrently with the creep apparatus program. The operator chose

between a sinusoidal or square wave RH profile, set the magnitude and amplitude, and the cycle period.

The programme calculated the RH set point every minute and updated the Eurotherm's set point. Changing the set point every minute gave a smooth sinusoidal RH profile. The operator interface and block diagram is shown in Appendix B.

4.8 System Operation

4.8.1 Sample Setup

Prior to running an experiment the operator positioned the test pieces and set up the creep apparatus and RH profile programs.

Test pieces were placed into the load frames with the doublebacker facing up so it would form the outer surface (i.e. in tension). Each load frame was then placed over the static supports such that the test piece was at a right angle to the static supports and in the centre of the load frame, and the load frame was not touching the static supports.

If sample moisture content was to be determined a test piece was suspended from the balance after taring the weight of the chain. The ability to monitor moisture content was added to the test system in the later part of the study.

4.8.2 PC Operation

The operating screen shown in Figure 4.7 shows the set up inputs on the left of the screen. These fields were set before starting a test. The *Test Description* text was stored in a data file header. The *mm for test piece* set the LDT movement distance in millimetres from the mechanical home position for each reading.

The *Pager* check box selected the pager in the case of environmental or stepper motor errors. The allowable error range for relative humidity and temperature was normally set to $\pm 3\%$ and $0.5°C$. The *Save data* check box selected the recording of data. The *Time delay* switch activated a delay between the end of one measurement

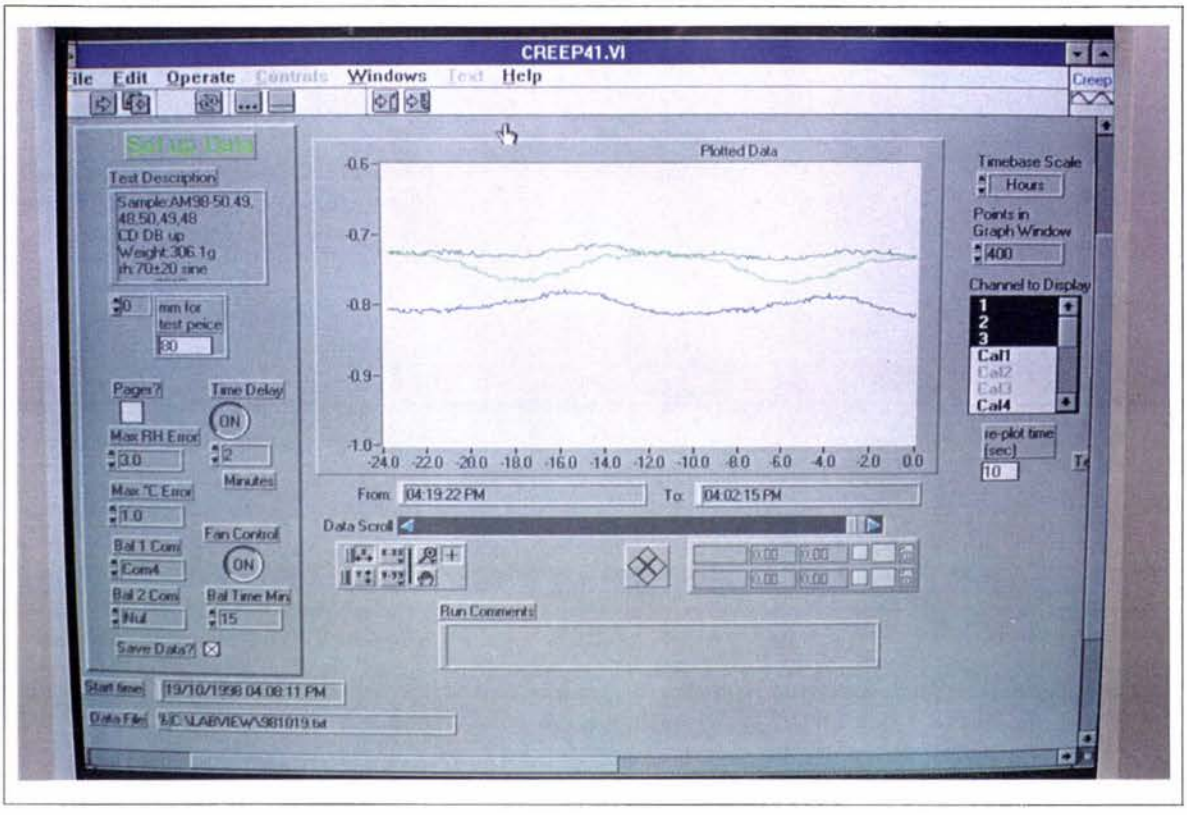

Figure 4.7: Creep System Operating Screen

cycle and the beginning of the next. The length of the delay was usually 2 minutes.

The balance(s) to be read and the corresponding serial port were selected prior to starting the test. Only one balance on Com 4 could be logged in this study. The *Fan Control* switch activated the fan control loop for switching the Thermoline fans off 10 seconds prior to and during a balance reading. The *Bal Time Min* dialog box set the approximate time between balance readings. Balance readings were not taken as often as deflection readings because stopping the fans every 3 minutes would have interfered with the relative humidity and temperature control and possibly damage the fan motors.

The ability to run the program without saving the data was included so that data did not have to be recorded during calibration or test runs. The program was started by selecting Run from the Operate menu.

The front panel *Comments* dialogue box allowed comments to be stored during

the experiment. These comments were stored in the data file next to the relevant time stamp. When the data was analysed comments could provide valuable reminders for otherwise unexplainable data (e.g. if the cabinet door was opened during an experiment causing a spike in the temperature and relative humidity).

Data to be graphed was selected from the *Channel to display* list on the right side of the graph. Multiple signals were be plotted by holding the <shift> key and selecting the channels to be plotted. The time scale was adjusted by selecting the number of points to graph. This is shown at the bottom of the graph. The sliding scale beneath the graph moved the time for data to be read from the circular buffer. The y axis scale was changed by double clicking either the top or bottom number and setting a new number. Data could also be copied onto a floppy disk for viewing or analysing on another PC during an experiment by copying the data file using Window's File Manager.

The test was stopped by clicking on the *STOP* button. The program finished the current cycle before it stopped operating.

4.9 Data File Handling

Data were saved in a tab delimited ASCII text file. This allowed the data to be imported into software such as Excel, Origin and SAS for data analysis and plotting.

4.9.1 Calibration

Data were imported into Microsoft Excel where the voltage measurements from the LDT were transformed to millimetres of deflection. Deflection was calculated by fitting the known measurements from the calibration block to the measured voltages by least squares linear regression. The slope and intercept from the regression was used to calculate the distance from the LDT to the specimen. This procedure was done for each measurement cycle. The deflection recorded in the first measurement of each test piece was subtracted from each subsequent measurement to calculate

the change in deflection for each time period i.e. creep.

$$\text{Deflection} = (V_t \times m_t + c_t) - (V_0 \times m_0 + c_0) \tag{4.1}$$

V_t	Measured voltage at time t
m_t	Slope of calibration block regression at time t
c_t	Offset of calibration block regression at time t
V_0	Measured voltage at time = 0
m_0	Slope of calibration block regression at time = 0
c_0	Offset of calibration block regression at time = 0

Chapter 5

Preliminary Experiments to Verify Creep Apparatus, Characterise Corrugated Fibreboard Bending Creep and Develop Model

5.1 Introduction

Initial experiments were conducted to check the reliability and calibration of the creep apparatus, to measure the effects of corrugated board orientation and conditioning, and thirdly to choose a model to describe the creep data.

The preliminary experiments used corrugated board identified as 'R' and 'S' to obtain creep curves for the evaluation of creep models. The samples used in the main experiments were not available at the begining of the study, and although they were different to the samples used in the preliminary tests, the main trends were expected to be the same for all types of corrugated board.

5.2 Instrumentation Verification

5.2.1 Plastic Hygrostability

Some plastic materials absorb small amounts of moisture from the atmosphere and are not dimensionally stable when the surrounding relative humidity changes. It was possible that the plastic components of the creep apparatus would move during

relative humidity cycling.

The frame from which the laser distance transducer was suspended and the housing for the transducer were fabricated from PVC plastic. Acrylic plastic was used to make the base plate and the stationery sample supports. PVC is slightly hygroscopic and it was thought it may exhibit hygroexpansion as a result. No hygrostability data was found for the plastics, so to eliminate this as a source of error it was decided to measure the hygrostability of the plastics in the Vacuum Compression Apparatus (VCA). The VCA can control the relative humidity in a small chamber and has three extensometers to measure in-plane strain while relative humidity is changed.

Samples of PVC and acrylic were roughened to provide a non-slip surface for extensometers to be placed on. The third extensometer was locked with a pin to stop it moving so that any transducer drift associated with changing relative humidity could be measured. The samples were then put in the VCA, the extensometers placed on the samples the relative humidity cycled from approximately 30% to 95% RH over a 500 minute period in the form of a square wave. The VCA logged relative humidity, temperature and the 3 strain gauges at approximately 41 second intervals over 54 hours. The results are plotted in Figure 5.1.

Figure 5.1 shows the changing atmosphere conditions, temperature and relative humidity, and the strain responses. There was a large amount of noise in the initial part of the experiment, however, the data in the later stages was quite clean. The pinned extensometer showed little movement. Thus, strain measured for the samples was not affected by extensometer stability.

The strain measured on the two plastic samples showed changes when the atmosphere was changed from one condition to the other. The grey PVC moved approximately 0.0002 mm/mm, and the clear plastic moved about 0.0006 mm/mm. The temperature of the VCA changed by about 1.2°C while controlling the relative humidity. According to data from the plastic supplier the coefficient of thermal

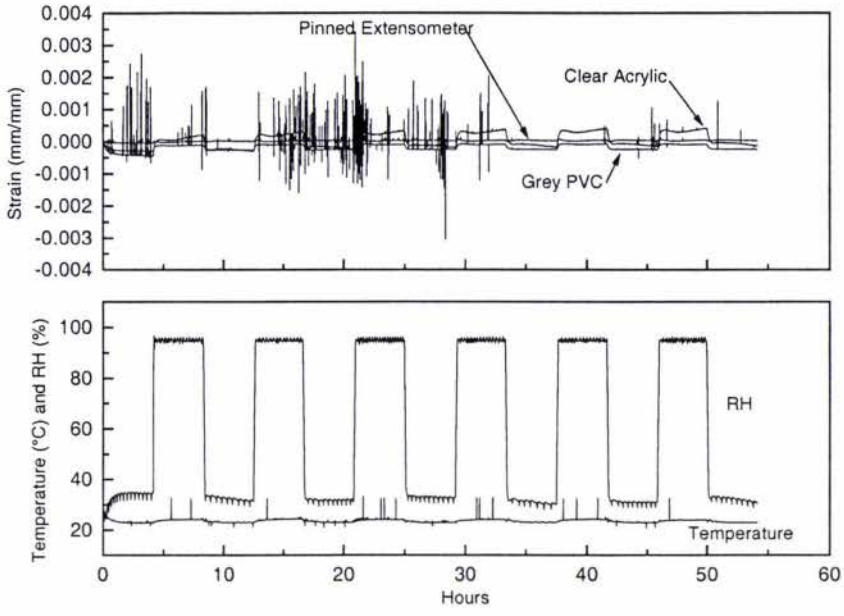

Figure 5.1: Hygrostability of creep apparatus plastic components

expansion of PVC was up to $18.5 \times 10^{-5}/°C$, depending on the formulation, giving a strain of up to 0.00022 mm/mm. It is therefore likely that the strain was due to thermal expansion rather than hygroexpansion. As a comparison, the coefficient of expansion for aluminium is $2.5 \times 10^{-5}/°C$. The strain response of the PVC was very rapid, and appeared to be too rapid for it to be moisture related, given that the water vapour transmission rate of PVC is very low.

Although not measured in this experiment, the hygroexpansivity of linerboard is of the order of 0.007 mm/mm (Chalmers, 1994a) under similar conditions. Therefore if the strain observed was entirely from the change in relative humidity, PVC is still about 30 times more stable than the paper products being measured. The temperature stability of the Thermoline cabinet environment was better than 1.2°C, and was typically ±0.2°C, minimising thermal expansion of the test rig components. With this in mind it was considered that any effect of moisture on the PVC components of the creep apparatus would not influence the measurement of corrugated fibreboard.

The movement of the acrylic sample was greater than that of the PVC sample. Manufacturer's data showed the coefficient of thermal expansion for acrylic plastic to be $5.9 \times 10^{-5}/°C$, so the strain measurements would have been expected to be smaller than that of the PVC. The sample tested was about 2mm thick, compared to 12mm for the creep apparatus. It is expected that if the measured strain was largely due to moisture swelling it would be smaller for the thicker material used to make the creep apparatus.

5.2.2 Laser Displacement Calibration

The laser displacement transducer output was checked for linearity prior to commencing creep testing. The slope of the response was more important than the intercept as the offset was subtracted during data analysis. The calibration results in Figure 5.2 showed that the LDT provided a linear output.

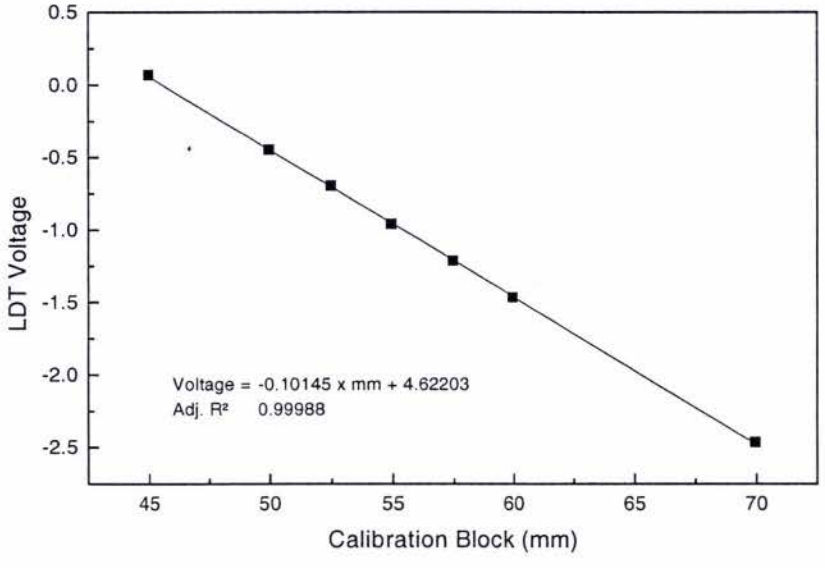

Figure 5.2: Laser displacement transducer calibration

5.2.3 Laser Displacement Transducer Stability

Although any lack of stability of the laser displacement transducer was accounted for in the data processing using the calibration block, it was decided to determine if the transducer was affected by relative humidity. LabVIEW was programmed to record LDT measurements from a stationary target while the relative humidity was cycled from 50 to 90% RH for a period of three 6 hour cycles.

Two hermetically sealed Schaevitz LVDTs were mounted in the Thermoline cabinet to provide reference measurements. One LVDT was mounted in a clamp on a steel retort stand as a stable reference. The other LVDT was mounted on the creep tester next to the LDT. This provided a reference in case the plastic frame of the creep tester moved with the changing relative humidity. Figure 5.3 shows the logged measurements. There was no movement recorded from the LVDT mounted on the

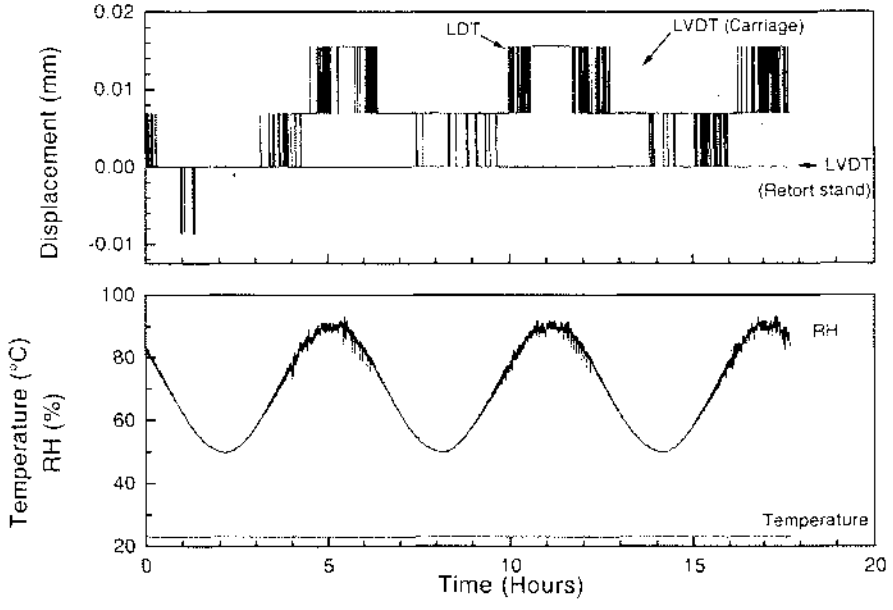

Figure 5.3: Transducer RH stability

retort stand. The other LVDT, mounted next to the LDT showed a small amount movement, but at the limit of detection of the data acquisition system. The laser displacement sensor was less stable, exhibiting a small cyclic deviation (< 0.03mm).

This small amount of deviation was only just detectable and was readily compensated for by the calibration measurements carried out during testing.

5.3 Characterisation of corrugated fibreboard bending creep

5.3.1 Experimental

Five experiments were conducted using the methods described in Chapter 4. The experimental conditions are tabulated in Table 5.1. Each experiment is identified by a 5 digit code which corresponds to an in-house labeling system. 'R' and 'S' specimens were arranged in an alternating series in the tester.

Experiments 71114 and 80218 were run to test the ability of the Pecht model to fit both short and longer term creep curves. Experiment 71205 was run under the same conditions except that the load was increased to 260g to determine the effect of increasing the load. Experiment 80629 was run to compare the effects of static (90%) relative humidity and cyclic (50-90%) relative humidity on creep deflection.

To determine if orientation had a significant effect on creep experiment 80311 was run with test pieces cut in the machine direction, however 167g was insufficient load to get reliable readings. The load was increased to 306g and the experiment was repeated (80403).

Table 5.1: Conditions for preliminary creep experiments

Experiment	Conditioning RH	Experiment time	RH	Load (g)	Orientation
71114	50%	5 days	$70 \pm 20\%$	167	CD
80218	50%	21 days	$70 \pm 20\%$	167	CD
80311	50%	16 days	$70 \pm 20\%$	167	MD
80403	50%	6 days	$70 \pm 20\%$	306	MD
71205	50%	3.5 days	$70 \pm 20\%$	260	CD
80629	50 and 90%	3 days	90%	167	CD

5.3.2 Results and Discussion of Preliminary Trials

5.3.2.1 Typical data set

A typical result is shown in Figure 5.4, which shows the deflection versus time curve with the measured relative humidity shown below. The recorded deformation

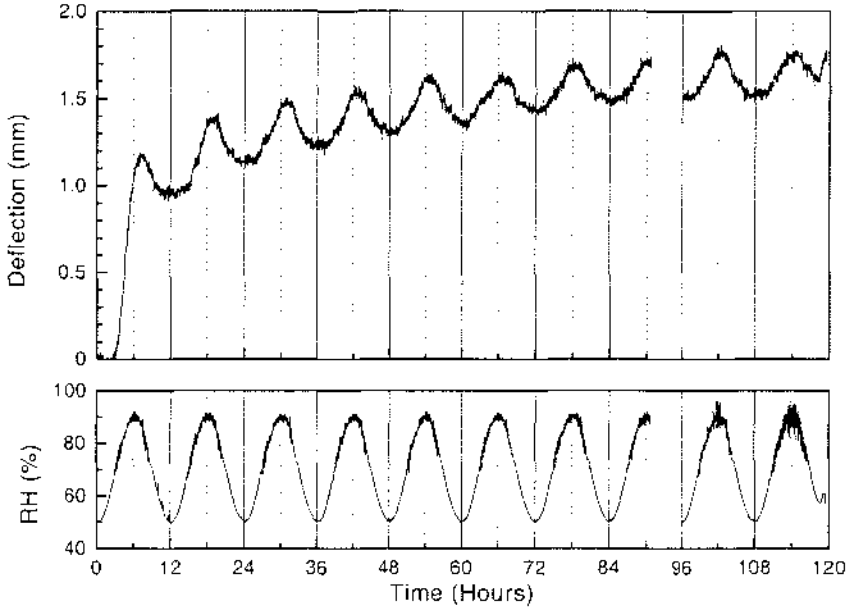

Figure 5.4: Typical creep deflection curve from experiment 71114 ('S'1)

followed a sinusoidal pattern, increasing as the relative humidity increased, and partially, but not totally, recovering as the humidity fell. There was a small time delay between the peak values of relative humidity and deformation which will be discussed in detail in Chapter 7. The cyclic deflection was opposite in direction to that reported by Söremark and Fellers (1993), but the same as reported by Laufenberg (1991). This will also be discussed in more detail in Chapter 7. The overall shape of the curves for both types of corrugated board were similar. All of the individual creep curves are shown in Appendix C.

The curves for some experiments have a gap in the data where the stepper motor moving the LDT jammed. This resulted in the loss of some measurement data but it did not affect the experimental conditions.

5.3.2.2 Effect of specimen orientation on bending creep

Averaged creep curves from experiments 71114 and 80403 are shown in Figure 5.5. The creep curves were sufficient to show that the CD orientation deflects more than

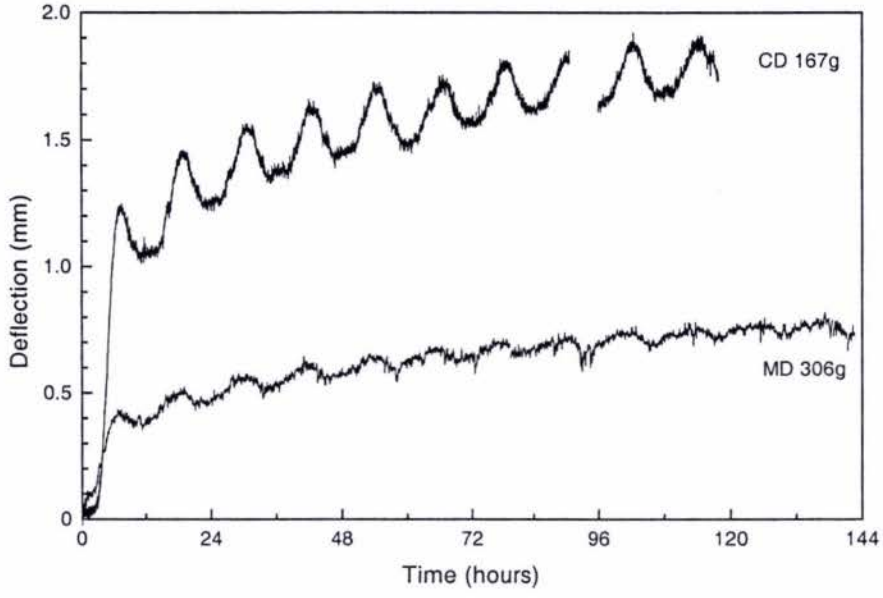

Figure 5.5: Effect of corrugated fibreboard orientation on creep response (averaged creep curves)

the MD. The cyclic response was noticeably lower for the MD specimen. Lower creep deflection and smaller cyclic response for MD specimens was not surprising as linerboard is stiffer and has lower hygroexpansivity in the machine direction. In terms of how direction relates to corrugated case performance it shows that in terms of creep, like compression strength, corrugated fibreboard is weaker in the cross machine direction.

No further experiments were done or analysis attempted, as the result confirmed the expected result. All subsequent creep tests were done in the CD direction, with the doublebacker forming the outer part of the bend.

5.3.2.3 Effect of load on corrugated fibreboard bending creep

It was expected that increasing the load would increase the initial deflection and increase the rate of creep. Data from experiments 71114 and 71205 using 167g and 260g loads on CD oriented specimens were conducted to check this. The conditions for the experiments are shown in Table 5.1.

Typical results in Figure 5.6 clearly show that increasing the load or bending moment increased the initial deflection during the first cycle and increased the rate of creep. The other creep curves are shown in Appendix C.

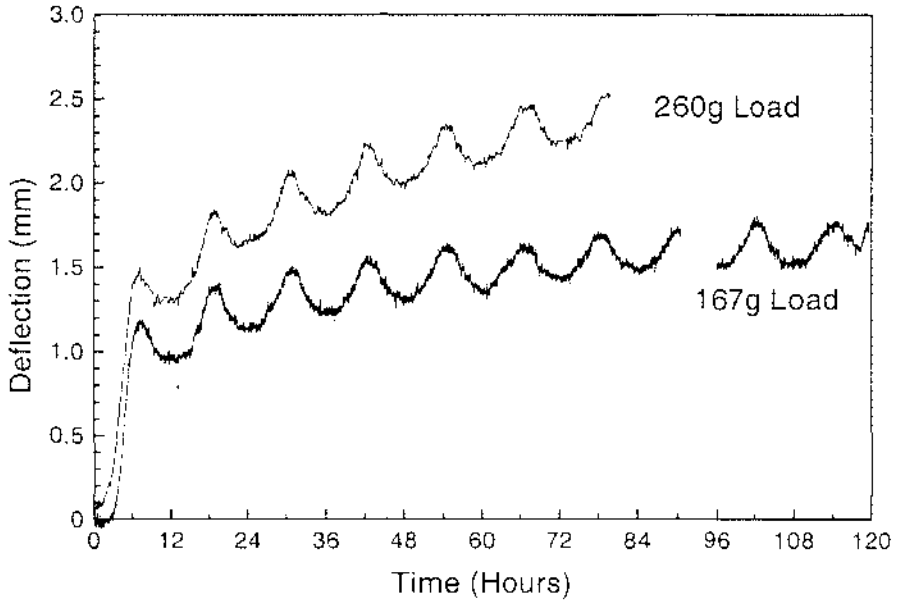

Figure 5.6: Creep response of 'S' corrugated fibreboard for two loads.

5.3.2.4 Effect of cyclic RH versus constant RH on corrugated fibreboard bending creep

Specimens of corrugated board were subjected to the same load (167g) in cycling and constant relative humidity environments in experiments 71114 and 80629 to determine if cyclic relative humidity causes more creep. Specimens tested at constant relative humidity were conditioned at the test relative humidity (90% RH). Specimens in the cyclic relative humidity test were conditioned according to the

procedure in Chapter 4. The conditions for the experiments are shown in Table 5.1.

Figure 5.7 clearly shows that specimen (a) which was exposed to cyclic relative humidity conditions had a greater initial deflection than specimen (b) which was exposed to constant high (90%) RH conditions. After the initial deflection the rate of creep was also greater (by a factor of apprximately 2) for the specimen in the cyclic relative humidity environment. This was consistant with the results of others. No further investigation was done. The complete set of creep curves are shown in Appendix C.

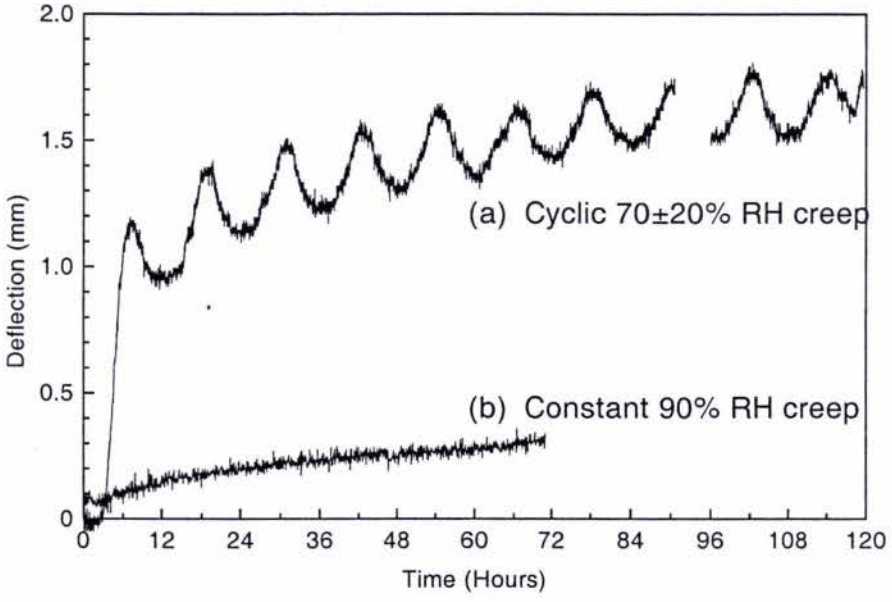

Figure 5.7: Constant 90% RH and cyclic RH creep at 167g load. Specimen (a) conditioned at 50% RH prior to cyclic RH creep test, specimen (b) conditioned at 90% RH prior to 90% RH creep test.

5.4 Cyclic Relative Humidity Creep Modelling - Attempts to Fit Preliminary Data to Existing and New Models

One of the objectives of this study was to model the creep response of corrugated board in a cyclic relative humidity environment. The literature review found two po-

tentially suitable models, one from Urbanik (1995) and the other by Pecht (Haslach et al., 1991). An empirical exponential model was also investigated.

Data from a 5 day experiment (71114) was used initially before data from a 21 day experiment (80218) was used to check the longer term suitability of the models. The 5 day experiment had three specimens of 'R' and three specimens of 'S' corrugated board. The 21 day experiment had 2 specimens of each. One typical result from each experiment was used for the model fitting. In the case of the 5 day experiment 'S' 1 was used, while 'R' 2 was used for the 21 day experiment. The other creep curves are in Appendix C.

5.4.1 Urbanik Model

Urbanik's (1995) model separated the hygroexpansion and mechanosorptive elements of creep deformation, and characterised the deformation in terms of:

- The amplitude and magnitude of a sinusoidal hygroexpansive response,
- The phase lag with respect to the relative humidity,
- Creep constants proportional to the primary and secondary creep rates,
- An exponential time constant to describe the change from primary to secondary creep.

This work made several assumptions which were unlikely to hold true for bending creep data, as noted in Section 3.8.2. Furthermore it was decided that the 'sign' element in the model (Urbanik, 1995: Equation 8) did not reflect the continuous nature of the creep deflection.

The bending creep curve shown in Figure 5.4 did not show any sign of a constant rate of creep associated with secondary creep. This was not surprising given that the test geometry is quite different to the constant load compression test used to generate the data used by Urbanik. It would not be possible to fit creep constants to the bending creep data. For these reasons it was decided to explore other models.

5.4.2 Exponential Empirical Model

The peaks for each cycle (which occurred close to the peak relative humidity) were found to be linear on a log Deflection vs log Time plot (Figure 5.8). Equation 5.1

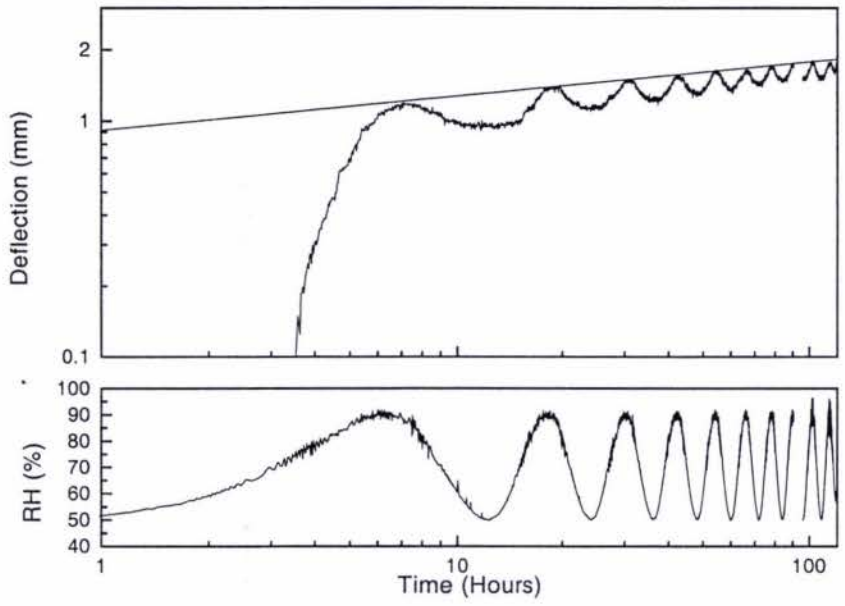

Figure 5.8: Log-log scale plot of deflection data (71114'S'1) showing a straight line across the peaks

was fitted to the deflection peaks as shown in Figure 5.9 on a linear - linear scale. This equation fitted the peaks reasonably well.

$$D(t) = e^a t^b \tag{5.1}$$

where

$D(t)$	=	Deflection at time t
e	=	Base of natural logarithms
t	=	Time
a	=	constant = -0.08681
b	=	constant = 0.14376

Although Equation 5.1 fitted data from experiments lasting less than a week it was found that longer term data could not be described by this function. At longer times the slope of the data curve reduced more quickly than the exponential

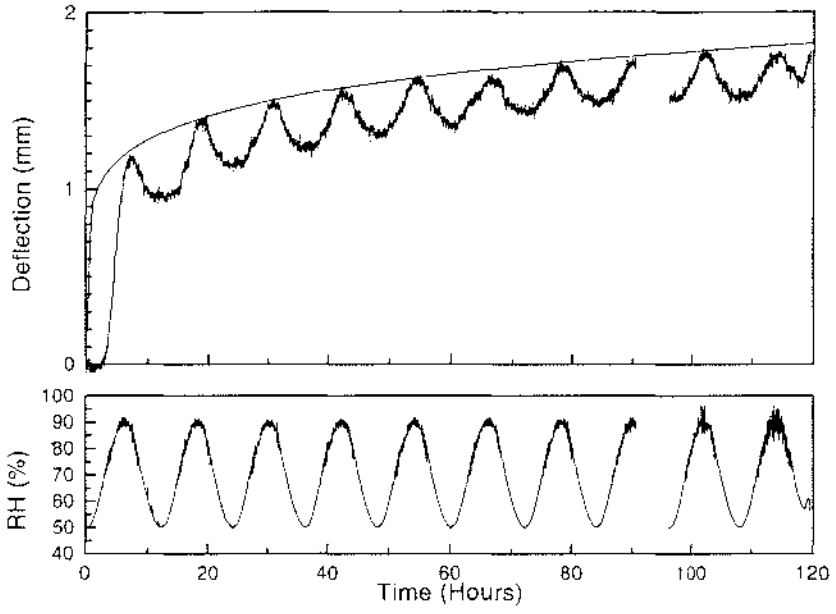

Figure 5.9: Linear - linear plot of equation 5.1 fitted to data peaks (71114'S'1)

function. This was similar to the findings of Brezinski (1956) who reported that creep behaviour at short times or low stress levels can be described by an exponential equation but creep behaviour over long times or at high loads required a log function to fit the data. Rather than using a step (which was not evident in the experimental data) in the model to change to a log function it was decided to modify the surds a and b with a time related function. A sigmoidal function could change a and b in a continuous function either rapidly, approaching a step function, or slowly. This is shown in Equation 5.2.

$$D(t) = e^{a\left(1-\frac{1-s}{1+e^{-k(t-t_c)}}\right)} t^{b\left(1-\frac{1-s}{1+e^{-k(t-t_c)}}\right)} \tag{5.2}$$

where
s, k, t_c = Constants

Equation 5.2 fitted the 21 day peak deflection data extremely well. Figure 5.10 shows the improvement in fit by adding the sigmoid function to the exponential function.

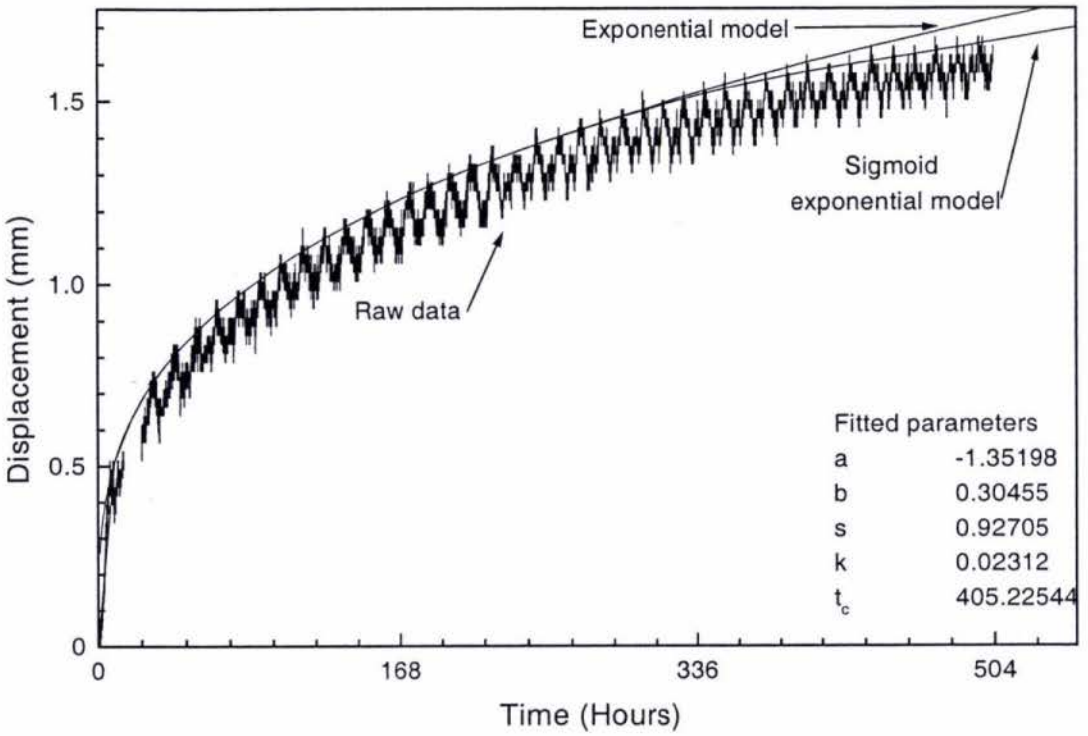

Figure 5.10: Sigmoidal exponential equation (Eq. 5.2) fitted to deflection peaks of Experiment 80218 data

However, fitting Equation 5.2 was very slow and sometimes unstable due to over parameterisation. Another drawback was that the model did not describe the deformation in terms of identifiable physical properties of corrugated fibreboard or paper.

5.4.3 Pecht Model

The Pecht model (Equation 3.5 on Page 26) combined logarithmic and exponential functions as suggested by Brezinski in a simple model with only 3 variables. Following the approach of Haslach et al. (1991), the Pecht model was fitted to cyclic relative humidity creep minima rather than maxima, as shown in Figure 5.11. The model was fitted to the cyclic minima because at those points the specimen would have returned to a moisture content close to that at the start of the experiment. If the moisture content was the same then there would have been no hygroexpan-

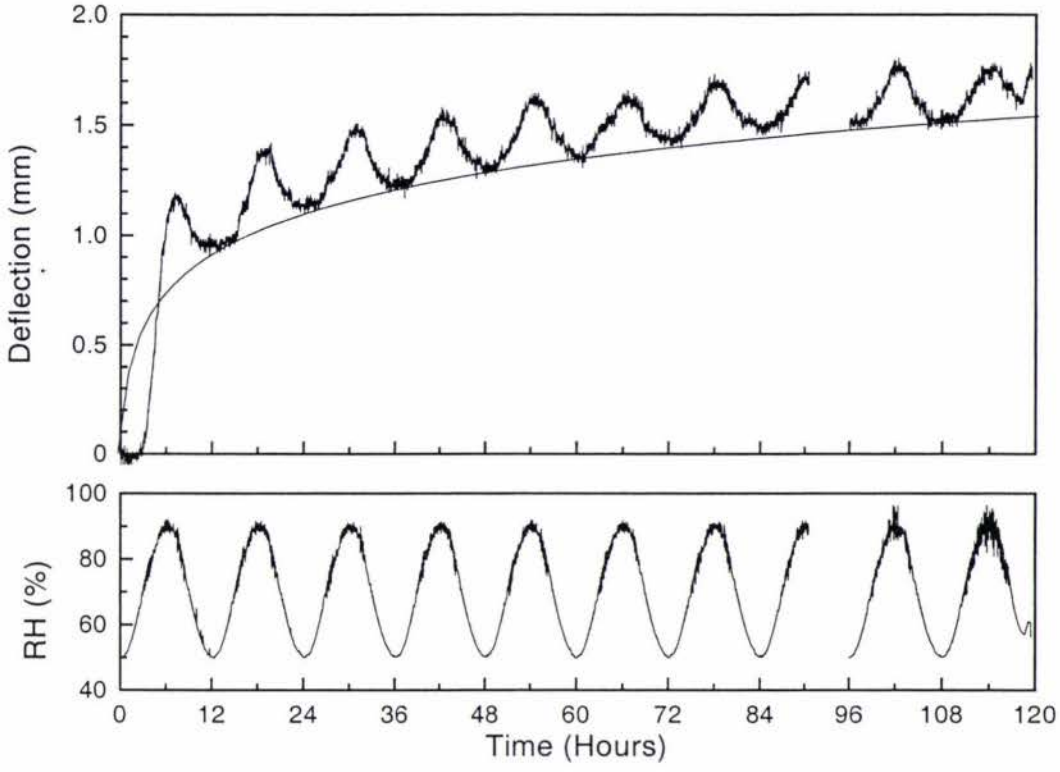

Figure 5.11: Pecht model (Equation 3.5) fitted to cyclic RH creep minima (71114'S'1)

sion component in the deflection i.e. the deflection at that point would be entirely due to creep. This also had the advantage of fitting only 2 points per day of experiment compared to trying to fit a curve through the middle of the data which would require a least squares fit using all of the data (approximately 480 points per day of experiment). The Pecht model also fitted the 21 day creep minima without modification.

However, the model was not always stable and would not necessarily converge using least squares fitting techniques. Haslach et al. (1991) commented on this. They determined the value of n by trial and error (Haslach, 1998). First a value of n was assumed then the values of B and c were fitted by least squares. They repeated this until a satisfactory fit was obtained for the creep strain at the initial relative humidity in each cycle. In this study the fitting software was allowed 50 iterations

to converge from initial values of 0.305, 5.1 and 0.7 for c, B and n respectively. If the fitting had not finished by 50 iterations the process was terminated and the fit reviewed. Usually no further iterations were done as the fit was not improving significantly.

Having determined that the Pecht model could fit the overall creep trend fitting the model to the cyclic displacement required an equation to describe the cyclic bending and straightening. The most simple form was likely to be the same form as the changing relative humidity, such as used by Urbanik. Equation 3.7 on Page 28 used by Urbanik was added to Pecht's equation to approximate the cyclic deflection on top of the creep trend (Equation 5.3).

$$D(t) = c\ln[1 + Bt^n] + A(1 + \sin(\omega t + \phi - \theta)) \tag{5.3}$$

where

$D(t)$	=	Deflection at time t, *mm*
c	=	Constant
B	=	Time shift factor
t	=	Time, *hours*
n	=	Material constant
A	=	Amplitude of the sinusoidal deflection, *mm*
ω	=	frequency of the sinusoidal deflection, *radians/hour*
ϕ	=	Phase offset, $-\frac{\pi}{2}$ radians
θ	=	Phase lag relative to relative humidity, *radians*

The sinusoidal function described the deflection quite well in the exploratory experiments (Figure 5.12). However there was no physical reason to expect it to follow the shape of the relative humidity waveform because of the non-linear interactions between relative humidity and moisture content, and the effect of the interaction between the rate of moisture content change and load on deflection (mechanosorption) as detailed in Chapter 3.

Figure 5.12 clearly shows the amplitude of the cyclic deflection decays over the first few cycles. However not all data showed a decay in the cyclic deflection, for example Figure 5.13 shows the Pecht model fitted to the minima and the same curve

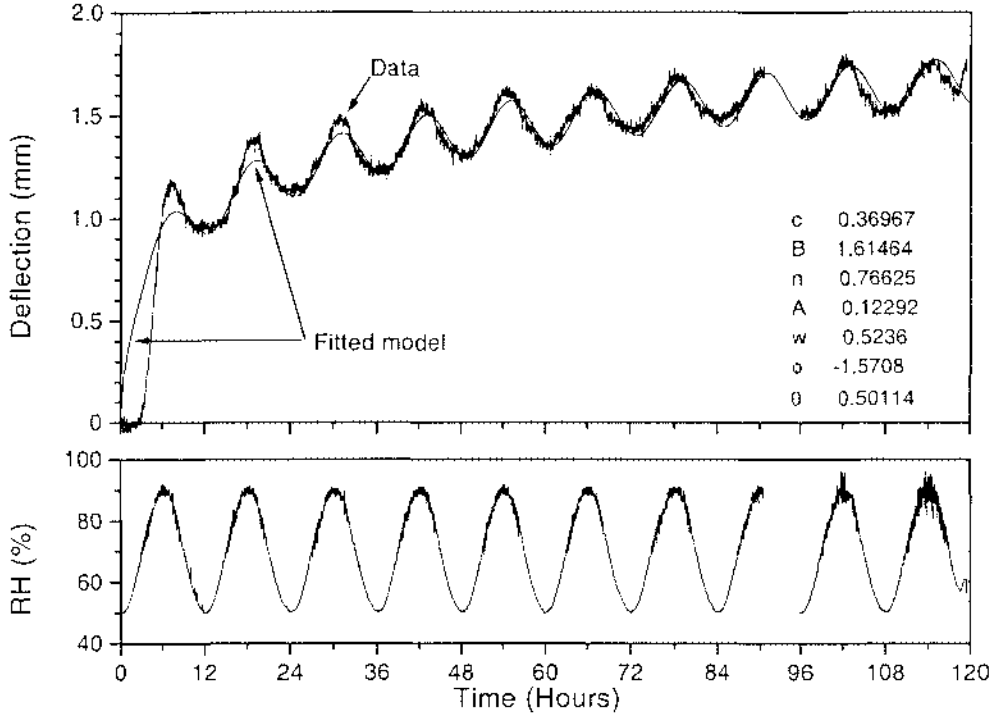

Figure 5.12: Equation 5.3 fitted to cyclic RH creep data (Experiment 71114'S'1)

translated +0.175mm showing it touching the maxima throughout the experiment. The amplitude therefore did not decay significantly in this case.

Although an exponential decay could easily be added to the model which could account for any decay, it was not included as there were inconsistant results from the experimental results and the literature had contradictory evidence as to whether the amplitude decreases or increases over time (Haslach, 1997).

There is still some doubt about using a function of the same form as the relative humidity to approximate the cyclic deflection, so not including a decay function would likely result in minimal loss of precision while being faster to fit. These shortcomings notwithstanding, the model fit in Figure 5.12 showed the cyclic behaviour lagged the relative humidity by 0.5 radians, or approximately 29°.

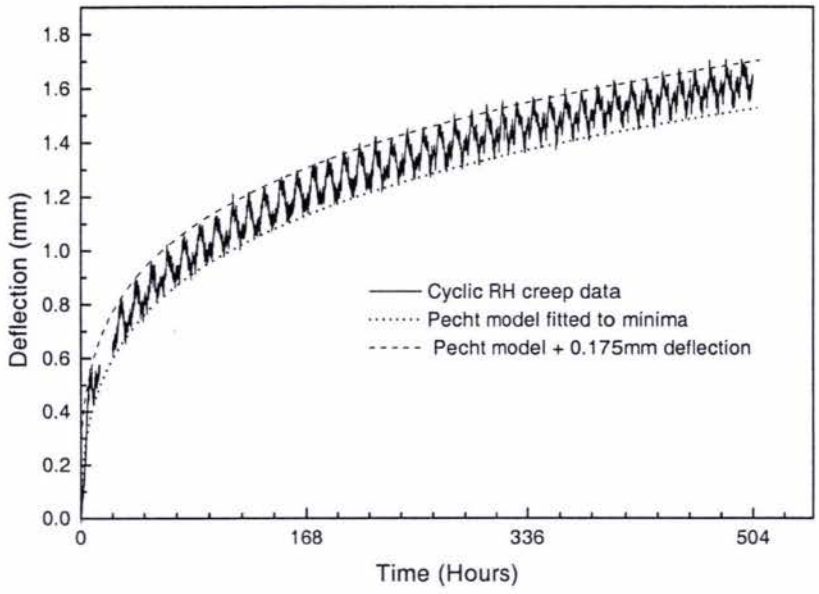

Figure 5.13: Cyclic RH creep curve showing no amplitude decay (80218'R'2)

5.5 Summary and Conclusions

The creep test apparatus was shown to provide sufficiently stable readings of displacement during cyclic relative humidity to enable the study to progress to measuring the characteristics of corrugated fibreboard bending creep in high and cycling relative humidity conditions.

Bending creep of corrugated fibreboard was found to be greatest in the cross machine direction. The initial deflection and creep rate increased with increasing load. Cycling the relative humidity caused the corrugated board to creep faster than a static relative humidity environment. The direction of the cyclic deflection was opposite to that reported by Söremark and Fellers (1993), but the same as reported by Laufenberg (1991).

Three models were investigated; Urbanik's model (1995), an exponential model and Pecht's model (Haslach et al., 1991). The Pecht model was found to fit the cyclic relative creep deflection minima over short (5 day) and long (21 day) tests. Although the Pecht model parameters were not as useful as those in Urbanik's

model, since they had no physical meaning, it fitted the data well, and was therefore a useful tool in the analysis of the creep curves. A sinusoidal function, of the form used to generate the cyclic relative humidity profile, was added to the Pecht model to decribe the cyclic relative humidity creep. The fit was reasonable but did not include an allowance for possible decay in the cyclic deflection as was noted in some experiments.

Chapter 6

Main Experiment

6.1 Experimental and Test Details

The bending creep response of three different corrugated fibreboard samples in static and cyclic relative humidity conditions were measured. The corrugated board types were identified as *CB1*, *CB2* and *CB3*.

Five experiments (80409, 80422, 80622, 80704 and 80714) were run to measure the cyclic relative humidity creep performance under four load conditions. These results were used to generate isometric and isochronous creep curves. One cyclic relative humidity experiment (80824) was run to test the hypothesis that a lower top relative humidity would reduce the cyclic and long term creep deflection. Two experiments (80709 and 80721) were conducted at constant relative humidity to act as indicators of the relative magnitude of the effect of cyclic relative humidity on creep performance. Tests were conducted as described in Chapter 4.

In addition, two previously unscheduled experiments (80921 and 81003) were performed to investigate further the cyclic deflection response observed in the preliminary experiments, which was opposite to that reported by Söremark and Fellers (1993). In these tests specimens were subjected to square wave relative humidity variation to establish if the sinusoidal variation of relative humidity made a difference to the direction of the moisture induced deflection. Specimens of 3.4mm thick wood veneer were included in the second experiment to see if the deflection response of corrugated fibreboard was in the same direction as that for wood.

6.2 Experimental conditions

Table 6.1 shows the experimental conditions chosen for the main experiments to generate isometric curves and isochrones. Table 6.2 shows the experimental conditions for the two experiments run to measure the static relative humidity creep performance. Table 6.3 shows the experimental conditions used in the square wave relative humidity profile experiments. Specimens were arranged in the tester with one specimen of each corrugated board type on each side of the calibration block.

Table 6.1: Cyclic relative humidity corrugated fibreboard experimental conditions

Experiment	Sample	RH	Period (Hours)	Load (g)	Orientation
80409	CB1	70 ± 20	12	306	CD
80409	CB1	70 ± 20	12	306	CD
80409	CB2	70 ± 20	12	306	CD
80409	CB2	70 ± 20	12	306	CD
80409	CB3	70 ± 20	12	306	CD
80409	CB3	70 ± 20	12	306	CD
80422	CB1	70 ± 20	12	306	CD
80422	CB1	70 ± 20	12	306	CD
80422	CB2	70 ± 20	12	306	CD
80422	CB2	70 ± 20	12	306	CD
80422	CB3	70 ± 20	12	306	CD
80422	CB3	70 ± 20	12	306	CD
80622	CB1	70 ± 20	12	167	CD
80622	CB1	70 ± 20	12	167	CD
80622	CB2	70 ± 20	12	167	CD
80622	CB2	70 ± 20	12	167	CD
80622	CB3	70 ± 20	12	167	CD
80622	CB3	70 ± 20	12	167	CD
80704	CB1	70 ± 20	12	120.7	CD
80704	CB1	70 ± 20	12	120.7	CD
80704	CB2	70 ± 20	12	120.7	CD
80704	CB2	70 ± 20	12	120.7	CD
80704	CB3	70 ± 20	12	120.7	CD
80704	CB3	70 ± 20	12	120.7	CD
80714	CB1	70 ± 20	12	397.3	CD
80714	CB1	70 ± 20	12	397.3	CD
80714	CB2	70 ± 20	12	397.3	CD
80714	CB2	70 ± 20	12	397.3	CD
80714	CB3	70 ± 20	12	397.3	CD
80714	CB3	70 ± 20	12	397.3	CD
80824	CB2	65 ± 15	12	167	CD
80824	CB2	65 ± 15	12	397.3	CD
80824	CB2	65 ± 15	12	120.6	CD
80824	CB2	65 ± 15	12	167	CD
80824	CB2	65 ± 15	12	120.6	CD
80824	CB2	65 ± 15	12	397.3	CD

Table 6.2: Static relative humidity corrugated fibreboard experimental conditions

Experiment	Sample	RH	Load	Orientation
80709	CB1	50	397.3	CD
80709	CB1	50	397.3	CD
80709	CB2	50	397.3	CD
80709	CB2	50	397.3	CD
80709	CB3	50	397.3	CD
80709	CB3	50	397.3	CD
80721	CB1	90	397.3	CD
80721	CB1	90	397.3	CD
80721	CB2	90	397.3	CD
80721	CB2	90	397.3	CD
80721	CB3	90	397.3	CD
80721	CB3	90	397.3	CD

Table 6.3: Square wave relative humidity experimental conditions

Experiment	Sample	RH	Period	Load	Orientation
80921	CB3	50 - 90	12	166.7	CD
80921	CB3	50 - 90	12	166.7	CD
80921	CB3	50 - 90	12	306	CD
80921	CB3	50 - 90	12	306	CD
80921	CB3	50 - 90	12	397	CD
80921	CB3	50 - 90	12	397	CD
81003	CB1	50 - 90	12	167	CD
81003	Wood Veneer	50 - 90	12	397	'MD'
81003	CB1	50 - 90	12	306	CD
81003	CB1	50 - 90	12	306	CD
81003	Wood Veneer	50 - 90	12	397	'MD'
81003	CB1	50 - 90	12	167	CD

6.3 Results

The main experiments gave trends similar to those detailed in the preliminary experiments section (Chapter 5). There were, however, some significant new observations from this series of experiments. The creep curves shown in this section were selected to be representative of the results. Individual graphs of the experimental data are shown in Appendix C.

Figure 6.1 combines creep curves from four experiments, these curves and features were typical of the other creep curves (see Appendix C for other creep curves). Higher loads increased the initial deflection during the first cycle and increased the

rate of creep deflection dramatically just as found in the preliminary experiments. Figure 6.1 also shows how increased load changed the shape of the cyclic deflection response to the sinusoidal relative humidity.

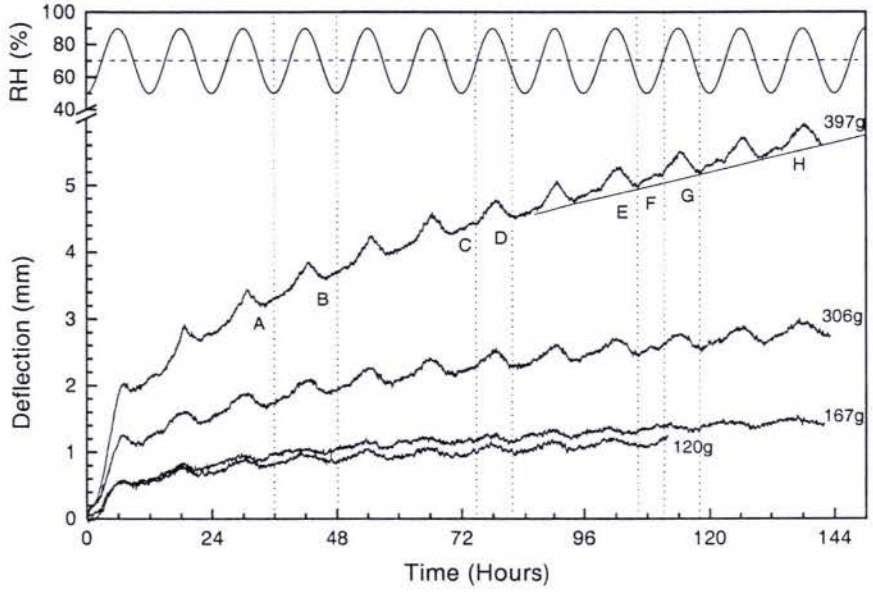

Figure 6.1: Bending creep response of CB3 corrugated board in a sinusoidal cyclic RH. Test loads are shown next to each curve.

Also evident in Figure 6.1 is the characteristic increase in deflection when the relative humidity increased and vice versa exhibited by all specimens in a sinusoidal 50 to 90% RH environment. Lines A and B define a single RH cycle to make this more evident. Lines C and D in Figure 6.1 show that the peak response from the 397g loaded specimen occurred between about 70% RH (increasing) and 60% RH (decreasing). Lines E and F define a region at the bottom of the RH cycle from approximately 60% RH (decreasing) to 70% RH (increasing). During this relative humidity phase there appears to be a small deflection peak. Line H was drawn as a baseline to emphasise this small peak. The relative humidity curve shown in this graph is the control signal (the measured relative humidity in each experiment was almost identical, since the response time of the cabinet was very small in comparison to the cycle frequency).

In experiment 80824 the relative humidity was cycled between 50 and 80% RH. An example is shown in Figure 6.2. The experiment showed that reducing the top RH reduced both the cyclic and long term deflection. This was the only experiment in which the cyclic displacement of some of the samples increased with decreasing relative humidity.

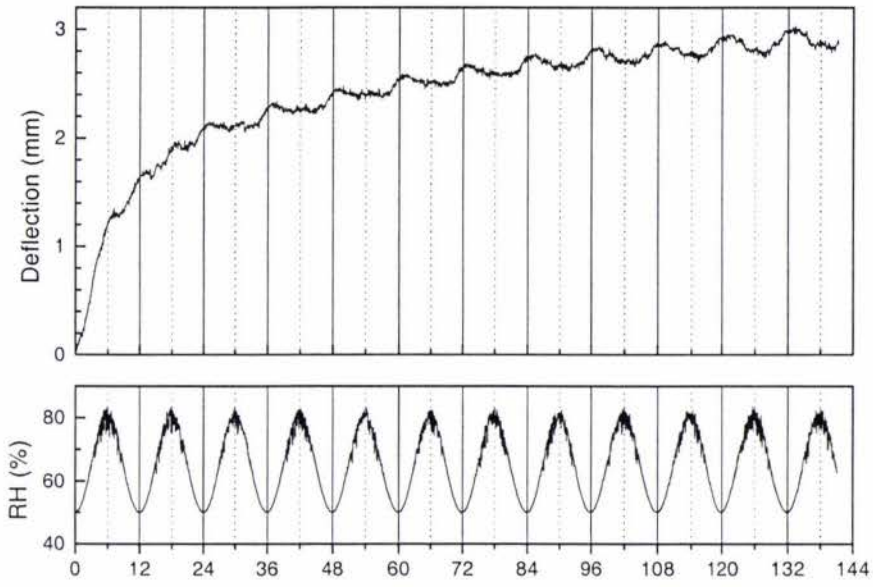

Figure 6.2: Bending creep response of CB2 corrugated board under 397g load in a sinusoidal cyclic RH over a range of 50-80% RH

In experiments 80921 and 81003 a square wave relative humidity cycle with 12 hour period (six hours at each condition) was used. The creep curves are shown in Figures 6.3 and 6.4.

Most noticeable in these experiments were spikes in the deflection when the relative humidity changed. The change from 50% to 90% RH caused the deflection to increase followed by a recovery period. Under high load (397g) the recovery was not complete, but at lower load (167g) the recovery was very close to complete. The change from 90% to 50% RH caused the deflection to reduce followed by a period of recovery. The deflection recovered almost completely for the low load but was incomplete for the high load.

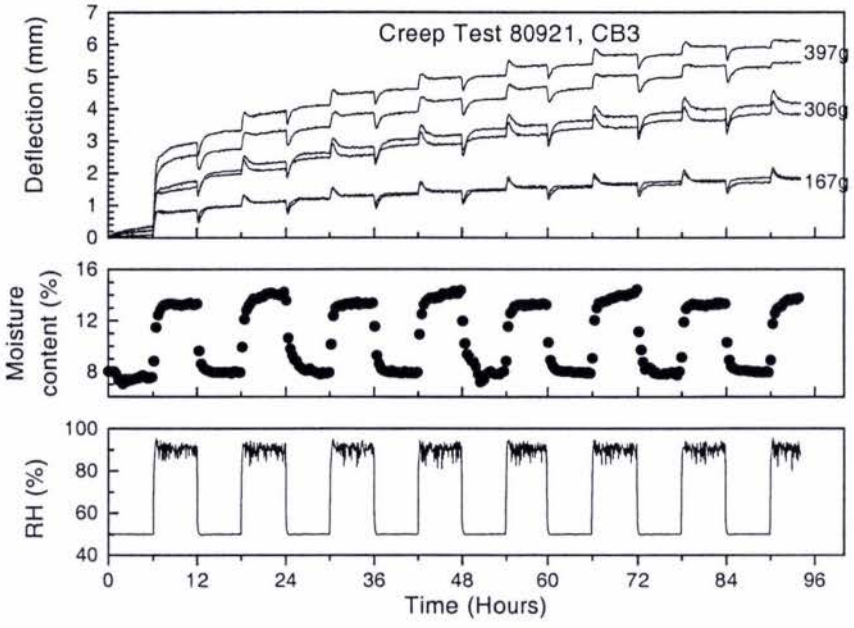

Figure 6.3: Bending creep response of corrugated board in a square wave cyclic RH (80921)

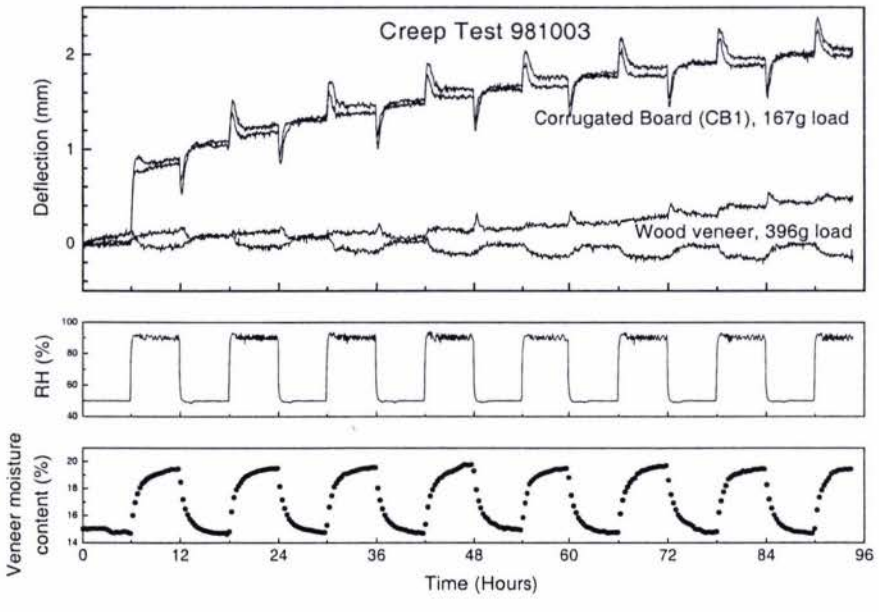

Figure 6.4: Bending creep response of corrugated board and wood veneer in a square wave cyclic RH (81003)

Regardless of the direction of the relative humidity change after 2 to 3 hours the specimens all resumed a condition of slow but steady creep. It was interesting to note

that during the periods of steady creep the rates at 50% RH and 90% RH for each specimen were very similar, and even the different loads had similar rates during these periods. However, the overall creep rates of the corrugated board specimens subjected to 306g and 397g loads were greater than the creep rates at either 50% or 90% RH conditions. This occurred because the deflection increase from the change from 50% to 90% RH plus the steady creep was greater than the combined effect of the recovery period and the deflection and recovery when the relative humidity changed from 90% to 50% RH. The complete deflection recovery of the specimens under the low load resulted in the overall creep rate being very close to the steady creep rates at 50% and 90% RH.

The different responses from the two wood veneer specimens cannot be explained, but the deflection response of both specimens was smaller and opposite in direction to that of the corrugated fibreboard. The reason for the drift shown by the lower creep curve was not apparent.

The moisture content of both specimen types followed the form of the relative humidity cycles but the rate of change reduced assymptotically as equilibrium moisture content was approached. The wood veneer moisture content responded more slowly than the corrugated fibreboard.

Chapter 7

Discussion

This chapter concentrates on interpreting the results of the main experiments detailed in Chapter 6 using corrugated fibreboard types *CB1*, *CB2* and *CB3*. The response to moisture sorption cycles is discussed before reviewing the fitting of the Pecht model and sinusoid to the creep deflection. Isometric and isochronous data derived from the model fitting were then used to rank the performance of the three corrugated fibreboard types.

7.1 Deflection Response to Moisture Sorption

7.1.1 Direction of cyclic deflection response

Data from experiments where the relative humidity was cycled between 50% and 90% showed increased deflection when the relative humidity increased and vice versa. The creep curves in Figure 6.1 on page 77 show this. Lines A and B define a single RH cycle to make it more evident. Laufenberg (1991) reported the same response as found in these experiments.

This was, however, opposite to the result reported by Söremark and Fellers (1993) who reported that specimen deflection increased when the relative humidity reduced. They observed that when the specimen was loaded at low relative humidity and the relative humidity was raised, the deflection increased. When the relative humidity was reduced the deflection increased again. Subsequent relative humidity cycles caused the deflection to decrease when the relative humidity rose and increase

during periods of reduced relative humidity. The small peak observed in Figure 6.1 between lines E and F is what might be expected if the deflection followed in part Söremark and Fellers observations.

Söremark and Fellers explanation for decreased bending during periods of moisture adsorption was based on the stress induced hygroexpansion of the linerboards in compression and tension. Increased hygroexpansivity of the linerboard in compression and reduced hygroexpansivity of the linerboard in tension forced the corrugated board to straighten as moisture was adsorbed. Moisture loss causing increased bending is also explained by this model of differential expansion and contraction

There is also an explanation for the cyclic bending response to cyclic relative humidity observed in these experiments and by Laufenberg (1991). As the relative humidity increased the linerboards on the corrugated board gain moisture which results in reduced stiffness. This would cause the corrugated board beam structure to lose bending stiffness which would cause the beam to deflect more under the constant load.

On the downward part of the relatiave humidity cycle the linerboard loses moisture and its strength and stiffness increase and it will also contract (Salmén, 1993). Söremark and Fellers explanation of stress induced hygroexpansion predicts that differential expansion of the two linerboards will cause increased bending. The other possibility is the increase in stiffness would release some of the strain energy causing the specimen to straighten.

Experiments 80921 and 81003 more closely resembled the stepped relative humidity used by Söremark and Fellers (but retain 90% RH as the top relative humidity). The square wave relative humidity cycle showed that a rapid change in moisture content from a step change in relative humidity maintained the deflection direction of corrugated board observed in the sinusoidal experiments ie: increasing RH increased the deflection and vice versa (Figure 6.3).

Wood veneer was included in the second experiment because the behaviour of

wood has always been reported as straightening with increasing moisture content. The wood veneer cyclic deflection reacted in the oppposite direction to that of the corrugated fibreboard (Figure 6.4). It matched the direction expected for wood (Hoffmeyer and Davidson, 1989). The direction of the wood veneer deflection was the same as Söremark and Fellers (1993) reported for corrugated board. Söremark and Fellers noted that their deflection observations for corrugated board were the same as had been reported for wooden beams. This showed that corrugated fibreboard could give cyclic deflections opposite to wood[1].

Experiment 80824 was the only experiment which showed cyclic deformation similar to that described by Söremark and Fellers. In this case, the relative humidity was cycled from 50 to 80% RH compared with 50 to 90% RH for other tests. It is useful to note that Laufenberg's (1991) experiments which had a cyclic response opposite to Söremark and Fellers were also conducted in a 50 to 90% RH cyclic atmosphere. This suggests that there may be different mechanisms operating above 80% RH.

Above about 80 - 85% RH the softening of the hemicellulose components of the fibre cause greater relaxation of the paper structure and irreversible changes in the stress/strain characteristics and hygroexpansivity (Salmén, 1993). The softened fibres and fibre-fibre bonds also change the viscoelastic behaviour of the paper.

Norimoto et al. (1992) suggested that although increased deflection during drying and vice versa under bending stress was regarded as a characteristic of mechano-sorptive creep it may be a geometrical or elastic effect. This backs up the concept that any changes in stress-strain properties caused by the peak level of the cyclic relative humidity will change the cyclic response of corrugated fibreboard.

The mechanism causing the change in mechanosorptive characteristics above 80% RH was not investigated as it was beyond the scope of this study. However,

[1]It should also be noted that, since the cyclic deflections of the wood veneer were in the expected direction, this confirmed that the creep tester was measuring the correct deflection direction

the finding that increasing the peak relative humidity from 80% to 90% RH changes the direction of the cyclic deflection response provides a solution to conflicting data in the literature on relative humidity cycling effects (Laufenberg, 1991; Söremark and Fellers, 1993). This should be the subject of further research in order to gain a better understanding of cyclic relative humidity creep phenomenon.

7.1.2 Cyclic deflection response shape

The cyclic deflection was not always a sinusoidal shape. An example of a non-sinusoidal response is shown by the response of the *CB3* specimen loaded with 397g in Figure 6.1 on page 77. This was not completely unexpected as hygroexpansivity and stiffness are related to the moisture content rather than relative humidity (Salmén, 1993), and above 80% RH there is a non-linear relationship between relative humidity and moisture content (as shown in Figure 2.4 on page 9). Furthermore, if the level of hygroexpansion is affected by the direction of stress (compressive or tensile), as proposed by Söremark and Fellers (1993), then hygroexpansion would not be the same in both liners resulting in curvature changes not proportional to the moisture content. Section 7.1.1 also shows mechanosorptive characteristics change dramatically above 80% RH which affects the shape of the cyclic deformation.

The shape of the curve notwithstanding, it was expected that the cyclic deflection response would be regular with respect to relative humidity and that there would have been a small time delay with respect to the relative humidity because of the finite time to sorb moisture as the relative humidity changed. This was not always observed. In some experiments the deflection peaks closely matched the time of the relative humidity and moisture peaks but the deflection minima were ahead of the relative humidity minima. This implied that the deflection response was anticipating the change in relative humidity. This was clearly unlikely. Figure 7.1 shows an example in which at the begining of the test the deflection peaks occur at the time of the relative humidity and moisture peaks but the deflection minima are

ahead of the relative humidity minima. In the later stages of the test the deflection peaks also occur before the relative humidity and moisture peaks.

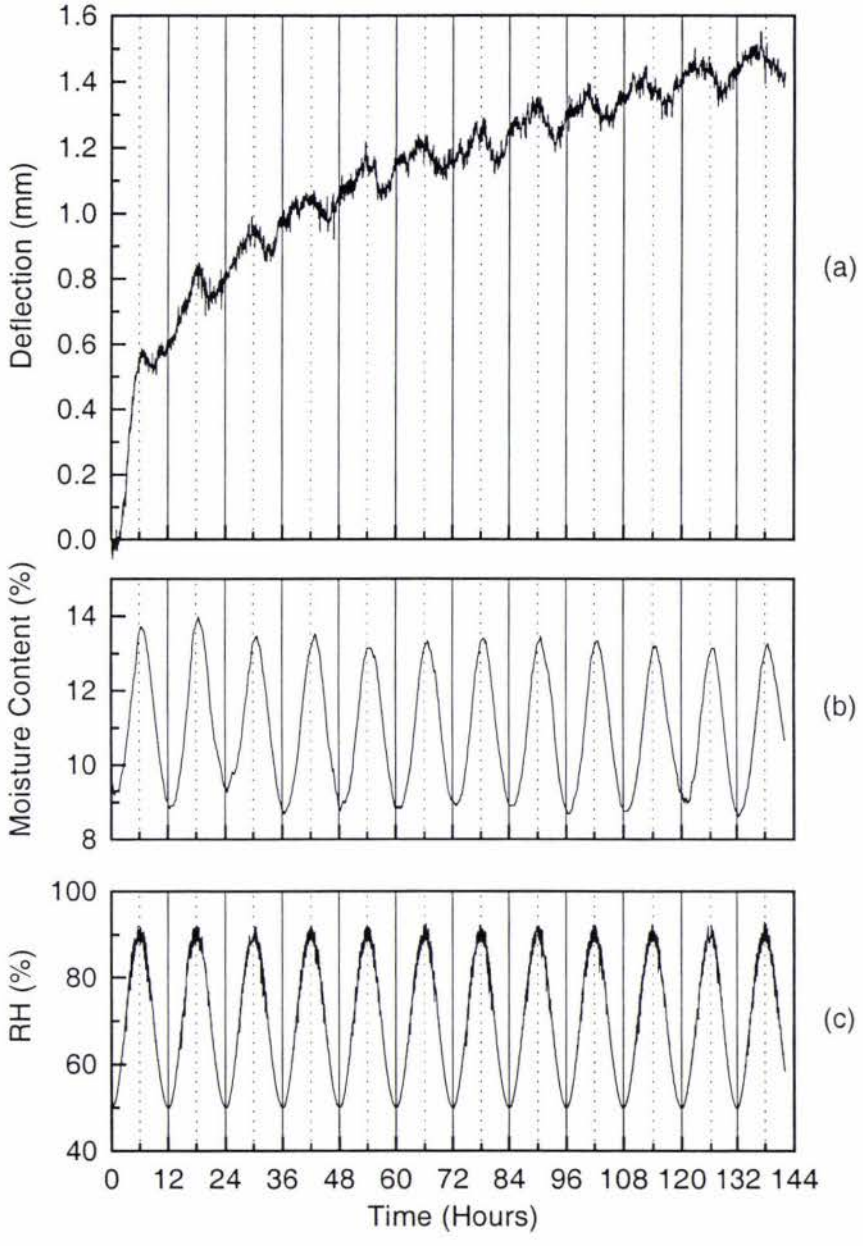

Figure 7.1: Example of corrugated board showing cyclic deformation showing lead (negative phase lag) with respect to RH (80622, CB3,1)

The experimental data were checked to make sure there were no timing errors between the measured relative humidity and the deflection, and no calibration errors.

No errors were found and it was concluded that the response was real.

Figure 7.1 shows that the moisture content closely followed the sinusoidal shape of the relative humidity, lagging slightly behind the relative humidity as expected. The lead in deflection minima was not explained by the moisture content. This also implies that the cyclic deflection response was not just related to moisture content otherwise it would be expected that the slight lagging of the moisture content would cause the deflection response to lag the relative humidity. It would also be expected that the cyclic deformation would follow a sinusoidal shape but the shape was clearly not sinusoidal.

It is thought that the mechanism causing both the cyclic deflection response to lead the relative humidity and moisture content and the non-sinusoidal response is related to that which causes the direction of the cyclic deformation to change depending on the peak relative humidity attained during cyclic relative humidity testing.

7.2 Creep Model Fit

The model postulated in Chapter 5 (Equation 5.3, page 70) was fitted to the sinusoidal cyclic relative humidity creep experiments. The parameters are shown in Table 7.1. The Pecht model parameters from static relative humidity experiments are shown in 7.2.

Values were fitted for the sinusoidal component of the model (i.e. ω, ϕ and θ), but fitting the cyclic deflection was not very successful since the response due to the cyclic relative humidity was not always well approximated by a sinusoidal model. The asymmetrical non-sinusoidal response made the amplitude term of the fitted model meaningless. An example of a non-sinusoidal response is shown by the response of the *CB3* specimen loaded with 397g in Figure 6.1 on page 77.

In some cases the fitted phase lag, θ, was negative which implied that the cyclic response was anticipating the change in relative humidity. This was due to the

Table 7.1: Cyclic relative humidity corrugated fibreboard creep model parameters

Experiment	Sample	c	B	n	A	ω	ϕ	θ
80409	CB1	2.01049	0.12955	0.57664	0.14041	0.5278	-1.5708	0.05467
80409	CB1	7.45929	0.05026	0.43076	0.12737	0.53176	-1.5708	0.22795
80409	CB2	7.46398	0.04838	0.40637	0.10844	0.53193	-1.5708	0.45412
80409	CB2	8.85917	0.04613	0.41058	0.12866	0.53077	-1.5708	0.3763
80409	CB3	2.53186	0.13343	0.48089	0.09902	0.53176	-1.5708	0.38292
80409	CB3	15.08142	0.02533	0.40634	0.11522	0.53213	-1.5708	0.45372
80422	CB1	0.92102	0.2699	0.88273	0.09298	0.52773	-1.5708	0.08553
80422	CB1	10.49537	0.05535	0.36974	0.11339	0.52783	-1.5708	0.3117
80422	CB2	14.84252	0.0318	0.3789	0.08143	0.52974	-1.5708	0.44128
80422	CB2	7.61112	0.05926	0.39629	0.13802	0.52721	-1.5708	0.20035
80422	CB3	16.67812	0.02964	0.38158	0.09783	0.53052	-1.5708	0.4403
80422	CB3	18.75292	0.02556	0.36604	0.11945	0.52709	-1.5708	0.24636
80622	CB1	0.8607	0.28425	0.56757	0.12951	0.52803	-1.5708	0.42437
80622	CB1	3.83993	0.0783	0.36625	0.14314	0.5274	-1.5708	0.27365
80622	CB2	1.65157	0.20135	0.37512	0.04477	0.54198	-1.5708	0.72513
80622	CB2	2.76507	0.09523	0.37976	0.07315	0.53315	-1.5708	0.24974
80622	CB3	1.11644	0.18833	0.52074	0.05489	0.54092	-1.5708	0.43934
80622	CB3	1.05113	0.2362	0.46525	0.08263	0.53759	-1.5708	0.26251
80704	CB1	0.86511	0.19853	0.56317	0.06417	0.53277	-1.5708	0.40023
80704	CB1	0.40518	0.38713	0.71464	0.13466	0.52775	-1.5708	0.19652
80704	CB2	1.11272	0.20434	0.3976	0.0406	0.53572	-1.5708	0.26142
80704	CB2	2.06568	0.09247	0.42424	0.06589	0.52911	-1.5708	-0.11582
80704	CB3	0.50857	0.39035	0.61882	0.06446	0.53489	-1.5708	0.37364
80704	CB3	1.1549	0.11987	0.5022	0.06753	0.52886	-1.5708	-0.02551
80714	CB1	22.62502	0.032	0.42516	0.1084	0.53098	-1.5708	0.78926
80714	CB1	11.70674	0.06054	0.46107	0.1106	0.53213	-1.5708	0.72803
80714	CB2	4.09754	0.20978	0.46207	0.08817	0.53401	-1.5708	0.76588
80714	CB2	16.91281	0.04529	0.41631	0.09012	0.53227	-1.5708	0.52641
80714	CB3	13.75709	0.05148	0.4618	0.10696	0.53133	-1.5708	0.71334
80714	CB3	0.55511	3.12104	1.53053	0.14886	0.52946	-1.5708	0.81006
80824	CB2 (120g)							
80824	CB2 (120g)							
80824†	CB2 (167g)	0.54774	0.30235	0.38982				
80824†	CB2 (167g)	0.47307	0.31665	0.47114				
80824†	CB2 (397g)	0.2697	3.14621	2.03034				
80824	CB2 (397g)							

Sinusoidal function not fitted to 80824. Missing data caused by either no peaks or mixed cyclic response.
† Cyclic response increasing with reducing RH and vice versa

Table 7.2: Static relative humidity corrugated fibreboard creep model parameters

Experiment	Sample	c	B	n
80709	CB1	0.10436	1.31764	1.07778
80709	CB1	0.0724	0.99011	1.59873
80709	CB2	0.12681	1.42973	1.06354
80709	CB2	0.17138	1.15236	0.83496
80709	CB3	0.02789	19.29197	3.00361
80709	CB3	0.3805	0.63873	0.66796
80721	CB1	0.27102	0.29492	1.1021
80721	CB1	0.52743	0.14773	0.85528
80721	CB2	0.50803	0.14439	0.7874
80721	CB2	0.60758	0.12742	0.78936
80721	CB3	0.46538	0.15763	0.82182
80721	CB3	0.60535	0.15198	0.89455

model trying to fit a regular sinusoidal response to an asymetric response. This was discussed earlier in Section 7.1.2.

In summary, although the attempt to model the cyclic deflection was not successful, the Pecht model fitted the cyclic deflection minima satisfactorily. The model was used to describe the creep deflection to calculate isometric and isochronous data to allow comparison of samples on a similar basis. No attempt was made to assign the model parameters to sample characteristics.

7.3 Isometric Creep Response

Figure 7.2 shows the time the corrugated board took to reach 2mm deflection, using values for 2mm calculated from the Pecht equation (Equation 3.5). 2mm deflection was chosen because it was approximately the initial deflection of the tests with the greatest load while minimising extrapolation of the low load data. Data for the 120.7g and 167g loads were predicted values based on extrapolating the fitted creep curves. All data points are shown.

The graph showed a logarithmic relationship between load and time.

Static 90% and 50% relative humidity creep times at 397g loads were also calculated using the Pecht model. These were about two and five orders of magnitude respectively longer than the cyclic relative humidity times, which indicate the severe effects of cyclic relative humidity.

7.4 Isochronous Creep Response

Isochronous deflection results calculated using the Pecht model were plotted for the *CB1*, *CB2* and *CB3* corrugated board samples. 50 hours was chosen because the creep deflection had begun to level off and for logistical reasons because it would enable creep analysis from tests lasting 4 days. Figure 7.3 shows the deflections after 50 hours of creep. It shows the deflection increased with greater load and that cyclic relative humidity caused much greater deflection than both constant 50% RH

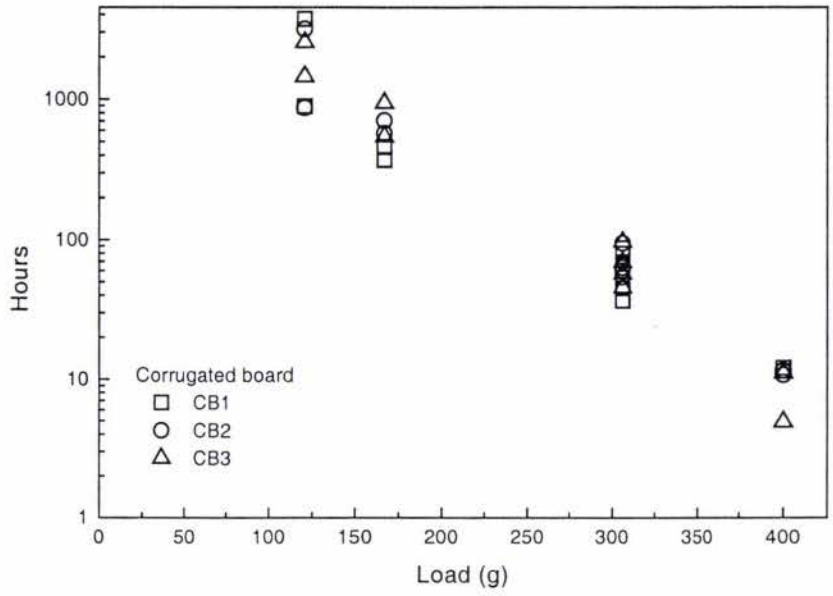

Figure 7.2: Creep times for 2mm deflection for corrugated board in a 12 hour 70±20% RH cyclic environment. CB1, CB2 and CB3 refer to the corrugated board sample label.

and constant 90% RH atmospheres.

Not shown on Figure 7.3 were the results of experiment 80824 where the relative humidity was cycled from 50% to 80% RH. The isochrone for this experiment was midway between the constant 90% RH isochrone and the 50% to 90% RH isochrones. This demonstrated that the peak relative humidity affects the rate of creep in a cyclic relative humidity environment.

100 hour deflections showed the same trends, with slightly greater separation between the data as the load was increased. This was a result of the rate of deflection increasing with greater load.

Söremark et al. (1993) described the slope of the linear section of a stress/strain isochronous curve for tensile creep tests as the *creep modulus*. A similar concept was used in this study to compare the bending creep isochrones of the specimens using load and deflection in place of stress and strain.

At low loads the deflection/strain isochrones were proportional to the load. This

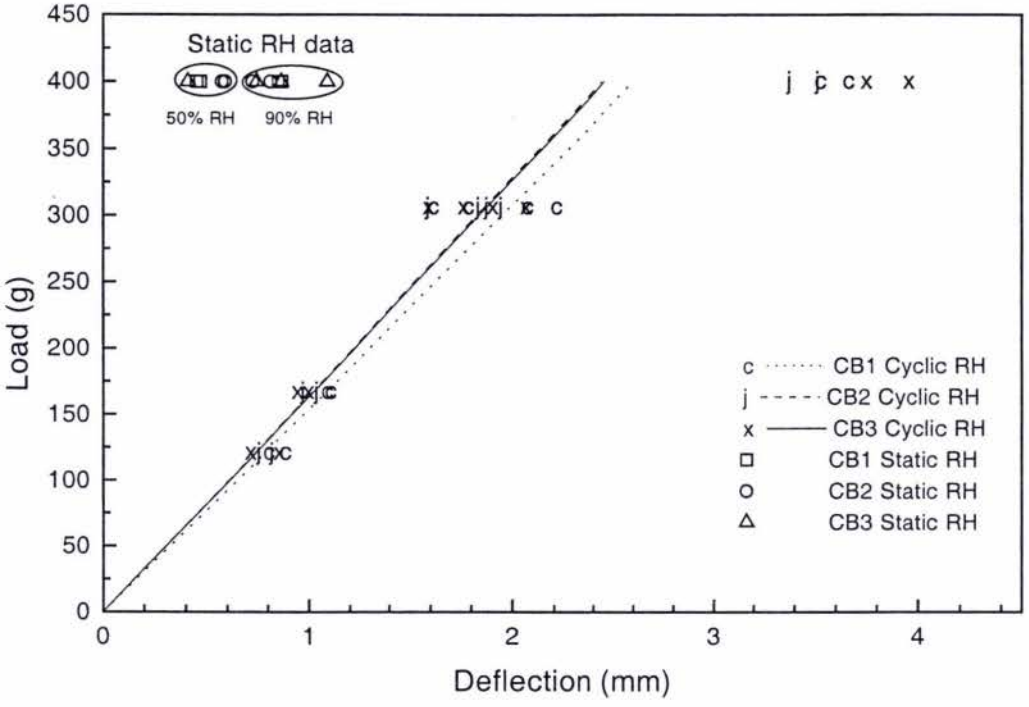

Figure 7.3: 50 hour isochronous data for CB1, CB2 and CB3 showing the creep modulus for 50 hour 50%-90% cyclic RH creep data

is characteristic of linear viscoelastic behaviour. However above about 300g the proportional limit of the isochrones was reached and non-linear viscoelastic behaviour occurred. Similar non-linear viscoelastic regions have been reported by Kolseth and De Ruvo (1983). The different material behaviours in these regions most likely account for altered order of responses amongst the corrugated board types. The 397g load results were excluded from modulus calculations as they were not on the linear part of the isochrones.

Figure 7.3 shows regression lines fitted to the linear region of the cyclic relative humidity creep isochrones using data from the 120g, 167g and 306g load levels. The creep modulus at constant 50% RH was greater than at constant 90% RH, which in turn is greater than the cyclic RH conditions. This was expected and is similar to the results reported by Söremark et al. (1993).

The creep modulus was modelled in SAS with the deflection dependent on the load in order to perform a least squares fit. The terms in the model were load, load×board type interaction and load×run interaction. The interaction terms were added to the model as these represent the slope differences due to the board type and the experimental run respectively. The load term was modelled as a continuous variable and interactions were continuous by class variables. Due to using one load per experimental run and only one experimental run for each load, except for the 306g load which was replicated, the load and load×run terms were partially confounded.

The results are shown in Table 7.3. The load and load×run interaction terms were statistically significant and the load×board type interaction term fell outside the p=0.05 level used to determine significance. This implied that the three board types were not significantly different at this level. However the p-value was only slightly greater than 0.05 so comparisons between board type pairs was done.

Table 7.3: SAS General linear model results for corrugated board 50 hour isochrones up to 306g load

Source	p-value type III SS
Load	0.0001
Load × Board type	0.0741
Load × Run	0.0001
Contrast	p-value
CB1 vs CB2	0.0398
CB1 vs CB3	0.0580
CB2 vs CB3	0.8501

Direct comparisons between each pair of moduli (Contrasts) were calculated for the board type×load interaction effect (Table 7.3). These comparisons showed the difference between the *CB1* and the *CB2* moduli was significant and the difference between the *CB1* and *CB3* moduli was close to significant. However the *CB2* and *CB3* moduli were not significantly different. Deflection residuals increased with increasing load which meant the variance was not equal. Thus the assumption

of equal variance was not valid. However, transforming the deflection metric to homogenise the variance would no longer give the creep modulus (ie: the slopes of the load-deflection isochrones).

The data were further analysed using a square root transformation to homogenise the variation over the load range. Analysis of the transformed metric ($\sqrt{\text{deflection}}$) was done using a mixed model with fixed effects of load and board type and the random effect of run within load (Table 7.4). The large p-value for the load term was due to the low number of replicates for each load. Contrasts were used to compare each sample with the other two. It confirmed the *CB1* mean was different to both the *CB3* and *CB2* means while the *CB3* and *CB2* samples were not significantly different.

Table 7.4: SAS General linear model results for corrugated board $\sqrt{\text{deflection}}$ up to 306g load

Source	p-value
Board type	0.0488
Load	0.1946
Run (Load)	0.0001
Contrast	p-value
CB1 vs CB2	0.0333
CB1 vs CB3	0.0313
CB2 vs CB3	0.9766

Based on the creep modulus analysis and the data analysis it can be said that the *CB1* corrugated board did not perform as well as the *CB2* and *CB3* boards. This result does need to be taken in cognisance of the limited number of tests and samples tested. Only one batch of each type of board was available to be sampled for testing and therefore there was no replication of each board type. A greater number of replicate tests would be essential before it could be conclusively said that *CB1* had inferior performance.

Although this study indicated that there may be a difference in creep modulus and hence creep performance between the *CB1* and the *CB2* and *CB3* corrugated

boards, there had been no data at the time of writing to suggest that a performance difference was evident in containers made from the different corrugated board types. Also, while the method may be capable of detecting a difference between board types, there are as yet no guidelines to decide the level of creep modulus which would be acceptable for a given end use.

Chapter 8

Conclusions

A testing apparatus and method have been developed to evaluate the bending creep performance of corrugated fibreboard in high and cycling relative humidity conditions. A number of experiments have been conducted to evaluate three samples of corrugated fibreboard.

The experiments have shown that cycling relative humidity between 50% and 90% caused more rapid bending creep than both static 90% RH and cycling relative humidity between 50% and 80% RH. This was in agreement with the findings of researchers in the field of corrugated fibreboard, paper and wood. Corrugated fibreboard subjected to bending stress was found to creep more in the cross machine direction than the machine direction.

The direction of the cyclic response of corrugated fibreboard under bending stress seems to be dependent on the peak relative humidity over the range of 80% to 90% RH. Corrugated board exposed to cyclic relative humidity which peaked at 80% RH showed bending increased when the relative humidity was decreasing and vice versa. The opposite pattern was observed when the peak relative humidity was 90% RH. This change in mechanosorptive behaviour was explained in terms of loss of stiffness of the linerboards and relaxation of bonds in the paper structure. Furthermore, in the 90% RH peak creep data the deflection appeared to reach a minima ahead of the relative humidity minima, so that the board bending was increasing as the relative humidity minima was reached. This was explained in terms of the change in mechanosorptive behaviour at over 80% RH. However, the

mechanism causing the change of mechanosorptive behaviour was not investigated but needs to be determined to further our understanding of cyclic relative humidity creep phenomenon.

Three models for describing cyclic bending creep were investigated. The model used by Urbanik was rejected on theoretical grounds, and an exponential model was found to fit the data, but this was also rejected after it was found that additional parameters needed to provide a fit made the model excessively complex. It was found that the long term creep trend could be modelled using an empirical curve fitting model proposed by Pecht. Cyclic deflection caused by the sorption of moisture in a cyclic relative humidity atmosphere was not modelled successfully.

Isochronous cyclic relative humidity bending creep results showed the *CB1* corrugated fibreboard had lower creep modulus than both the *CB2* and the *CB3* corrugated fibreboard. However, the difference was not significant at a level of p=0.05 (p=0.074). Analysing the deflection data as opposed to the creep modulus and homogenising the variance using a square root transform of the deflection data the *CB1* board was found to be statistically significant (p=0.049).

It is important to take into account that this result came from only one sample batch of each type of corrugated fibreboard. More samples of each type of corrugated fibreboard need to be tested to clarify the result.

Creep performance data from corrugated fibreboard and containers is needed to be able relate bending creep modulus to container creep performance and to set a level of bending creep performance which is required to ensure satisfactory performance of corrugated containers.

If the performance of corrugated fibreboard packaging in cycling relative humidiy environments is to be improved the following further research is recommended:-

1. Further cyclic creep testing of corrugated fibreboard and cyclic creep testing of containers to relate bending creep modulus to container performance.

2. Develop a better understanding of the mechanisms affecting cyclic deflection caused by sorption.

Appendix A

Data Acquisition Specifications

The specifications in Sections A.1 and A.2 were taken from documentation included with the National Instruments equipment.

A.1 Voltage Input Module Specifications

Table A.1: Voltage Input Module Characteristics

Input range	±5V
Output range	±5V
Accuracy	±0.02% ±0.2 mV
Gain Stability	±50 mV / °C
Non-linearity	±0.2% FSR
Normal-mode Input Protection	240 Vrms, continuous
Common-mode voltage isolation	1500 Vrms, continuous

A.2 PC DAQ Card

Table A.2: Data Aquisition Card Specifications

Model	AT-MIO-16E-10
No. Analogue channels	16 single ended or 8 differential
Digitising resolution	12 bit, 1 in 4096
Nominal input	10 V
Programmable gain	0.5, 1, 2, 5, 10, 20, 50, 100
No. digital I/O lines	8
Maximum sampling frequency	100 000 samples/s

A.3 Data Aquisition Hardware Components

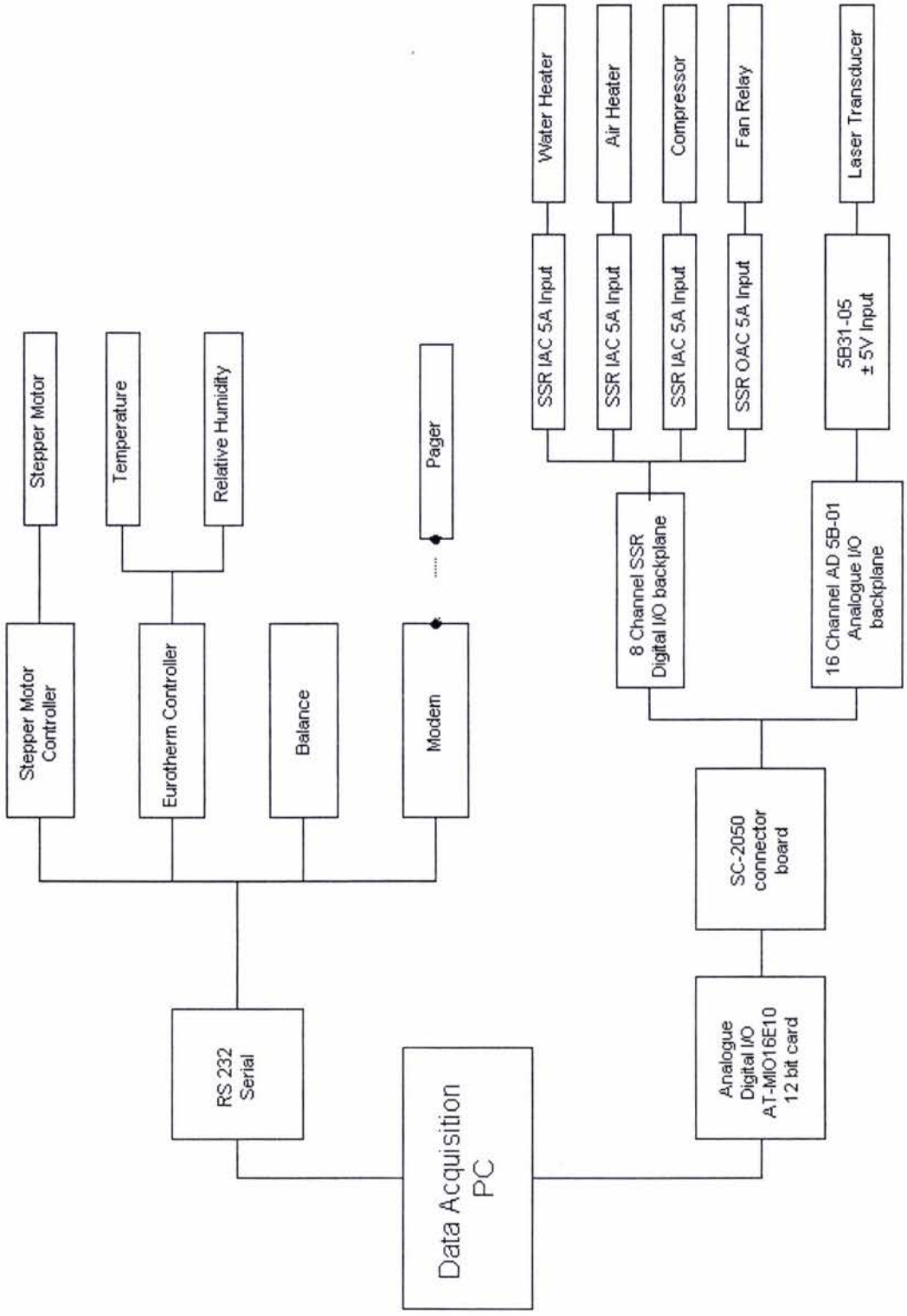

Appendix B

LabVIEW© Program

B.1 Creep test apparatus control program

The Creep apparatus LabVIEW program diagram is printed in the following four figures on pages 99 to 102

B.2 Thermoline RH control program

The figure on page 103 is the screen of the virtual instrument which controls the Thermoline RH setpoint. The figure following this is the program diagram for the virtual instrument which controls the Thermoline RH setpoint.

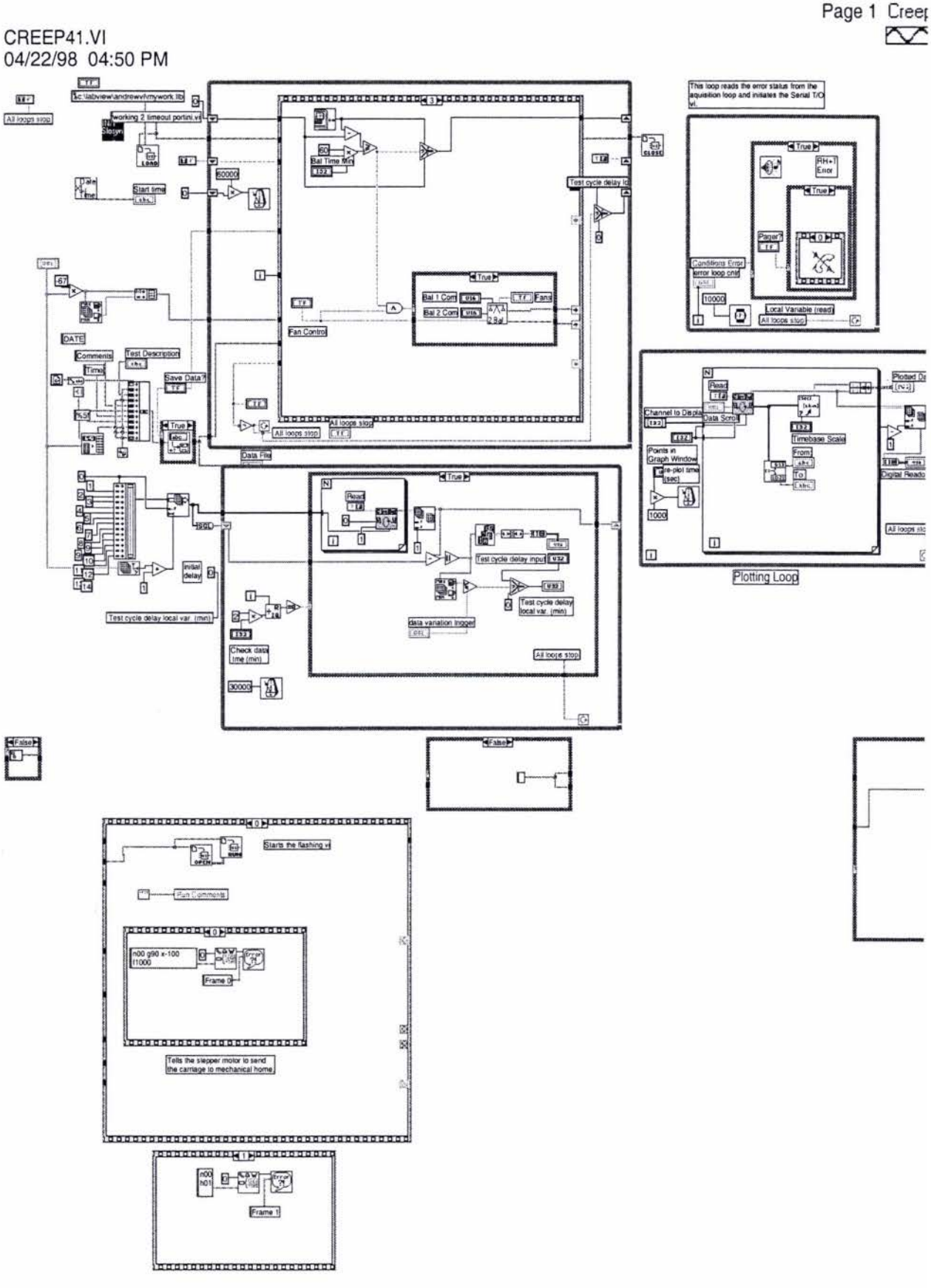
Page 1 Creep
CREEP41.VI
04/22/98 04:50 PM
All loops stop
working 2 timeout portini.vi
Start time
Bal Time (hr)
Test cycle delay (s)
Bal 1 Comm
Bal 2 Comm
Fans
Fan Control
DATE
Comments
Test Description
Save Data?
Data File
This loop reads the error status from the aquisition loop and initiates the Serial I/O vi.
RH+ Error
Pager?
Conditions Error
error loop cnfg
Local Variable (read)
Channel to Display
Data Scroll
Timebase Scale
Points in Graph Window
Plotting Loop
Read
Initial delay
Test cycle delay local var. (min)
Test cycle delay input
Test cycle delay local var. (min)
data variation trigger
Check data (mn (min)
Starts the flashing vi
Fan Comments
n00 g90 x-100 f1000
Frame 0
Tells the stepper motor to send the carriage to mechanical home
Frame 1

CREEP41.VI
04/22/98 04:50 PM

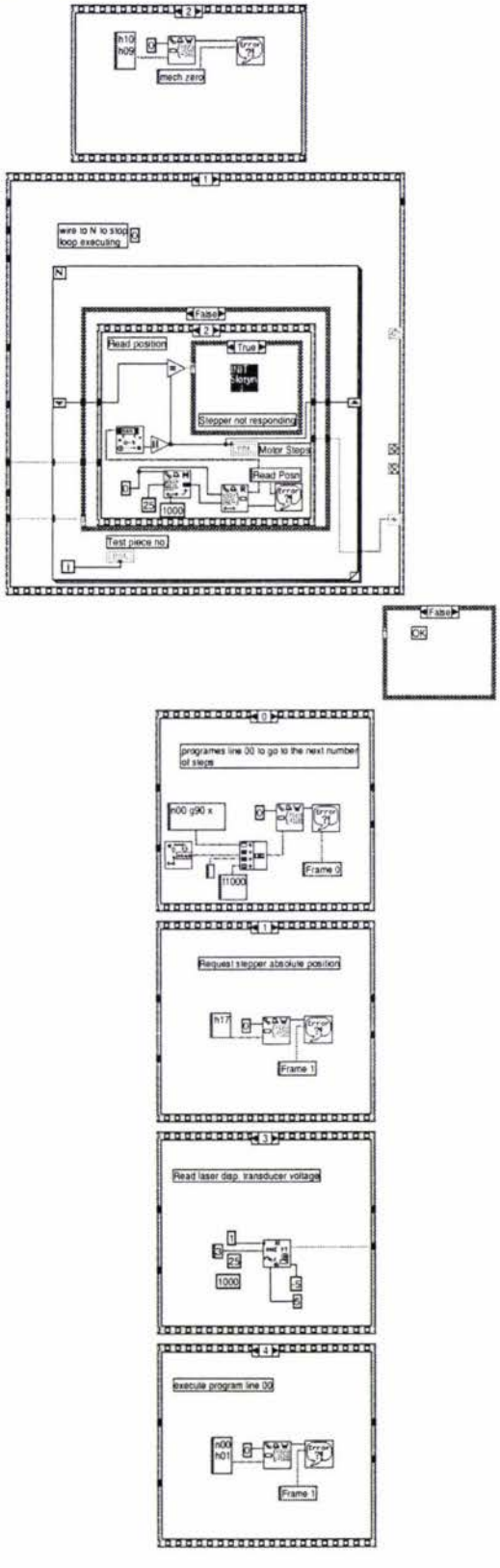

CREEP41.VI
04/22/98 04:50 PM

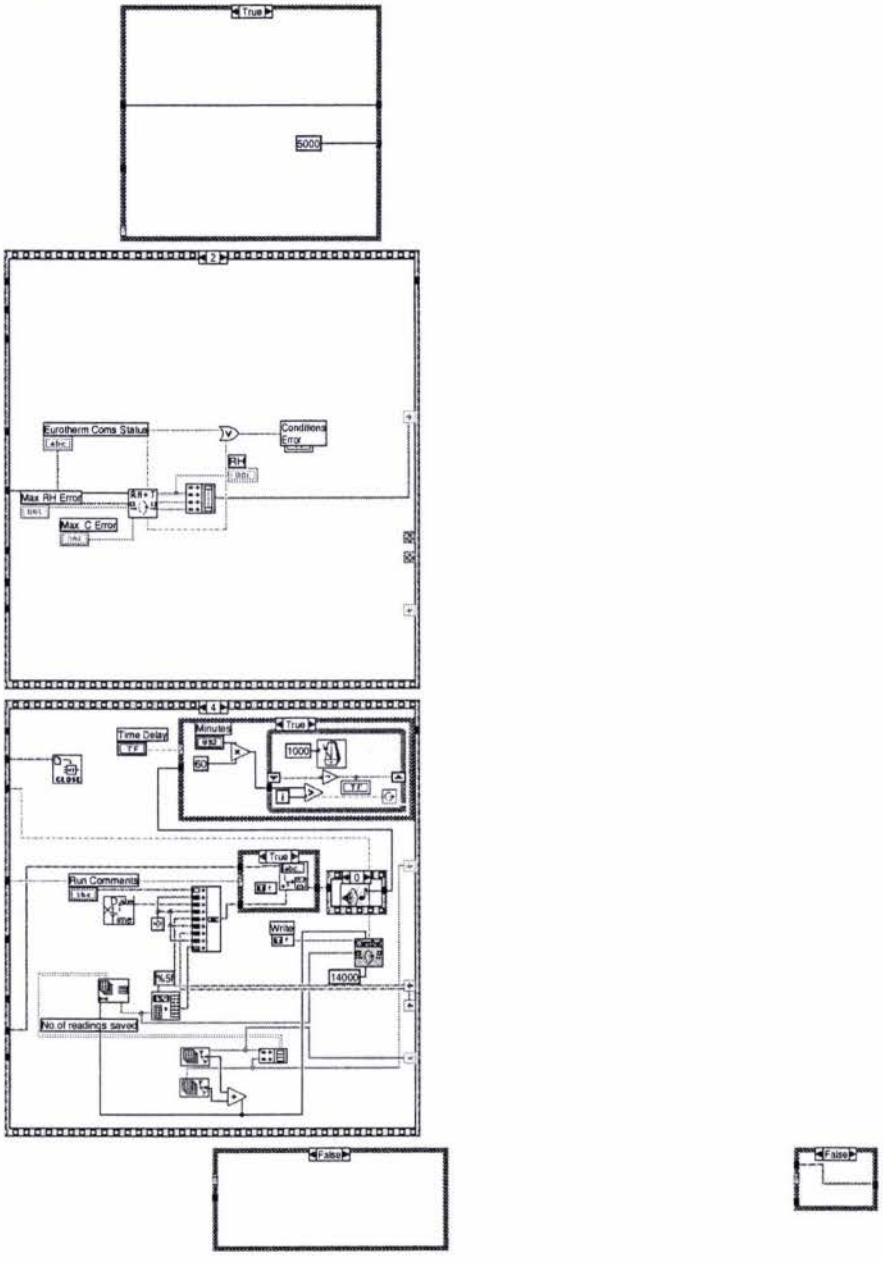

CREEP41.VI
04/22/98 04:50 PM

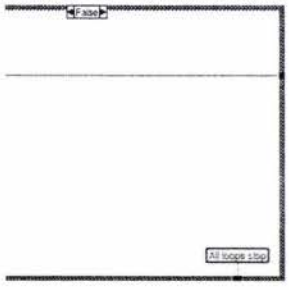

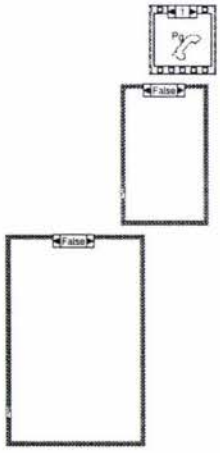

Page 1

SINERH4.VI
04/28/97 11:46 AM

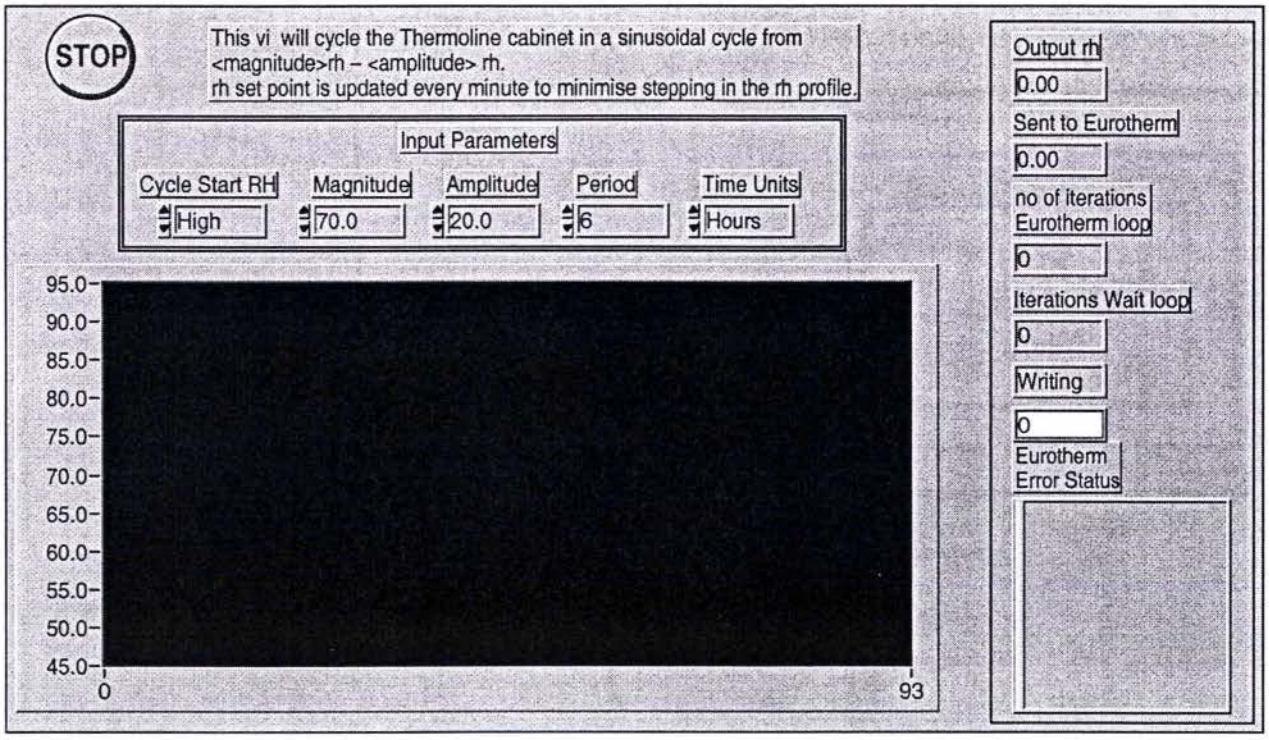

Page 1

SINERH4.VI
04/28/97 11:46 AM

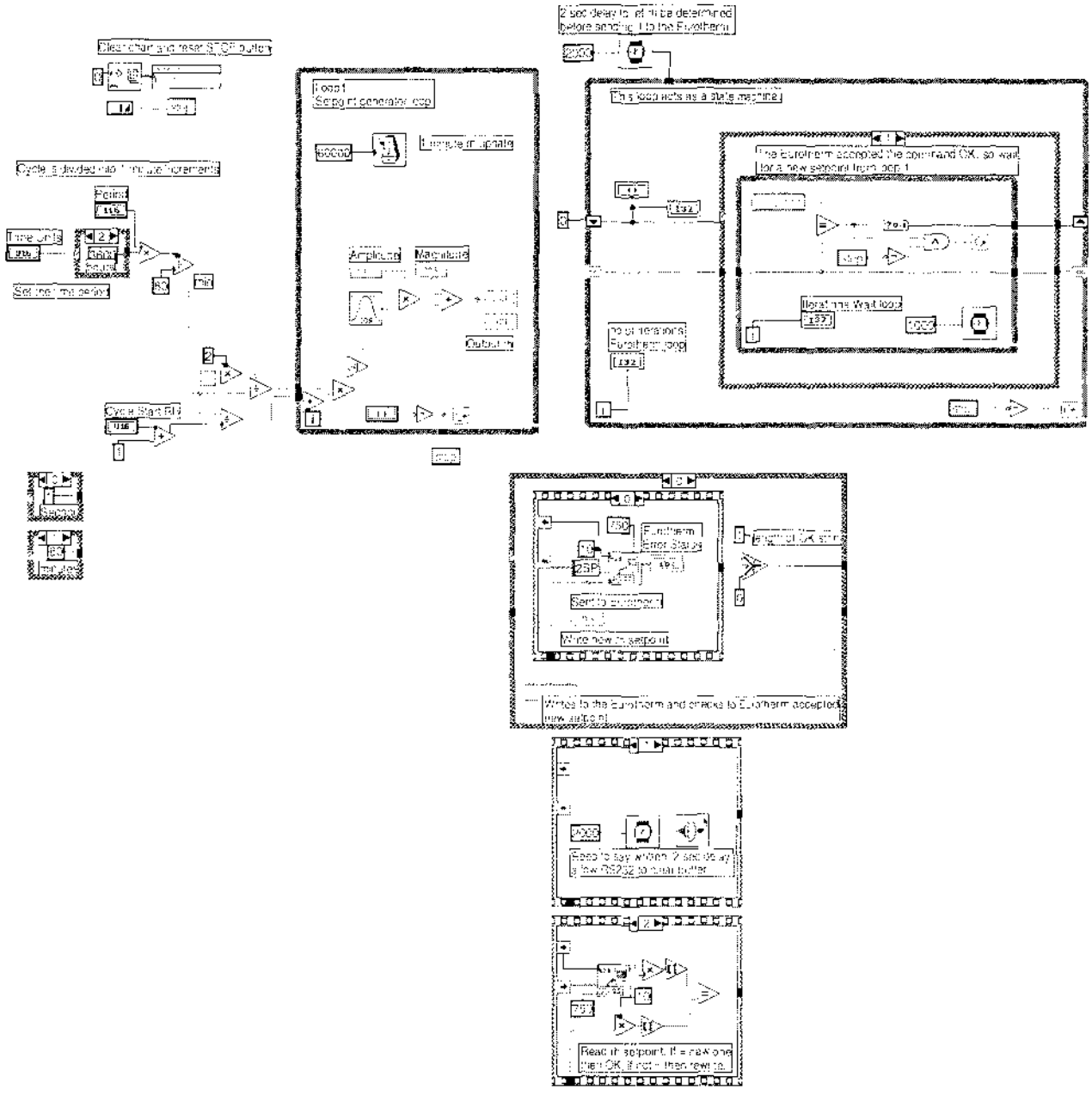

Appendix C

Creep Experiment Graphs

The following pages have the individual creep crurves.

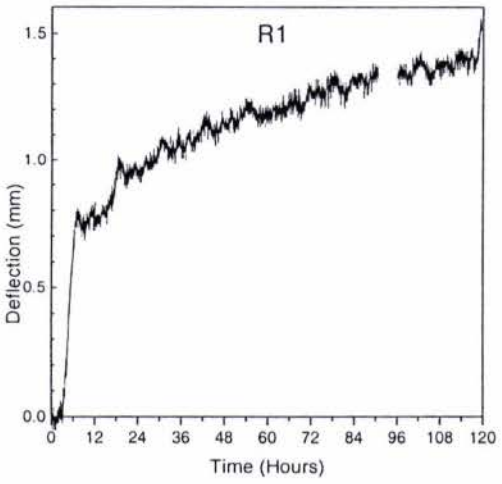

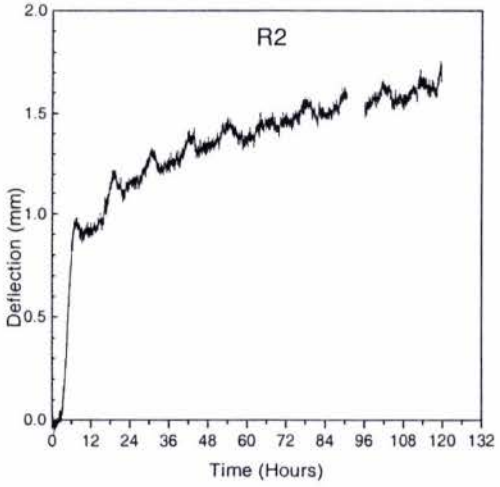

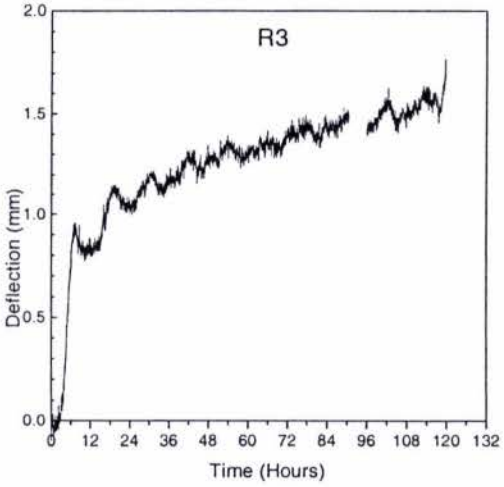

Creep test 71114

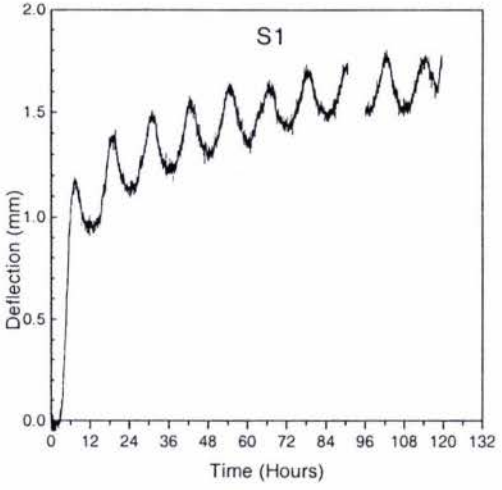

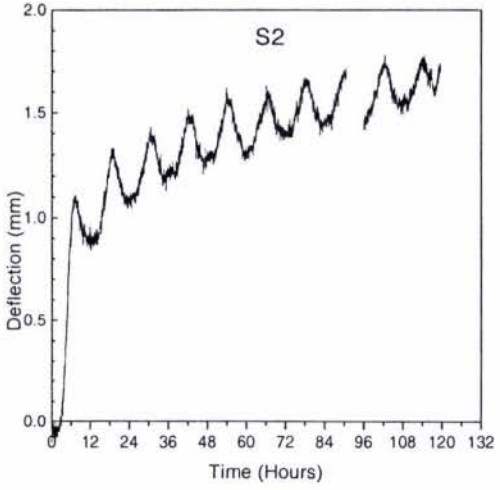

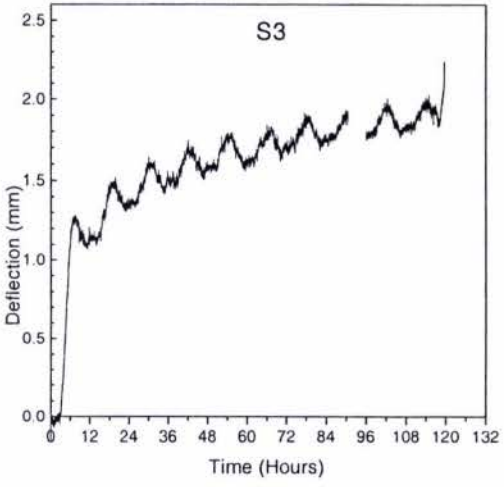

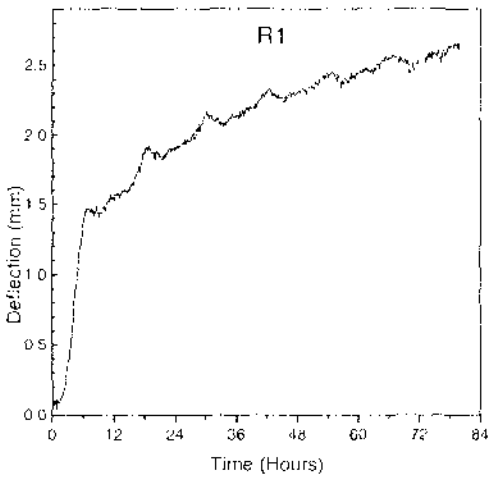

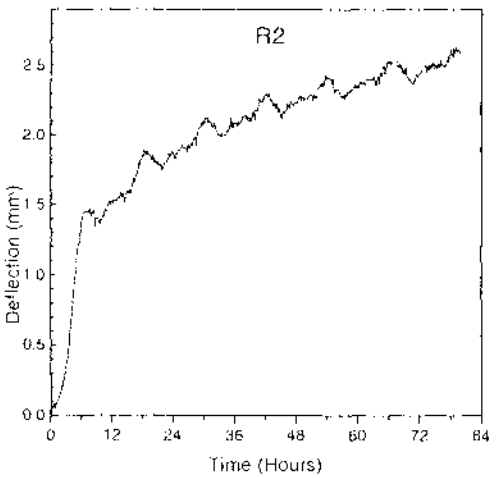

Creep Test 71205

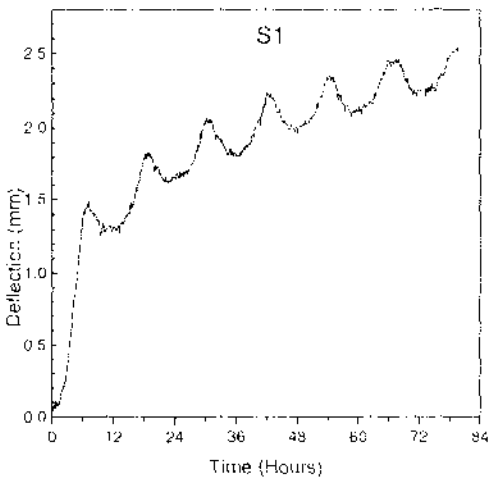

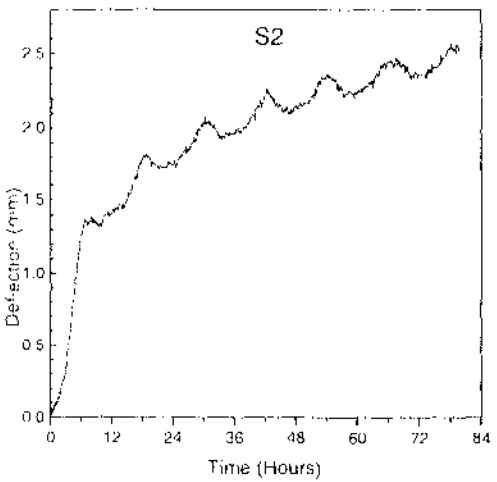

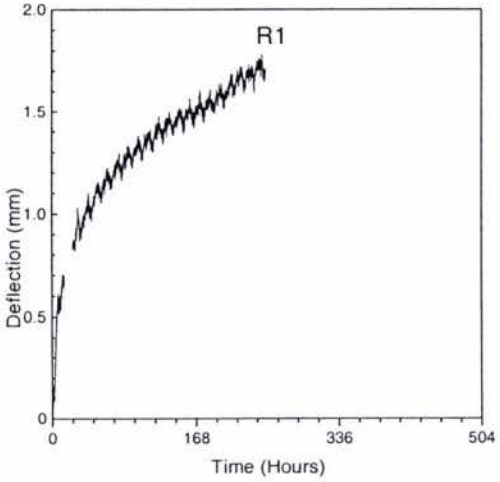

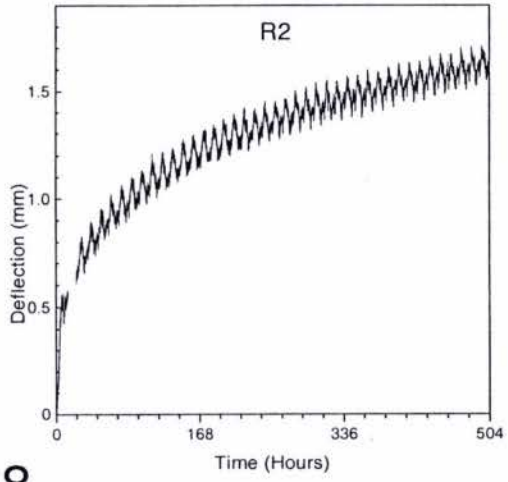

Creep Test 80218

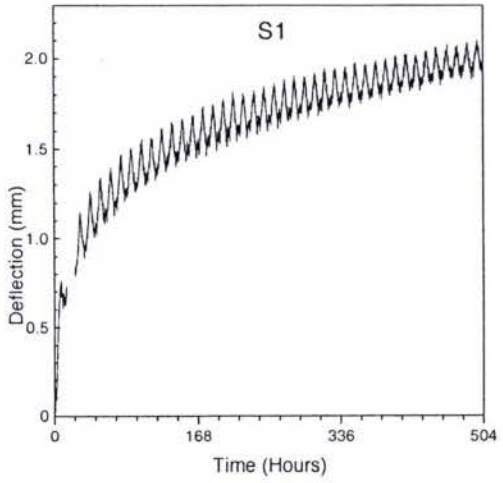

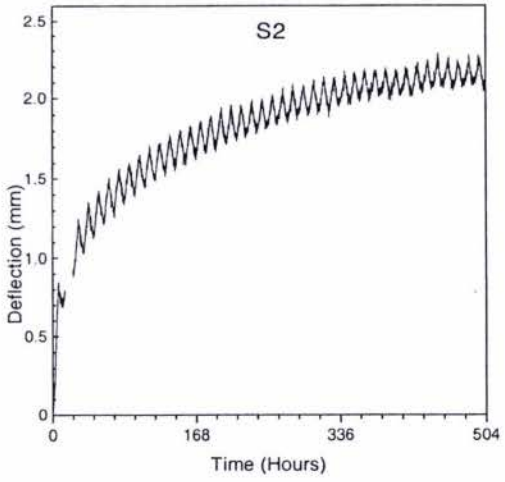

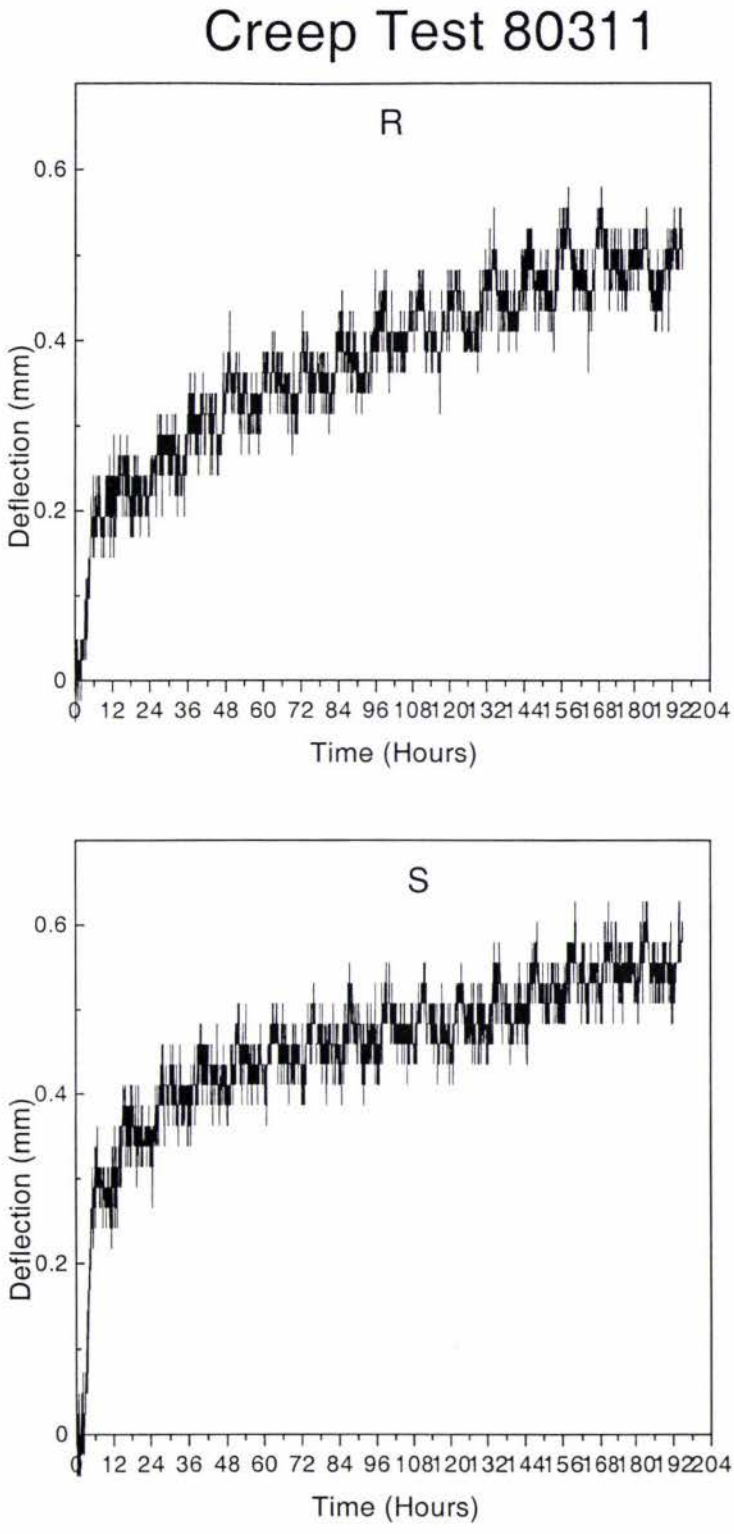
Creep Test 80311
R
Deflection (mm)
0
0.2
0.4
0.6
0 12 24 36 48 60 72 84 96 108 120 132 144 156 168 180 192 204
Time (Hours)
S
Deflection (mm)
0
0.2
0.4
0.6
0 12 24 36 48 60 72 84 96 108 120 132 144 156 168 180 192 204
Time (Hours)

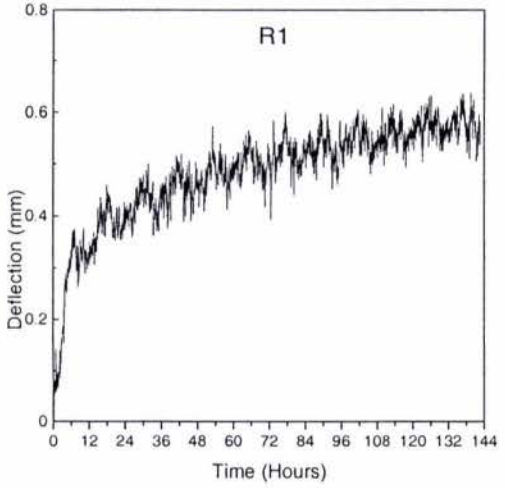

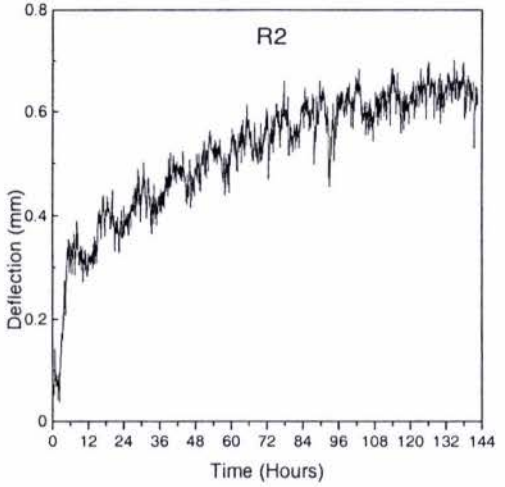

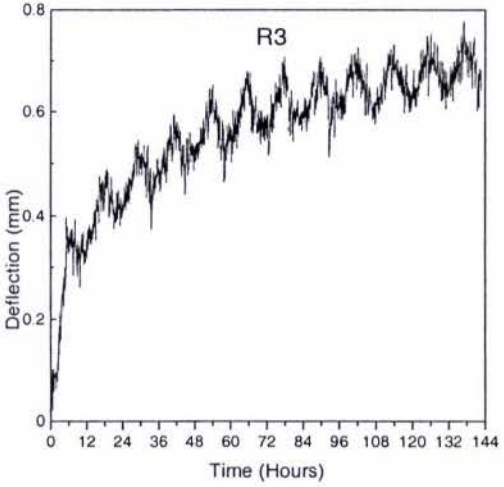

Creep Test 80403

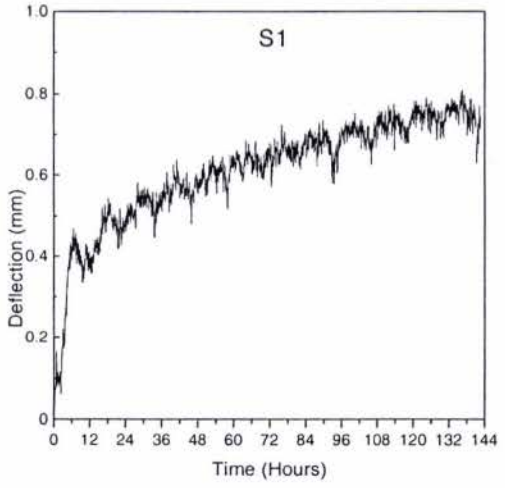

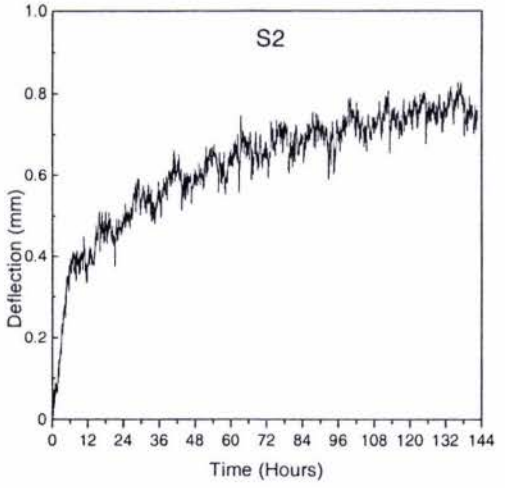

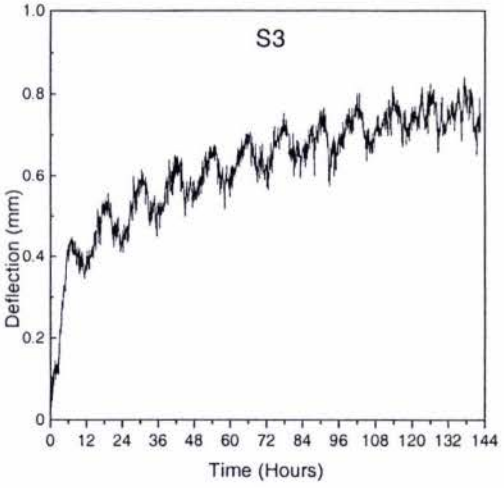

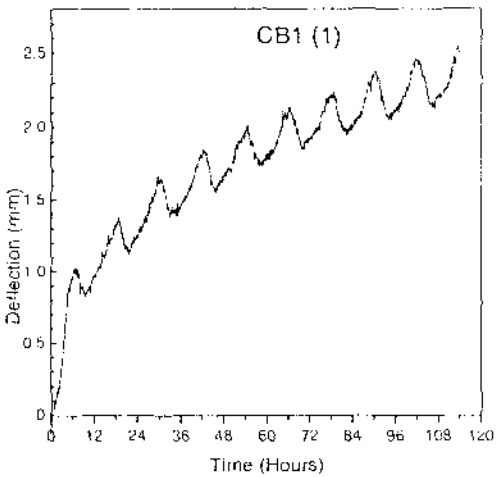

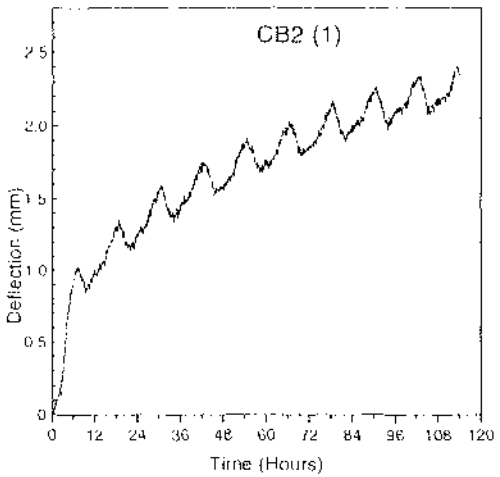

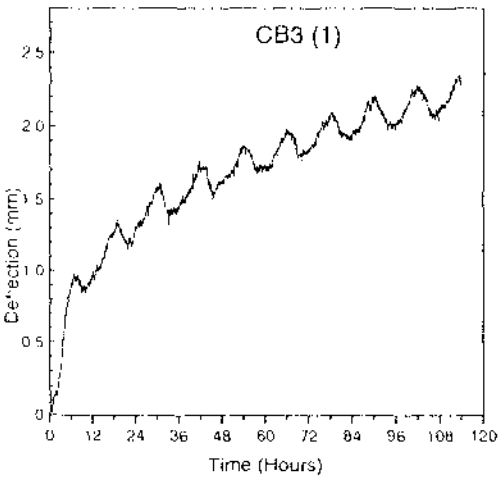

Creep Test 80409

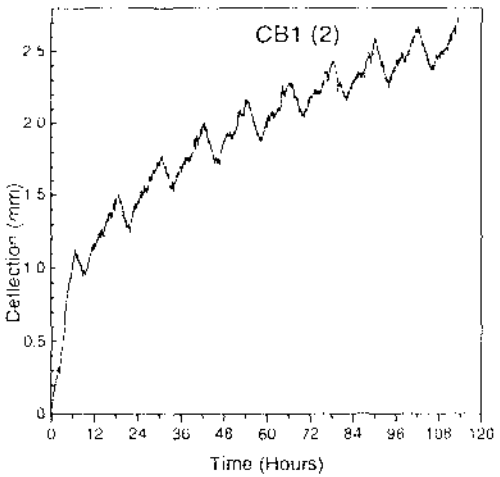

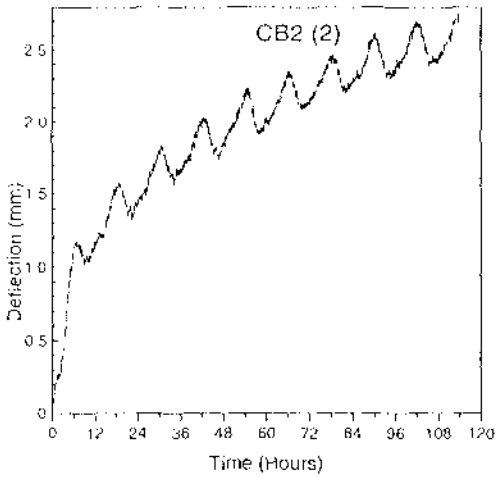

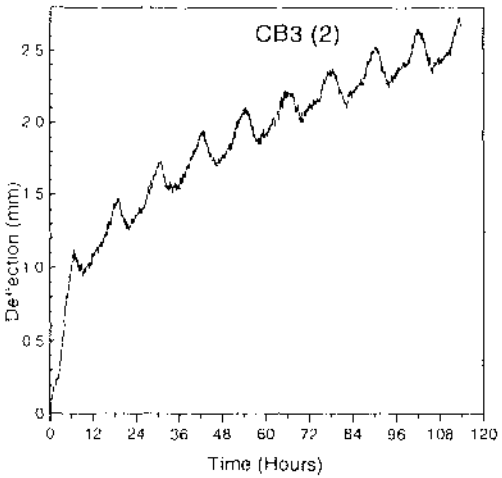

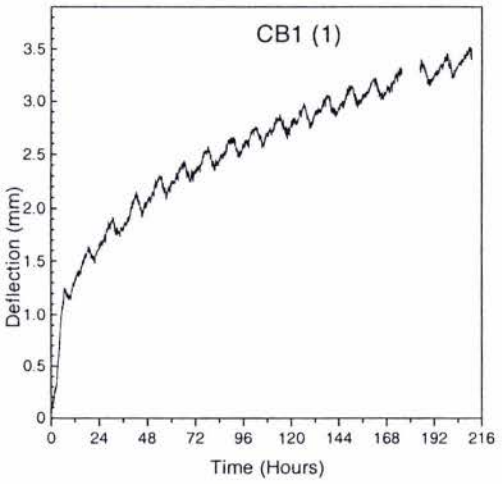

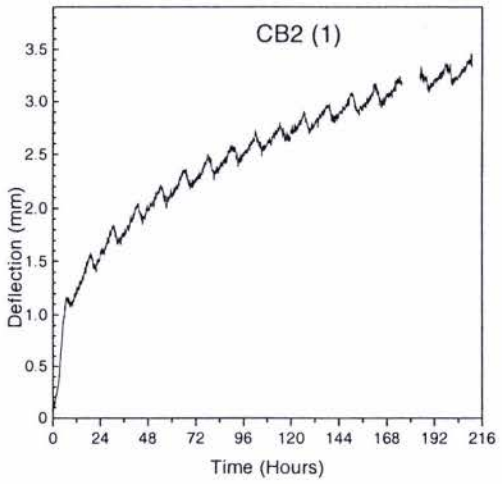

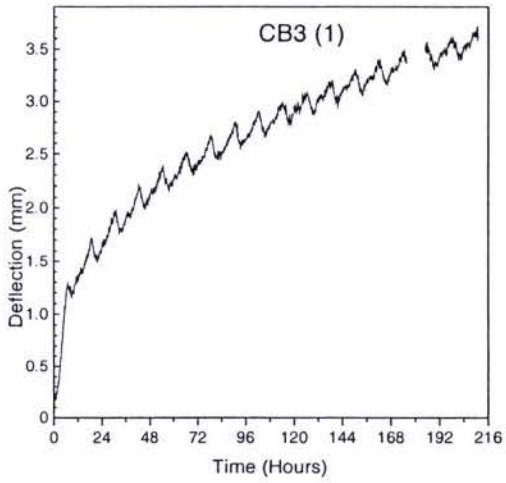

Creep Test 80422

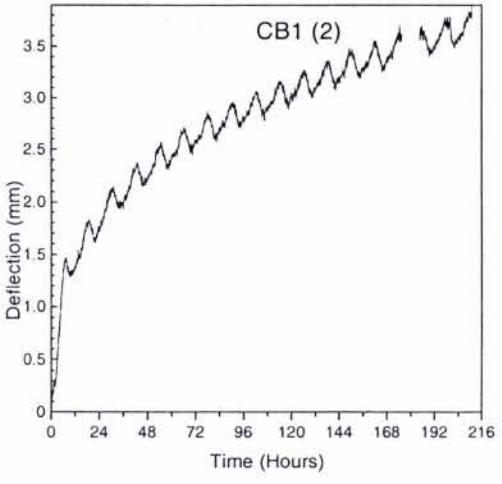

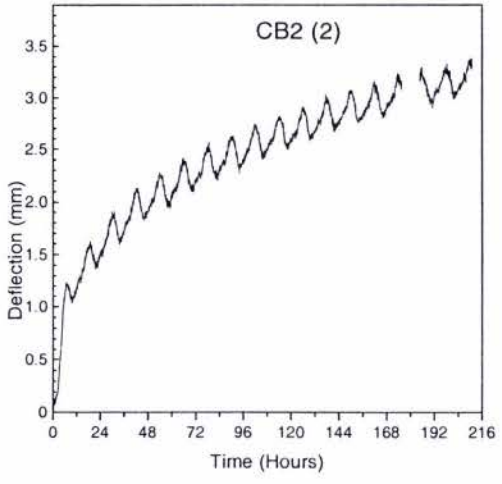

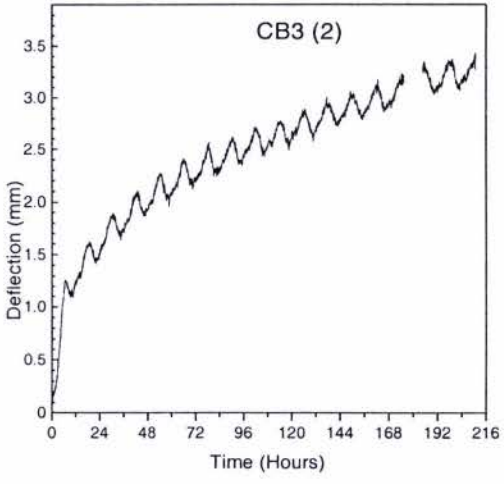

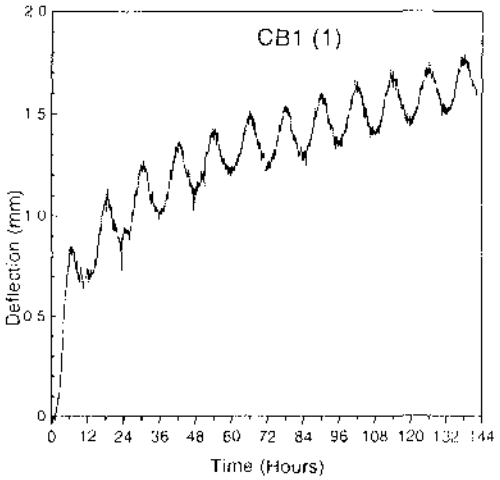

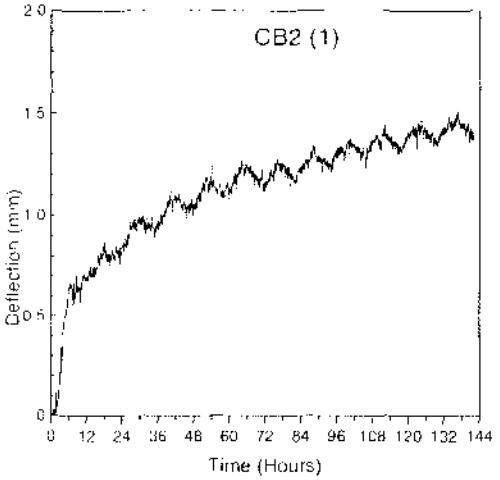

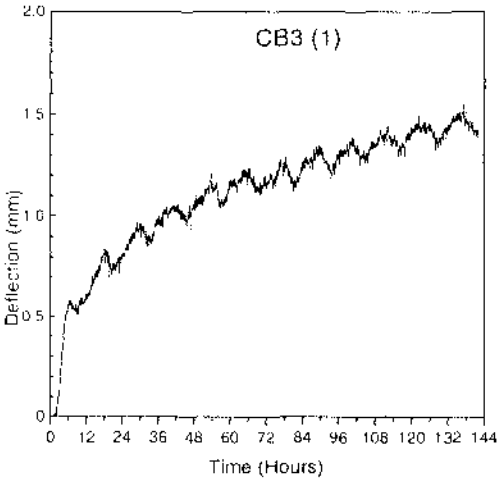

Creep Test 80622

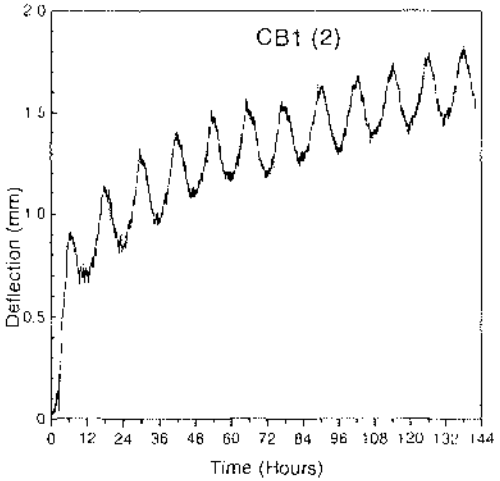

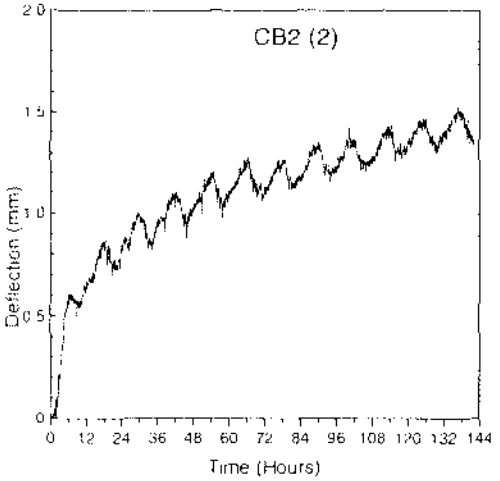

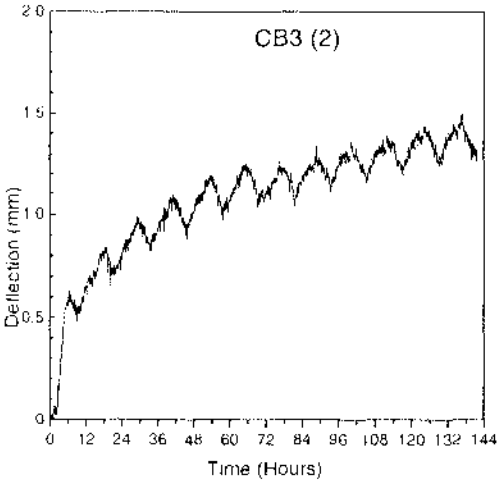

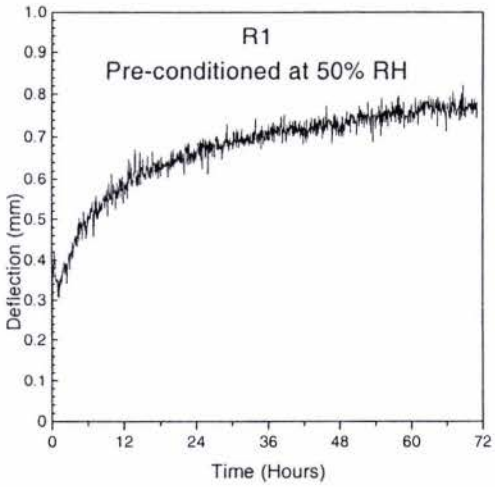

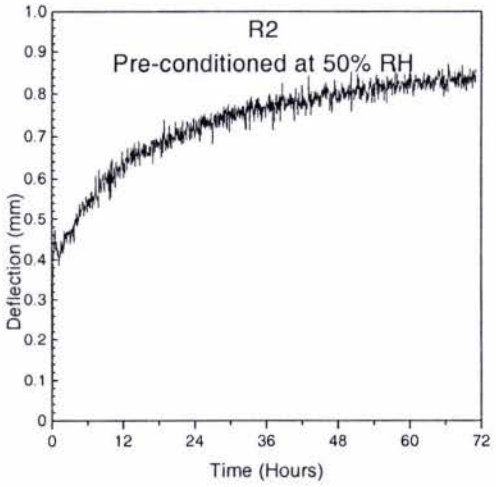

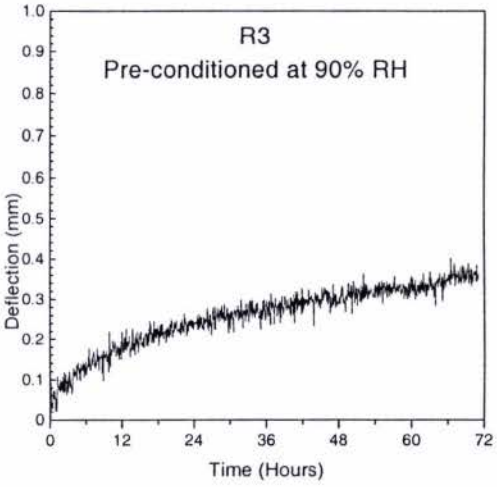

Creep Test 80629

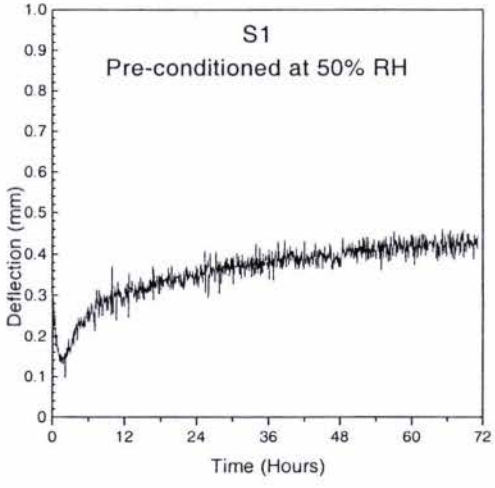

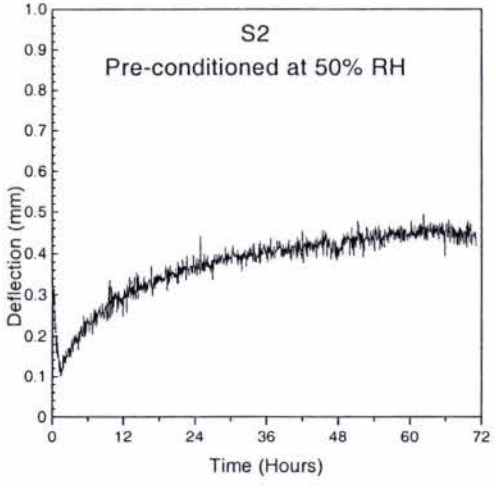

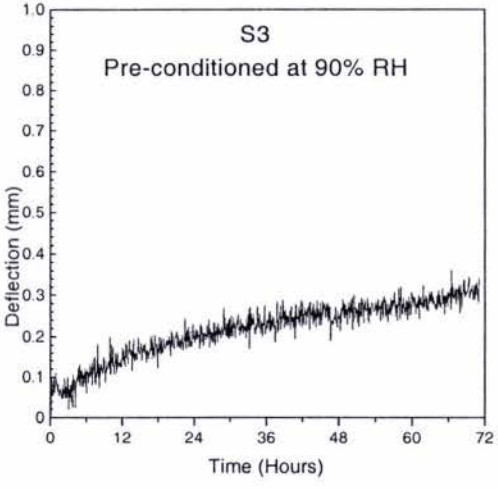

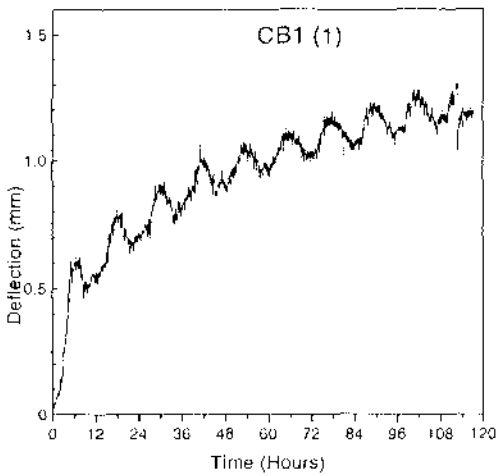

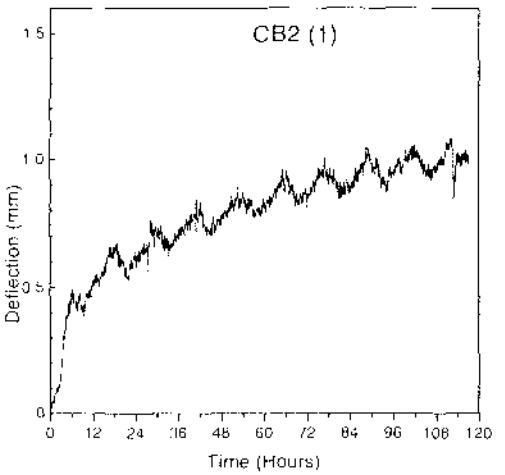

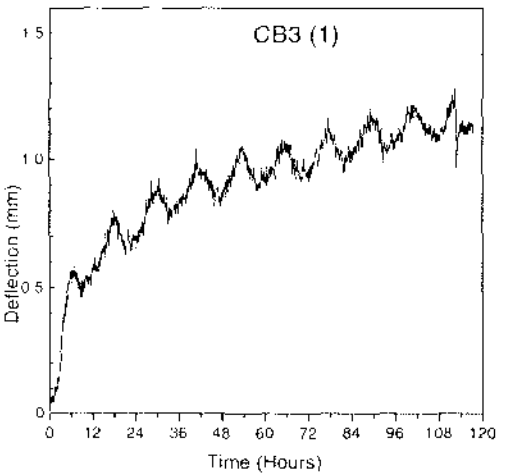

Creep Test 80704

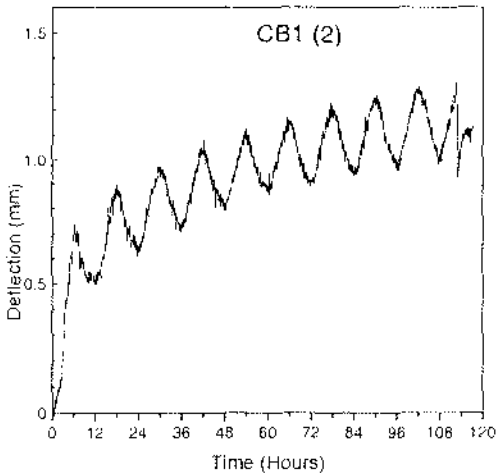

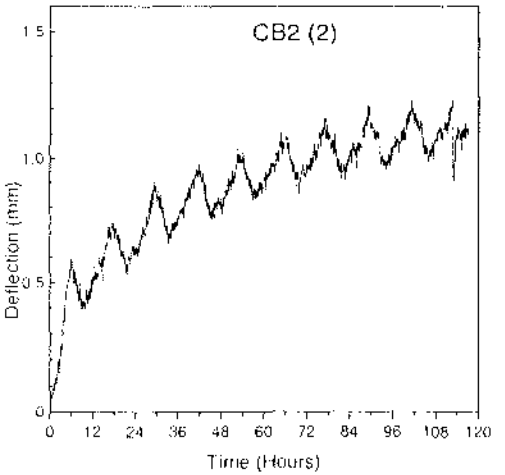

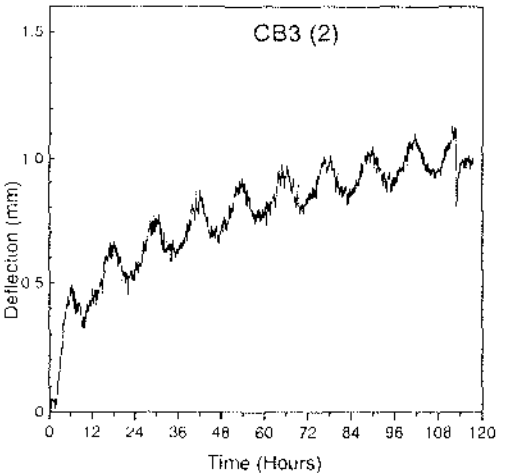

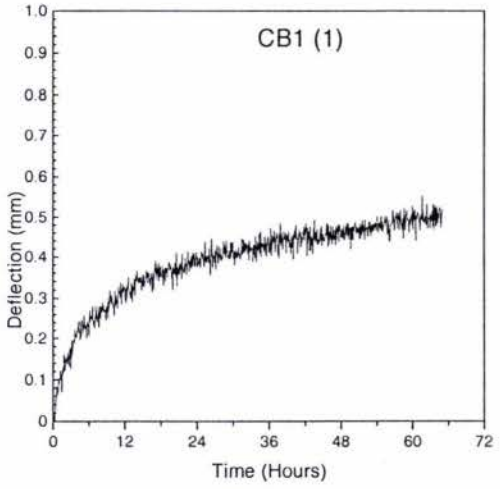

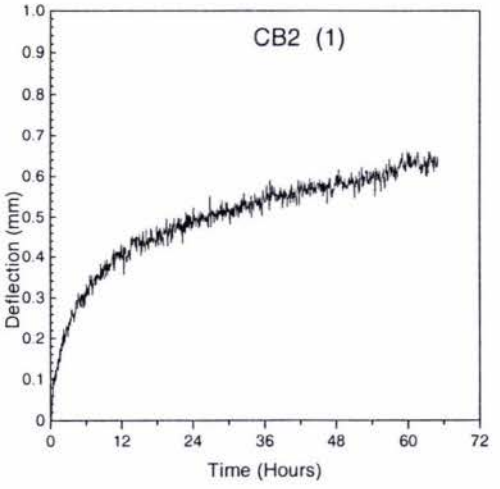

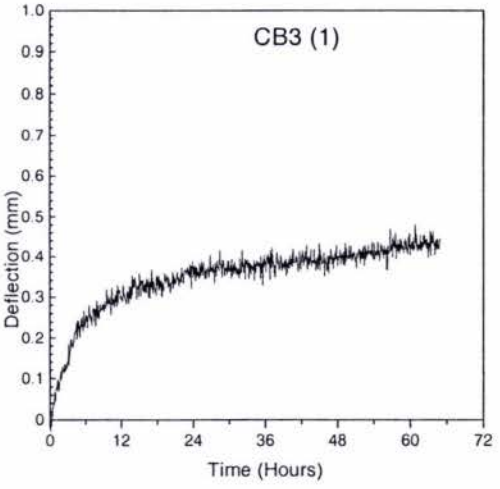

Creep Test 80709

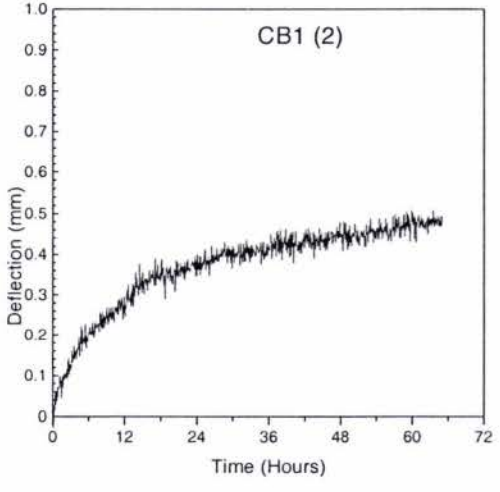

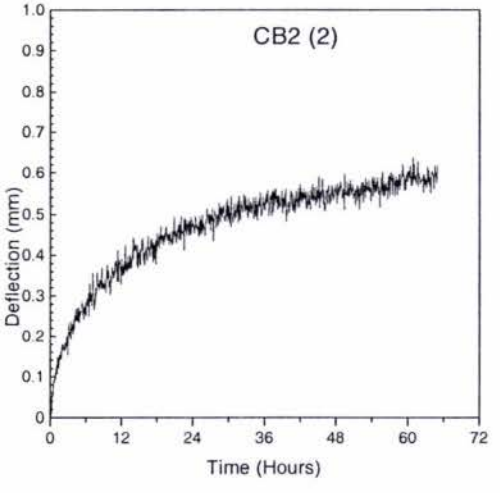

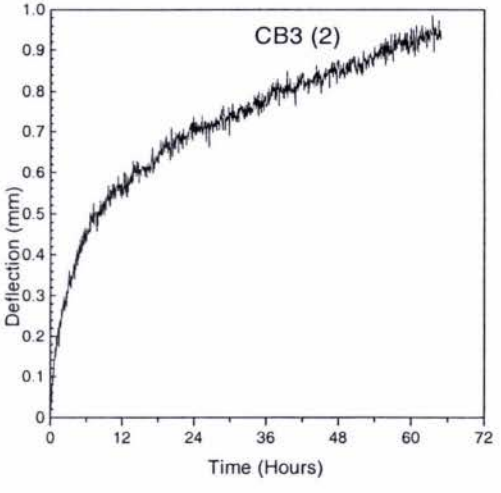

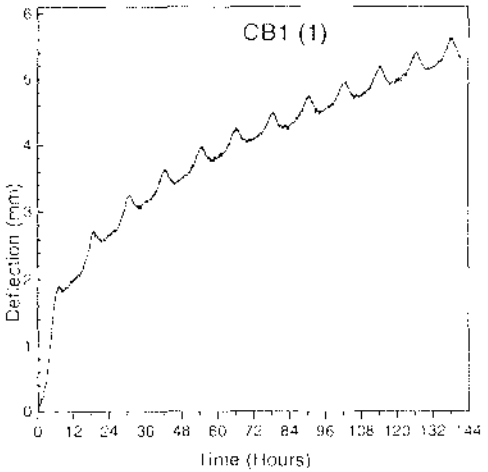

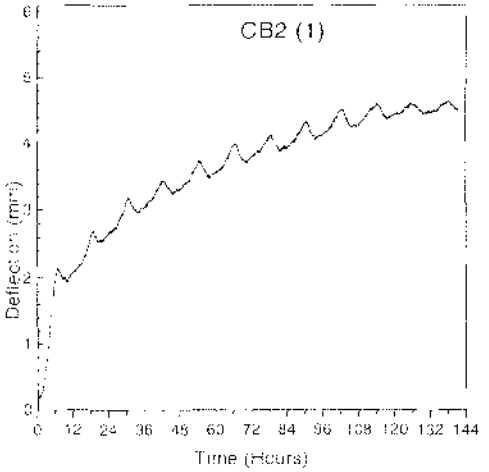

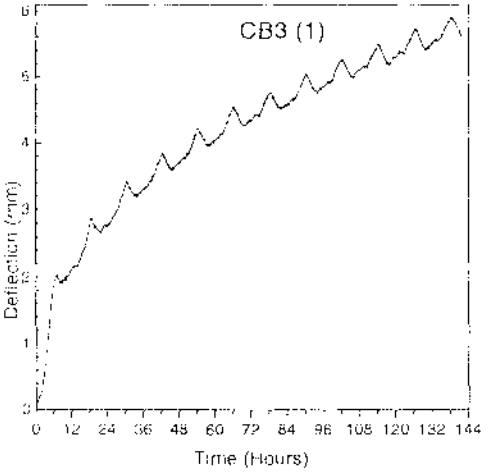

Creep Test 80714

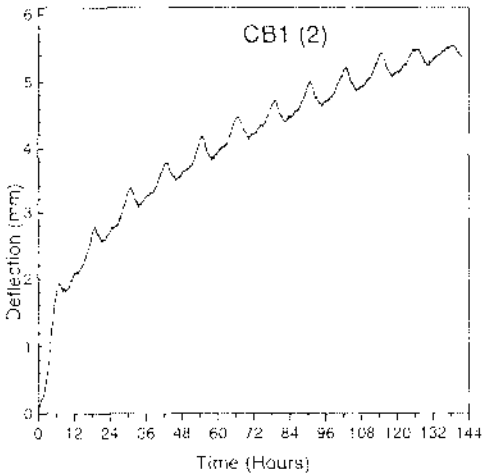

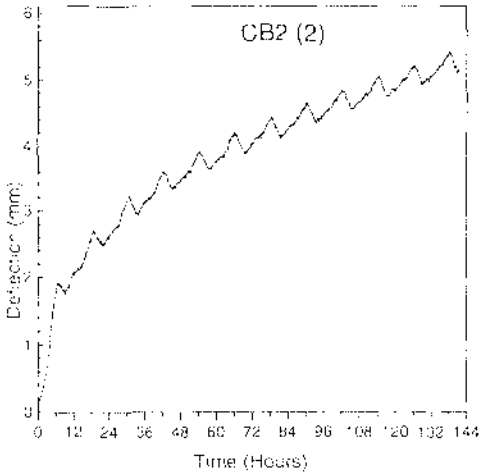

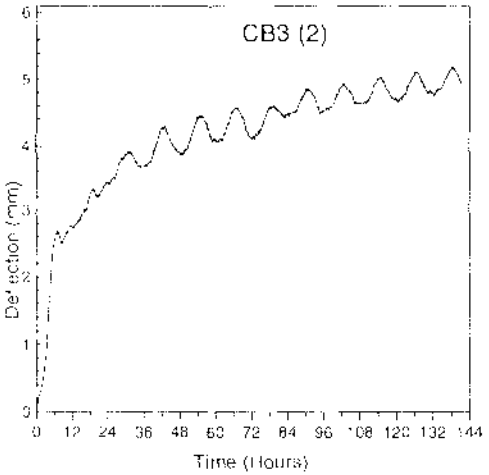

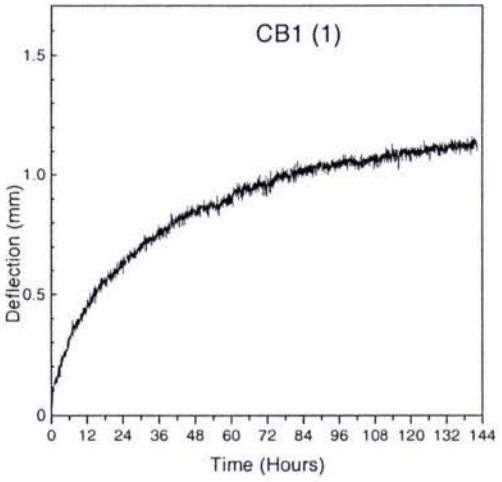

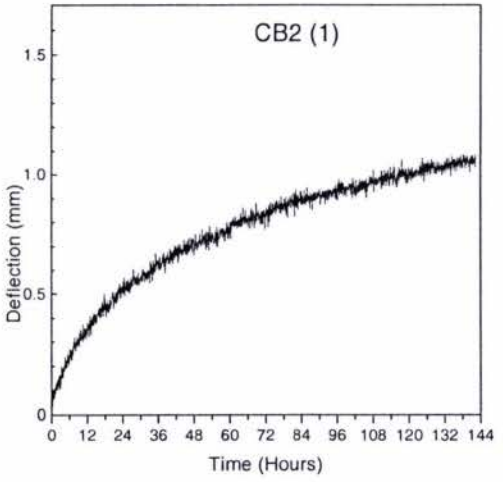

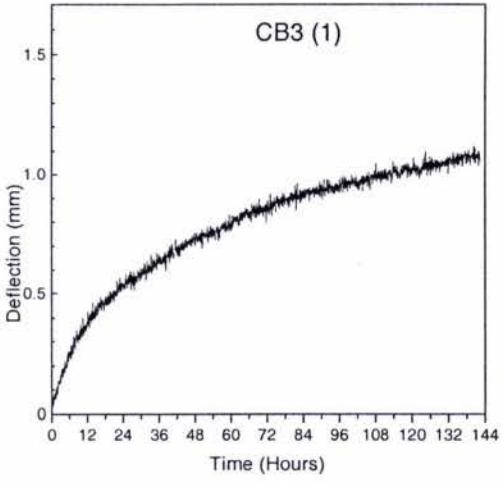

Creep Test 80721

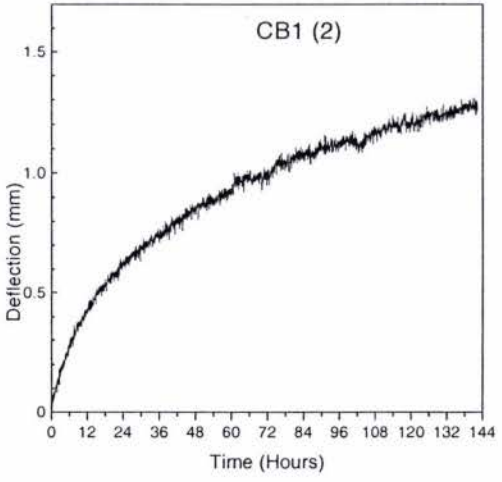

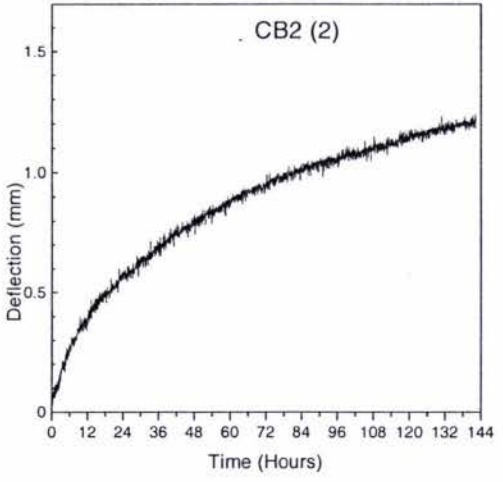

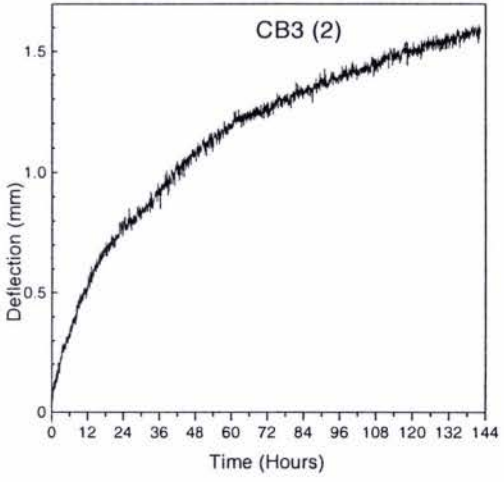

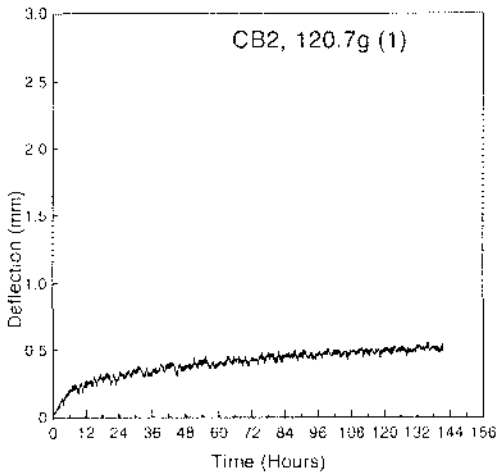

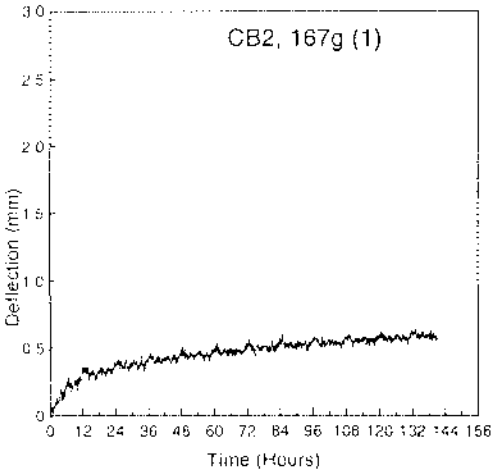

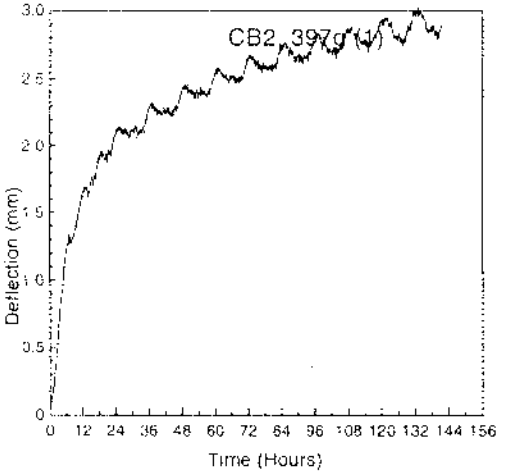

Creep Test 80824

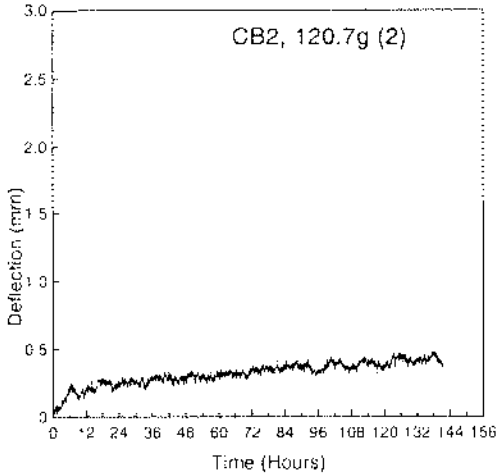

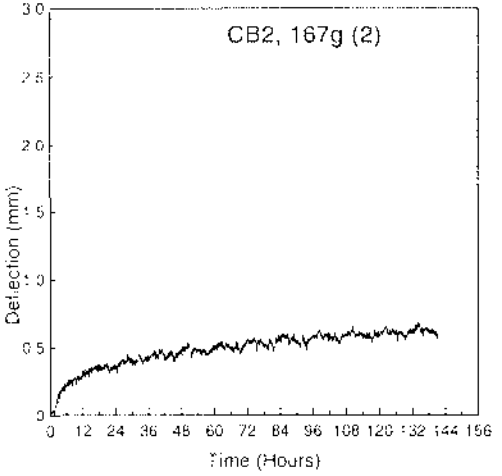

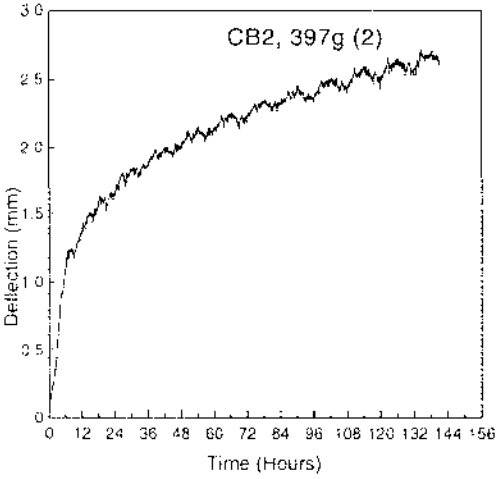

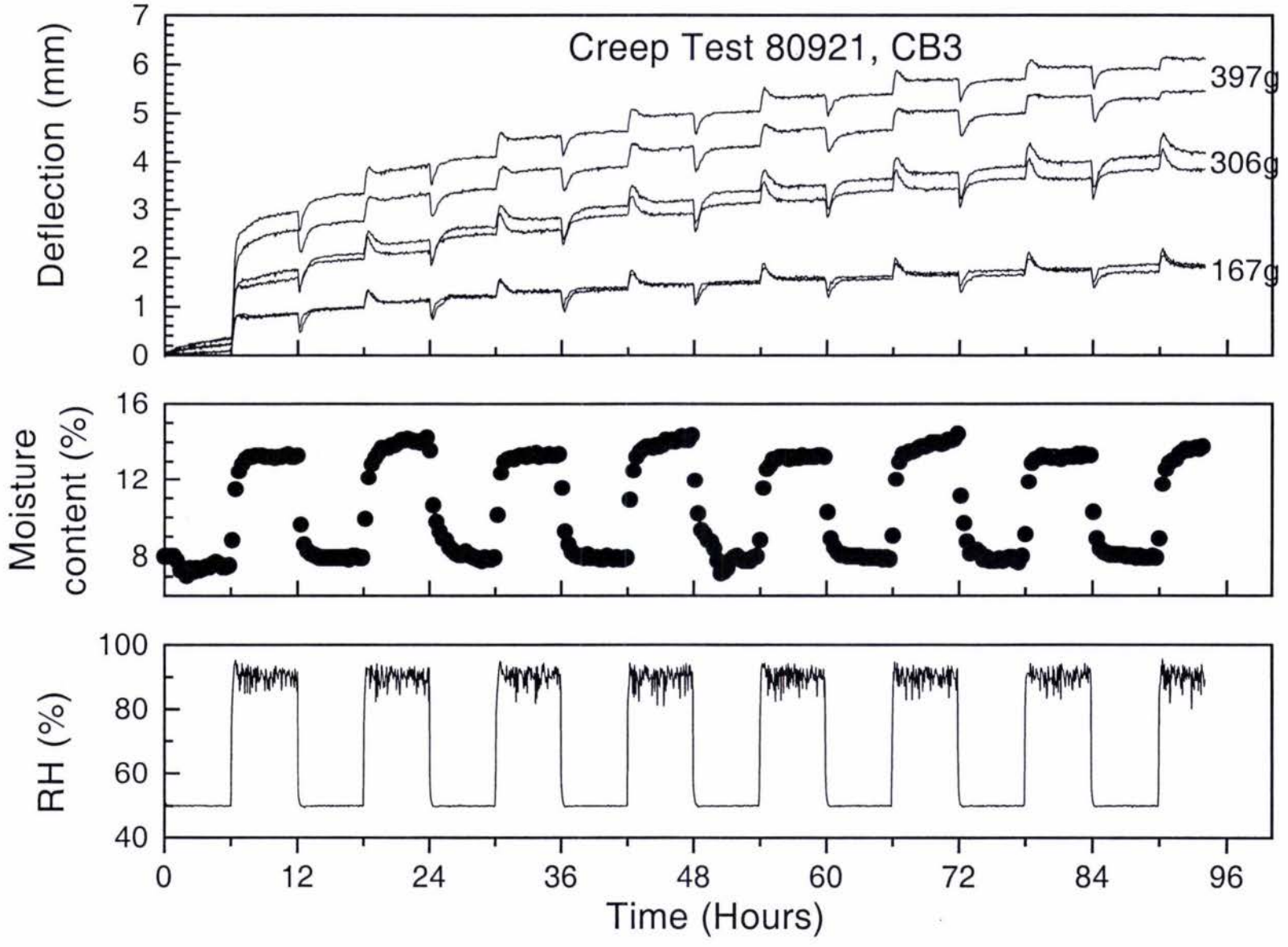
Creep Test 80921, CB3
397g
306g
167g
Deflection (mm)
0
1
2
3
4
5
6
7
Moisture content (%)
8
12
16
RH (%)
40
60
80
100
0
12
24
36
48
60
72
84
96
Time (Hours)

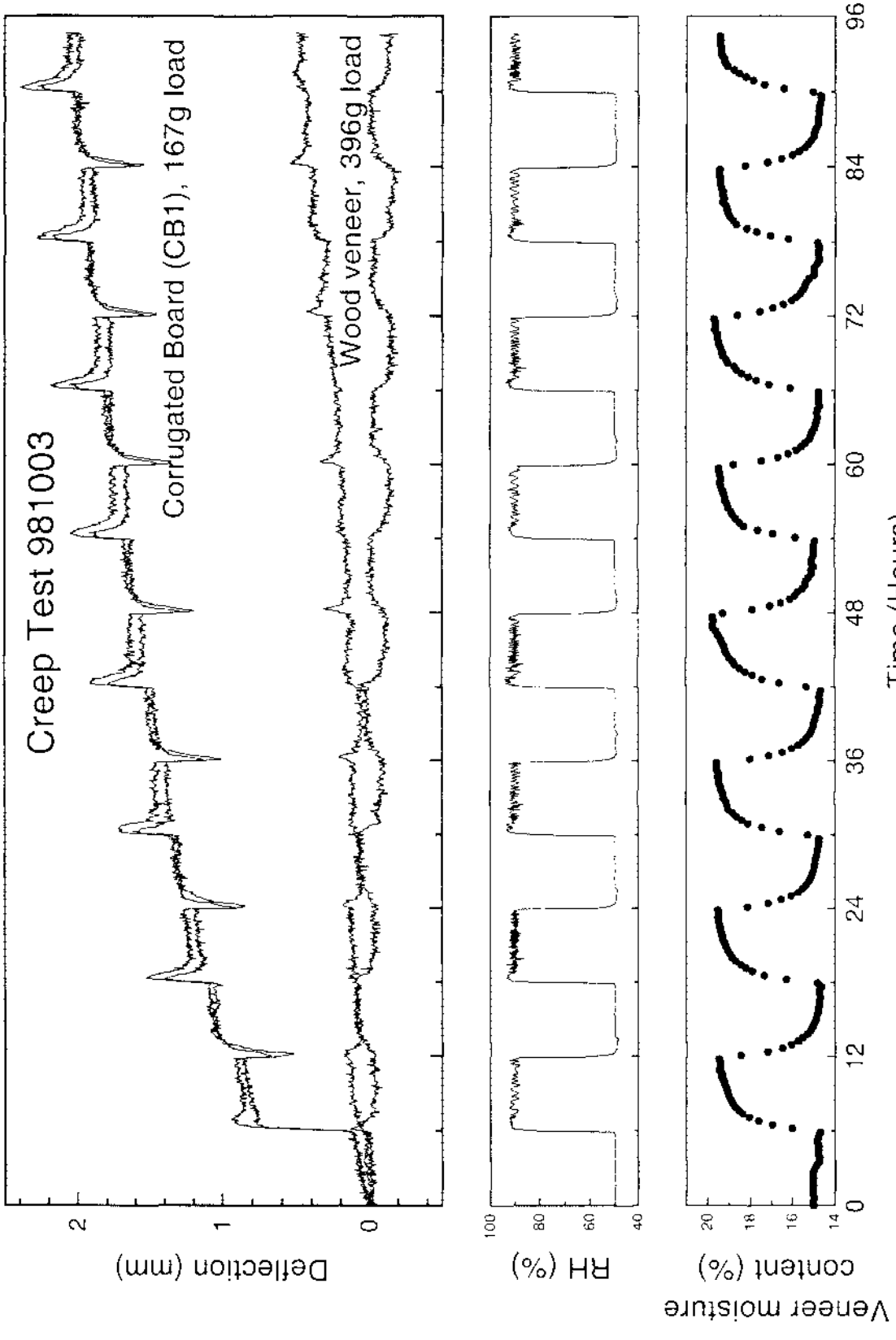
Creep Test 981003
Corrugated Board (CB1), 167g load
Wood veneer, 396g load
Deflection (mm)
RH (%)
Veneer moisture content (%)
Time (Hours)

References

Biermann, C.J. (1996) *Handbook of Pulping and Papermaking. 2nd ed.* Academic Press Inc.: San Diego

Brezinski, J.P. (1956) "The creep properties of paper." *Tappi* 39(2):116-128

Bronkhorst, C.A. (1997) "Towards a more mechanistic understanding of corrugated container creep deformation behaviour." *Journal of Pulp and Paper Science* 23(4):J174-J181

Byrd, V.L. (1972) "Effect of Relative Humidity Changes During Creep on Handsheet Paper Properties." *Tappi Journal* 55(2):247-252

Chalmers, I.R. (1994a) "Cyclic Humidity - Dimensional stability and theta angle on linerboard." : PAPRO Report C510, New Zealand Forest Research Institute, Rotorua, NZ

Chalmers, I.R. (1994b) "Mechanical Performance of Packaging Grade Paper Under High and Cycling Relative Humidity" : PAPRO Report C526, New Zealand Forest Research Institute, Rotorua, NZ

Chalmers, I.R. (1997) "Conference discussion", *Proceedings: 3rd International Symposium, Moisture and Creep Effects on Paper, Board and Containers, 20-21 February 1997, Rotorua, NZ.* (Chalmers, I.R. ed.) pp.201-214: PAPRO NZ, Appita, US Forest Products Laboratory United States Department of Agriculture/Forest Service.

Considine, J.M. (1992) "Investigation of role of hygroexpansivity on the compressive creep behaviour of paperboard." in *Proceedings: Cyclic Humidity Effects on Paperboard Packaging, 14-15 September 1992, Madison, Wi, USA.* (Laufenberg, T.L. and Leake, C.H. ed.) pp.79-92: US Forest Products Laboratory United States Department of Agriculture/Forest Service.

Considine, J.M.; Stoker, D.L.; Laufenberg,T.L.; Evans,J.W. (1994) "Compressive creep behaviour of corrugating components affected by humid environment." *Tappi Journal* 77(1):87-95

Fridley, K.J.; Tang, R.C.; Soltis, L.A. (1992) "Creep behaviour model for structural lumber." *Journal of Structural Engineering* 118(8):2261-2277

Gunderson, D.E.; Laufenberg, T.L. (1994) "Apparatus for evaluating stability of corrugated board under load in cyclic humidity environment." *Experimental Techniques* 18(1):27-31

Gunderson, D.E.; Tobey, W.E. (1990) "Tensile creep of paperboard - effect of humidity change rate." *Materials Research Society Symposium Proceedings Materials Interactions Relevant to the Pulp, Paper, and Wood Industies.* (Caulfield, D. F., Passaretti, J. D.; Sobczynski, S.F. ed.) pp.213-216: Materials Research Society.

Haraldsson, T.; Fellers,C.; Kolseth,P. (1993) "The edgewise compression of paperboard." *Products of Papermaking - Transactions of the Tenth Fundamental Research Symposium, September 1993, Oxford, UK.* (Baker, C.F. ed.) pp.601-637: Pira International, Leatherhead

Haraldsson, T.; Fellers, C.; Söremark, C. (1997) "Creep properties of paper - principles of evaluation." *Proceedings: 3rd International Symposium, Moisture and Creep Effects on Paper, Board and Containers, 20-21 February 1997, Rotorua, NZ.* (Chalmers, I.R. ed.) pp.237-246: PAPRO NZ, Appita, US Forest Products Laboratory United States Department of Agriculture/Forest Service.

Haslach Jr., H.W. (1998) University of Maryland, Private Communication, 12 August.

Haslach Jr., H.W. (1997) "Relaxation of moisture accelerated creep, backstress and hygroexpansion." *Mechanics of Cellulosic Materials - 1997, The 1997 Joint ASME/ASCE/SES Summer Meeting, 29 June-2 July 1997, Evanston, Il, USA* (Perkins, R. ed.) pp.45-53: The American Society of Mechanical Engineers

Haslach Jr., H.W.; Pecht, M.G.; Wu, X. (1991) "Variable humidity and load interaction in tensile creep of paper." *Proceedings: 1991 TAPPI International Paper Physics Conference, 22-26 September 1991, Kona, HI, USA* pp.219-224: Tappi Press, Atlanta, GA

Hoffmeyer, P.; Davidson, R. W. (1989) "Mechano-sorptive creep mechanism of wood in compression and bending." *Wood Science and Technology* 23(3):215-227

Jönson, G. (1993) *Corrugated Board Packaging.* : Pira International, Leatherhead, UK

Kocurek, M.J. (ed) (1983-1993) *Pulp and Paper Manufacture. 3rd ed. Vols 1-10.* : Joint Textbook Committee of the Paper Industry, Canada

Kolseth, P.; de Ruvo, A. (1983) "The measurement of viscoelastic behaviour for the characterization of time-, temperature-, and humidity dependent properties." in *Handbook of physical and mechanical testing of paper and paperboard.* (Mark, R.E. ed.) pp.255-322: Marcel Dekker Inc., New York

Kuskowski, S.J.; Considine, J.M. and Lee, S.K. (1995) "Corrugating components and their relationship to combined board performance." *Moisture-Induced Creep Behaviour of Paper and Board, 5-7 December 1994, Stockholm, Sweden* (Fellers, C.; Laufenberg, T.L. ed.) pp.223-231: US Forest Products Laboratory United States Department of Agriculture/Forest Service.

Laufenberg, T.L. (1991) "Characterisation of paperboard, combined board, and container performance in the service moisture environment." *Proceedings: 1991 TAPPI International Paper Physics Conference, 22-26 September 1991, Kona, HI, USA* pp.299-30: Tappi Press

Luo, S.; Suhling, J.C.; Laufenberg,T.L. (1995) "Bending and twisting tests for the measurement of the stiffnesses of corrugated board." *Mechanics of Cellulosic Materials-1995.* (Perkins, R. ed.) pp.91-109 : The American Society of Mechanical Engineers

Mark, R.E. (ed) (1983) *Handbook of Physical and Mechanical Testing of Paper and Paperboard. Vols 1 and 2.*: Marcel Dekker Inc. New York

Markström, H. (1991) *The Elastic properties of paper - test methods and measurement instruments.* :Lorentzen & Wettre

McDougall, A. (1994) *Achievement Report.* Unpublished

McKee, R.C.; Gander, J.W.; Wachuta, J.R. (1963) "Compression strength formula for corrugated board." *Paperboard Packaging* 48(8):149-159

Mohager, S.; Toratti, T. (1993) "Long term bending creep of wood in cyclic relative humidity." *Wood Science and Technology* 27(1):49-59

Niskanen, K.J.; Kuskowski,S.J.; Bronkhorst,C.A. (1997) "Dynamic hygroexpansion of paperboards." *Nordic Pulp and Paper Research Journal* 12(2):103-110

Nordstrand, T.; Hägglund, R. (1997) "Predicting sagging of a corrugated board tray bottom using isochrones." in *Proceedings: 3rd International Symposium, Moisture and Creep Effects on Paper, Board and Containers,20-21 February 1997, Rotorua, NZ.* (Chalmers, I.R. ed.) pp.215-220: PAPRO NZ, Appita, US Forest Products Laboratory United States Department of Agriculture/Forest Service.

Norimoto, M.; Gril, J.; Rowell, R.M.X. (1992) "Rheological properties of chemically modified wood: relationship between dimensional and creep stability." *Wood and Fiber Science* 24(1):25-35

Padanyi, Z.V. (1991) "Mechano-sorptive effects and accelerated creep in paper." *Proceedings: 1991 TAPPI International Paper Physics Conference, 22-26 September 1991, Kona, HI, USA* pp.397-411: Tappi Press, Atlanta, GA

Pecht, M.G. (1985) "Creep of regain-rheologically simple hydrophilic polymers." *Journal of Strain Analysis* 20(3):179-181

Peterson, W.S. (1983) "Flute / liner interaction for bending of combined board beams." *Paperboard Packaging* August 1983:37-41

Pierce, C.B.; Dinwoodie, J.M.; Paxton, B.H. (1979) "Creep in chipboard Part 2: The use of fitted response curves for comparative and predictive purposes." *Wood Science and Technology* 13:265-282

Salmén, L. (1993) "Responses of moisture properties to changes in moisture content and temperature." *Products of Papermaking - Transactions of the Tenth Fundamental Research Symposium, September 1993, Oxford, UK.* (Baker, C.F. ed.) pp.369-430: Pira, Leatherhead

Smook, G.A. (1992) *Handbook for pulp and paper Technologists. 2nd ed.*: Angus Wilde Publications, Vancouver

Söremark, C.; Fellers, C. (1993) "Mechano-sorptive creep and hygroexpansion of corrugated board in bending." *Journal of Pulp and Paper Science* 19(1):J19-J26

Söremark, C.; Fellers, C.; Henriksson, L. (1993) "Mechano-sorptive creep of paper." *Products of Papermaking - Transactions of the Tenth Fundamental Research Symposium, September 1993, Oxford, UK.* (Baker, C.F. ed.) pp.547-574: Pira, Leatherhead

Thorpe, J.; Choi, D. (1992) "Linear image strain analysis details corrugated container compression failure modes." *1992 TAPPI Corrugated Containers Conference, 11-15 October 1992, Washington DC, USA* pp.71-76: Tappi Press, Atlanta GA

Uesaka, T.; Moss, C.; Nanri,Y. (1992) "The characterisation of hygroexpansivity of paper." *Journal of Pulp and Paper Science* 18(1):J11-J16

Urbanik, T.J. (1981) "The principle of load sharing in corrugated fiberboard." *Paperboard Packaging* November 1981:122-128

Urbanik, T.J. (1995) "Hygroexpansion-creep model for corrugated fiberboard." *Wood and Fiber Science* 27(2):134-140

Urbanik, T.J. (1998) USDA Forest Products Laboratory, Madison Wisconsin, Private Communication

Urbanik, T.J.; Lee, S.K. (1995) "Swept sine humidity schedule for testing cycle period effects on creep." *Wood and Fiber Science* 27(1):68-78

Wink, W.A. (1961) "The effect of relative humidity and temperature on paper properties." *Tappi Journal* 44(6):171A-180A